CLONING AND CHARACTERIZATION OF THE *IRON-REGULATED TRANSPORTER* (*IRT*) GENES AND THEIR TRANSCRIPTION FACTORS IN *POPULUS*

A Dissertation
Submitted to the Graduate Faculty
of the
North Dakota State University
of Agriculture and Applied Science

By

Danqiong Huang

In Partial Fulfillment of the Requirements
for the Degree of
DOCTOR OF PHILOSOPHY

Major Department:
Plant Sciences

December 2014

Fargo, North Dakota

North Dakota State University
Graduate School

Title

CLONING AND CHARACTERIZATION OF THE *IRON-REGULATED TRANSPORTER* (*IRT*) GENES AND THEIR TRANSCRIPTION FACTORS IN *POPULUS*

By

Danqiong Huang

The Supervisory Committee certifies that this ***disquisition*** complies with North Dakota State University's regulations and meets the accepted standards for the degree of

DOCTOR OF PHILOSOPHY

SUPERVISORY COMMITTEE:

Dr. Wenhao Dai
Chair

Dr. Edward L. Deckard

Dr. Michael Christoffers

Dr. Xiwen Cai

Dr. Anne Denton

Approved:

03/26/2015 — Date

Richard D. Horsely — Department Chair

ABSTRACT

Iron deficiency causes chlorosis in many plant species, resulting in yield loss and poor quality. Many tree species including poplar are susceptible to iron deficiency. Trees suffering from iron deficiency often show interveinal chlorotic leaves and in severe cases, branches or an entire tree may die.

In this study, two trees of *Populus tremula* L.'Erecta' growing near each other but with contrasting leaf color phenotypes were used to study the causes of chlorosis and the mechanisms of tolerance or susceptibility to iron chlorosis in poplar. A leaf analysis revealed that the iron deficiency tolerant tree (PtG) had a higher level of dry matter content, chlorophyll (a+b), Chl a/b ratio, Zn and Fe content than the iron chlorosis susceptible tree (PtY). A hydroponic culture confirmed the differences in aforementioned physiological parameters between PtG and PtY responding to iron deficiency.

Two *iron-regulated transporter* genes (*PtIRT1* and *PtIRT3*), the native promoter of the *PtIRT1* gene (PtIRT1-pro), and two *basic helix-loop-helix* (*bHLH*) transcription factors (*PtFIT* and *PtIRO*) were cloned and characterized for their responses to iron deficiency in PtG and PtY. Deduced amino acid analysis revealed that *PtIRT1*, *PtIRT3*, *PtFIT*, and *PtIRO* in PtG were identical to those in PtY. Phylogenetic and putative domain analyses showed that *PtIRT1*, *PtFIT*, and *PtIRO* may function in iron homeostasis, while *PtIRT3* may play a role in zinc transport in poplar. The expression of *PtIRT1* and *PtFIT* are root-specific and up-regulated by iron deficiency. The expression of a GUS gene derived by PtIRT1-pro in tobacco was also up-regulated by iron deficiency, but was not root-specific. The expression of *PtIRT3* is ubiquitous and up-regulated by iron deficiency, but significantly down-regulated by zinc deficiency. A high correlation in the expression between *PtFIT* and *PtIRT1* was observed in PtG, but not in PtY.

Transgenic poplars overexpressing *PtIRT1* or *PtIRT3* did not have enhanced Fe accumulation; however, an enhanced tolerance to iron deficiency was found in transgenic plants overexpressing *PtFIT*. The results suggested that the transcription factor *PtFIT* may be involved in iron deficiency response through regulation of *PtIRT1* and *PtFIT* itself may be regulated by other factors in poplar.

ACKNOWLEDGMENTS

I sincerely appreciate those people who helped and supported me during my PhD study at NDSU.

Firstly, I would like to express my gratitude to my major advisor, Dr. Wenhao Dai, for his full support, patience, and encouragement throughout my whole study process.

I would also like to thank the members of my graduate committee, Drs. Xiwen Cai, Michael J. Christoffers, Edward Deckard, Ann Denton, and Shahryar Kianian for their useful comments.

I would like to give thanks to Vicki Magnusson, my dear friend, for the technical support in the lab and heart support in my life. My thanks also go to Dr. Hongxia Wang, Mr. Ryan Lenz, Dr. Yinghai Liang for their help and friendship.

I thank Dr. Ted Helms and Dr. Qi Zhang for their suggestions and comments on the experimental design and data analysis.

I thank Mr. Justin Hegstad, Dr. Lynn Dahleen and Miss Cayley Steen for allowing me to perform real-time PCR in their lab and their assistance in data analysis.

My thanks go to the people in the Department of Plant Sciences, especially the office staff, for helping me have a wonderful study at NDSU.

I thank my friends at NDSU, Yueqiang Leng, Naiyuan Dong, Rui Wang, Xianwen Zhu, Wei Zhang, Guojia Ma, Gongjun Shi and others, for their kindness and the great time we spent together.

I thank my parents and parents-in-law for their endless love and financial support.

Finally, my greatest gratitude goes to my husband, You Wu and my lovely daughter, Di Windy Wu, for their love and support provided in my life.

TABLE OF CONTENTS

LIST OF TABLES

LIST OF FIGURES

CHAPTER I. GENERAL INTRODUCTION

Iron (Fe) is an essential plant nutrient involved in biosynthesis and functional maintenance of chlorophyll in plants (Abadia, 1992). Iron is an important component of the ferredoxin/thioredoxin system that catalyzes several photosynthesis enzymes and plays a key role in regulating many metabolic pathways in the chloroplast (Malkin and Niyogi, 2000). The structure and composition of photosynthetic membranes in chloroplasts changed under the condition of iron deficiency, causing interveinal chlorotic leaves with a network of green veins, which dramatically affected the entire photosynthetic system of higher plants (Terry, 1983; Morales et al., 1994; Bertamini et al., 2001; Andaluz et al., 2006). The iron chlorosis symptoms first occur on the young leaves in the early growing stage and will continue to develop on all leaves during the growing season. In severe cases, leaves turn brown and gradually die, and eventually, branches or even an entire tree may die. Iron chlorosis is often seen in calcareous and alkaline soils and will cause loss of productivity and yield (Mori, 1999). Many tree species including apple, citrus, banana, grape, pines, and poplar are susceptible to iron deficiency (Tagliavini and Rombolà, 2001).

The mechanism of iron acquisition by higher plants can be distinctly classified into two strategies, reduction-based and chelation-based (Römheld and Marschner, 1986; Römheld, 1987; Mori, 1999; Guerinot and Yi, 1994; Kim and Guerinot, 2007). Non-graminaceous higher plants (known as Strategy I plants) employ the reduction-based strategy to uptake iron from the soil with the help of H^+-ATPases, membrane-bound Fe(III)-chelate reductases, and Fe(II)-specific cation transporters. Graminaceous species (known as Strategy II plants) transfer the iron into roots by chelating soluble Fe(III) that is formed as a complex of Fe(III)-chelators in the rhizophere of plants.

Under iron deficiency, Strategy I plants induce a number of mechanisms to alleviate the stress. One mechanism is to release H^+, reductants, and chelators. Enhancement of proton excretion in the rhizosphere can increase the ferric reduction capacity at the root surface to reduce Fe(III) to Fe(II). Release of chelators enhances the transport of Fe(II) through the plasmamembrane (Santi et al., 2005; Santi and Schmidt, 2008). It has been well documented that Fe(III) reduction is regulated by the genes in the *FRO* (*Ferric Reductase Oxidase*) family. Iron uptake and transport in plants is controlled by *IRT* (*Iron-Regulated Transporter*) genes belonging to the ZIP (zinc-regulated transporter, iron-regulated transporter-like protein) family (Guerinot, 2000; Morrissey and Guerinot, 2009; Jeong and Connolly, 2009; Waters and Sankaran, 2011; Jain et al., 2014). These genes can be induced by iron deficiency and regulated by *bHLH* (*basic helix-loop-helix*) transcription factors (Colangelo and Guerinot, 2004; Jakoby et al., 2004; Yuan et al., 2005; Yuan et al., 2008; Long et al., 2010; Sivitz et al., 2012; Wang et al., 2013; Thomine and Vert, 2013).

The genus *Populus*, belonging to the family *Salicaceae*, is comprised of 30-40 species classified into five sections based on leaf and flower characters. Poplar is widely used in paper (pulp production), energy (biofuel), forest (wood), and agforestry (shelterbelt) industries. Poplar has been a model tree species for both applied and basic research because of its rapid growth, well-developed micropropagation and transformation system, great genetic diversity, and small genome size (~ 500 Mbp) (Tuskan et al., 2004, 2006; Jansson and Douglas, 2007). A total of 41,427 genes are predicted in the poplar nuclear genome according to *Populus trichocarpa Poptr2_0* submitted by US DOE Joint Genome Institute (http://www.ncbi.nlm.nih.gov/genome/98) and released in 2006 and then modified in 2013. This genome information has been used by researchers worldwide in various areas, such as

comparative genomics, molecular biology, and genetics (Tuskan et al., 2004; Jansson and Douglas, 2007; Polle and Douglas, 2010).

In this study, two trees of European aspen (*Populus tremula*) 'Erecta' grown close to each other (3 meters apart) on the NDSU campus were found have contrasting phenotypes. One tree (PtG) grows normally with green leaves during the growing season. The other tree (PtY) has interveinal chlorotic leaves. The chlorosis symptom suggested that the two trees may suffer from iron deficiency stress. The objectives of this research were to analyze the physiological responses to iron deficiency and to identify and characterize genes involved in the iron metabolism in poplar trees.

References

Abadia, J. 1992. Leaf responses to Fe deficiency: a review. J. Plant Nutri. 15:1699-1713

Andaluz, S., López-Millán, A.F., De las Rivas, J., Aro, E.M., Abadia, J. and Abadia, A. 2006. Proteomic profiles of thylakoid membranes and changes in response to iron deficiency. Photosynth. Res. 89:141-155

Bertamini, M., Nedunchezhian, N. and Borghi, B. 2001. Effect of iron deficiency induced changes on photosynthetic pigments, ribulose-1,5-bisphosohate carboxylase and photosystem activities in field grown grapevine (*Vitis Vinifera* L. cv. Pinot Noir) leaves. Photosynthetica 39:59-65

Colangelo, E.P. and Guerinot, M.L. 2004. The essential basic helix-loop-helix protein FIT1 is required for the iron deficiency response. Plant Cell 16:3400-3412

Guerinot, M.L. 2000. The ZIP family of metal transporters. Biochim. Biophy. Acta 1465:190-198

Guerinot, M.L. and Yi, Y. 1994. Iron: Nutritious, noxious, and not readily available. Plant Physiol. 104:815-820

Jain, A., Wilson, G.T. and Connolly, E.L. 2014. The diverse roles of FRO family metalloreductases in iron and copper homeostasis. Front. Plant Sci. 5:100

Jakoby, M., Wang, H.Y., Reidt, W., Weisshaar, B. and Bauer, P. 2004. FRU(BHLH029) is required for induction of iron mobilization genes in *Arabidopsis thaliana*. FEBS Lett. 577:528-34

Jansson, S. and Douglas, C. 2007. *Populus*: a model system for plant biology. Annu. Rev. Plant Biol. 58:435-458

Jeong, J. and Connolly, E.L. 2009. Iron uptake mechanisms in plants: Functions of the *FRO* family of ferric reductases. Plant Sci. 176:709-714

Kim, S.A. and Guerinot, M.L. 2007. Mining iron: iron uptake and transport in plants. FEBS Lett. 581:2273-2280

Long, T.A., Tsukagoshi, H., Busch, W., Lahner, B., Salt, D.E. and Benfey, P.N. 2010. The bHLH transcription factor POPEYE regulates response to iron deficiency in *Arabidopsis* roots Plant Cell 22:2219-2236

Malkin, R. and Niyogi, K. 2000. Photosynthesis. In: Buchanan, B. B., Gruissem, W., and Jones, R., eds. Biochemistry and Molecular Biology of Plants. American Society of Plant Physiologists, Rockville, MD, pp. 575-577

Morales, F., Abadia, A., Belkhodja, R., and Abadia, J. 1994. Iron deficiency-induced changes in the photosynthetic pigment composition of field-grown pear (*Pyrus communis* L.) leaves. Plant Cell Environ. 17:1153-1160

Mori, S. 1999. Iron acquisition by plants. Curr. Opin. Plant Biol. 2:250-253

Morrissey, J. and Guerinot. M.L. 2009. Iron uptake and transport in plants: the good, the bad, and the ionome. Chem. Rev. 109:4553-4567

Polle, A. and Douglas, C. 2010. The molecular physiology of poplars: paving the way for knowledge-based biomass production. Plant Biology 12:239-241

Römheld, V. 1987. Different strategies for iron acquisition in higher plants. Physiol. Plant 70:231-234

Römheld, V. and Marschner, H. 1986. Evidence for a specific uptake system for iron phytosiderophores in roots of grasses. Plant Physiol. 80:175-180

Santi, S. and Schmidt, W. 2008. Laser microdissection-assisted analysis of the functional fate of iron deficiency-induced root hairs in cucumber. J. Exp. Bot. 59:697-704

Santi, S., Cesco, S., Varanini, Z. and Pinton, R. 2005. Two plasma membrane H^+-ATPase genes are differentially expressed in iron-deficient cucumber plants. Plant Physiol. Biochem. 43:287-292

Sivitz, A.B., Hermand, V., Curie, C. and Vert, G. 2012. *Arabidopsis bHLH100* and *bHLH101* control iron homeostasis via a *FIT*-independent pathway. PLoS ONE 7:e44843

Tagliavini, M. and Rombolà, A.D. 2001. Iron deficiency and chlorosis in orchard and vineyard ecosystems. Eur. J. Agron. 15:71-92.

Terry, N. 1983. Limiting factors in photosynthesis. IV. Iron stress-mediated changes in light harvesting and electron transport capacity and its effects on photosynthesis in vivo. Plant Physiol. 71:855-860

Thomine, S. and Vert, G. 2013. Iron transport in plants: better be safe than sorry. Curr. Opin. Plant Biol. 16:322-327

Tuskan, G., Difazio, S., Jansson, S., et al. 2006. The genome of black cottonwood, *Populus trichocarpa* (Torr. & Gray). Science 313:1596-1604

Tuskan, G., DiFazio, S. and Teichmann, T. 2004. Poplar genomics is getting popular: the impact of the poplar genome project on tree research. Plant Biology 6:2-4

Wang, L., Cui, Y., Liu, Y., Fan, H., Du, J., Huang, Z., Yuan, Y., Wu, H. and Ling, H.Q. 2013. Requirement and Functional Redundancy of Ib subgroup bHLH proteins for iron deficiency responses and uptake in *Arabidopsis thaliana*. Mol. Plant 6:503-513

Waters, B.M. and Sankaran, R.P. 2011. Moving micronutrients from the soil to the seeds: Genes and physiological processes from a biofortification perspective. Plant Sci. 180:562-574

Yuan, Y., Wu, H., Wang, N., Li, J., Zhao, W., Du, J., Wang, D. and Ling, H.Q. 2008. FIT interacts with AtbHLH38 and AtbHLH39 in regulating iron uptake gene expression for iron homeostasis in *Arabidopsis*. Cell Res. 18:385-397

Yuan, Y., Zhang, J., Wang, D.W. and Ling, H.Q. 2005. AtbHLH29 of *Arabidopsis thaliana* is a functional ortholog of tomato FER involved in controlling iron acquisition in strategy I plants. Cell Res. 15:613-621

CHAPTER II. LITERATURE REVIEW

Iron is an essential nutrient for plants

Iron (Fe), an essential micronutrient, is involved in biosynthesis and functional maintenance of chlorophyll in plants (Abadia, 1992). As an important component of the ferredoxin/thioredoxin system, iron catalyzes several photosynthesis enzymes and participates in the regulation of many metabolism pathways in the chloroplast (Malkin and Niyogi, 2000). Accumulated evidences show that iron functions as a co-factor involved in the formation of δ-aminolevulinic acid (ALA) that intermediates chlorophyll synthesis in higher plants (Pushnik et al., 1984). The structure and composition of photosynthetic membranes in chloroplasts changed under iron deficiency. In several plant species, iron deficiency may decrease the number of thylakoid membranes and other photosynthetic units such as granal and stomatal lamellae (Spiller and Terry, 1980) and lower the efficiency of photosynthesis system II (PS II) (Belkhodja et al., 1998; Bertamini et al., 2001; Naumann et al., 2005). These structural and compositional changes impair the electron transport chain and the light harvesting system which results in the dramatical inhibition of the entire photosynthetic system of higher plants (Terry, 1983; Morales et al., 1994; Andaluz et al., 2006). Meanwhile, iron is an essential nutrient for human beings and iron deficiency leads to the major human nutritional disorder of anemia, particularly in populations of children and women (http://www.who.int/nutrition/topics/ida/en/index.html).

Iron deficiency and its management in plants

In plants, iron deficiency causes a decrease of chlorophyll content and alternates the chlorophyll structure, resulting in plant chlorosis. Iron chlorosis is one of the major problems in calcareous soils, especially in arid and semi-arid regions. Worldwide, about 30% of the cultivated soils are calcareous in which iron chlorosis limits agricultural production (Mori,

1999). Many tree species including apple, citrus, banana, grape, pines, and poplars are susceptible to iron deficiency (Tagliavini and Rombolà, 2001). Iron chlorosis has a primary symptom of interveinal chlorosis that shows a bright yellow leaf with a network of green veins. Symptoms first occur on the young leaves in the early growing stage and will continue to develop on all leaves during the growing season. In severe cases, leaves turn brown and gradually die, and eventually, branches or even an entire tree may die.

Considerable research has been done on the control of iron chlorosis (Tagliavini and Rombolà, 2001; Abadia et al, 2011). Current practical methods for correcting iron chlorosis include 1) using species or cultivars tolerant to iron deficiency; 2) creating ideal soil/root environments to improve iron availability; 3) applying iron fertilizers to the soil and/or to the plant directly. Lack of iron deficiency tolerant germplasm and long breeding times make it difficult to develop cultivars having tolerance to iron deficiency *via* traditional breeding, especially for woody species. Creating an ideal soil/root environment, such as acidifying the soil and applying organic compounds to the soil to make iron more available is not always practical and desirable to large crop fields and landscapes. Soil application of iron elements has variable results and relatively high cost, and sometimes plants may be slow to respond to the iron supplies. Foliar spray and trunk injection may cause temporary leaf and trunk injury and have short-lasting effects. Compared with studies on annual crop species, limited research has been done for correcting iron chlorosis on woody plants. So far, there is no satisfactory method to control tree chlorosis throughout the entire life span of trees either in natural stands or in urban forestry.

Iron availability in the soil

Iron is sufficient in most cultivated soils with an average concentration of 20-40 g/kg (Cornell and Schwertmann, 2003). Iron is present in the soil in two forms, mineral Fe including

Fe(II) in primary minerals and Fe(III) in secondary minerals; and absorbable Fe including soluble and exchangeable Fe and Fe-complexes bound to the organic matter (Colombo et al., 2014). Most iron, particularly in calcareous or alkaline well-drained soils, predominantly exists in the ferric oxidation state [goethite (α-FeOOH) and hematite (α-Fe_2O_3)] that is not available for plants to uptake (Guerinot and Yi, 1994). Generally, the Fe concentration needs to be 10^{-9} -10^{-4} M to keep the optimal growth of plants (Römheld and Marschner 1986). However, the concentration of inorganic Fe is as low as 10^{-10} M in aqueous aerated soil solution and that of soluble Fe(II) and Fe(III) are less than 10^{-15} M in well-aerated soil (Marschner, 1995; Boukhalfa and Crumbliss, 2002). Iron can be solubilized from mineral sources via weathering, but it is a slow process regulated by pH, oxygen concentration and the dissolution-precipitation process of minerals (Lindsay, 1988; Mengel, 1994). Reduction of Fe(III) to Fe(II) increases the Fe solubility, but further studies found that Fe(II) is not stable in the aerobic environment that is suitable for healthy growth of most plants. Therefore, the major concern is not only how much Fe(II) is reduced from Fe(III), but also how fast the plant is able to uptake and transport Fe(II) to the target site (Guerinot and Yi, 1994; Briat and Lobreaux, 1997). These findings resulted in a conclusion that the major role of Fe nutrition is played by Fe forms available to plant roots rather than the amount of inorganic Fe (Guerinot and Yi, 1994; Briat et al., 1995).

Iron uptake, transport, and metabolism in plants

The mechanism of iron acquisition by higher plants can be distinctly classified into reduction- and chelation-based strategies (Takagi, 1976; Römheld and Marschner, 1986; Römheld, 1987; Guerinot and Yi, 1994; Mori, 1999; Kim and Guerinot, 2007). Non-graminaceous higher plants, known as Strategy I plants, employ a reduction-based strategy. The iron is acquired from the soil to roots through a coordinated action of H^+-ATPases, membrane-

bound Fe(III)-chelate reductases, and Fe(II)-specific cation transporters. In graminaceous species, also called Strategy II plants, Fe(III) chelators are used to acquire soluble Fe(III) from the rhizophere and the complex of Fe(III)-chelators are then transport into roots by the iron transporter.

Under iron deficiency, a number of mechanisms have been induced in plants to alleviate the stress. In Strategy I plants, these mechanisms include release of reducing and chelating substances (reductants and chelators) and enhancement of proton excretion in the rhizosphere, which increases the reduction of Fe(III) to Fe(II) and benefits the transport of Fe(II) through plasmamembranes (Santi et al., 2005; Santi and Schmidt, 2008). In *Arabidopsis*, H^+-ATPase (AHA) plays a role in iron deficiency response with its activity being found in iron-deficient roots (Colangelo and Guerinot, 2004; Dinneny et al., 2008). The Fe(III) reduction capacity positively correlated to iron deficiency resistance in some annual plants, such as soybean (Jolley et al., 1992), dry bean (Ellsworth et al., 1997), and some woody species (De la Guardia and Alcantara, 2002). Evidence showed that increased reductase activities under iron deficiency stress enhanced reduction of soluble Fe(III) to Fe(II), consequently increasing iron uptake by plants (Römheld, 1987). In strategy II species, plants produce iron-chelating mugineic acids that belong to phytosiderophores (PSs) and are present at the root surface to chelate Fe(III) under iron deficiency. The complex of Fe(III)-PSs is then transported into roots via *YS1* (*Yellow Stripe 1*) and *YSL1* (*Yellow Stripe 1-Like*) transporters (Curie et al., 2001, 2009). It is interesting that Fe(II) could be taken up in addition to Fe(III)-PSs complexes in rice without H^+-ATPase and Fe (III)-chelate reductase activity which was often found in Strategy I plants (Cheng et al., 2007).

Iron homeostasis in plants

It has been well documented that Fe(III) reduction is regulated by the genes in the *FRO* (*Ferric Reductase Oxidase*) family and Fe uptake and transport is controlled by the *IRT* (*Iron-Regulated Transporter*) genes belonging to the ZIP (zinc-regulated transporter, iron-regulated transporter-like protein) family in plants (Guerinot, 2000; Morrissey and Guerinot, 2009; Jeong and Connolly, 2009; Water and Sankaran, 2011). Various iron deficiency inducible genes including *IRT* and *FRO* are regulated by the *bHLH* (*basic helix-loop-helix*) transcription factors (Colangelo and Guerinot, 2004; Jakoby et al., 2004; Yuan et al., 2005; Yuan et al., 2008; Long et al., 2010; Sivitz et al., 2012; Thomine and Vert 2013; Wang et al., 2013).

Ferric reduction oxidase (*FRO*) gene family

The mechanism of iron reduction has been well characterized (Schmidt, 1999). Previously, an externally oriented reductase has been found to be responsible for the reduction of ferric iron and was localized on the root-cell plasma membrane (Bienfait et al., 1983; Buckhout et al., 1989; Holden et al., 1991; Schmidt, 1999). The *FRO* gene encodes Fe(III)-chelate reductase, reducing Fe(III) to soluble Fe(II). As a member of the flavocytochrome family, Fe(III)-chelate reductase has a function of transporting electrons across membranes and its activity increases when iron is deficient (Robinson et al., 1999; Bienfait, 1985). By contrast, iron deficiency decreases the activity of Fe(III)-chelate reductase in leaf mesophyll protoplasts, which may resulted in chlorotic leaves because of lower active Fe used for chlorophyll formation (Gonzalez-Vallejo et al., 2000; Mengel, 1994). In *Arabidopsis*, *AtFRO2* is the main Fe(III)-chelate reductase expressed in the epidermal cells of iron-deficient roots (Robinson et al., 1999). A loss-of-function mutant (*frd1*) of *FRO2* that was extremely chlorotic when grown on iron deficiency medium showed a defective iron uptake when iron was supplied as a Fe(III)-chelate

form (Connolly et al., 2003). In the other hand, overexpression of *AtFRO2* in soybean increased the root ferric reductase activity and enhanced tolerance to iron deficiency induced chlorosis (Vasconcelos et al., 2006). In addition to *AtFRO2*, seven other *AtFRO* genes (*FRO1*, *FRO3*, *FRO4*, *FRO5*, *FRO6*, *FRO7*, and *FRO8*) were identified in *Arabidopsis* based on the sequence similarity (Wu et al., 2005; Mukherjee et al., 2006). The expression of the *AtFRO* genes in various tissues suggests that the *AtFRO* genes function differently in iron uptake. The *AtFRO1* and *AtFRO4* genes are barely detected in all tissues. The *AtFRO2* and *AtFRO5* genes are primarily expressed in roots while *AtFRO6*, *AtFRO7*, and *AtFRO8* genes are shoot-specific. The *AtFRO3* is expressed at a higher level in roots and shoots. Besides, the promoter of *FRO6* has multiple light-responsive elements, since the reporter gene driven by the *AtFRO6* promoter was activated when exposed to light (Feng et al., 2006). Indeed, transgenic tobacco overexpressing *AtFRO6* has higher ferric reductase activity in leaves than the control, leading to increased concentrations of ferrous iron, chlorophyll as well as reduced iron deficiency chlorosis (Li et al., 2011). In summary, evidence suggested that the *AtFRO* genes appear to play important roles in uptake and subcellular compartmentalization of iron (Jain et al., 2014). It is well demonstrated that *AtFRO2* serves to reduce solubilized Fe(III) to usable Fe(II) in roots. The *AtFRO6* gene functions to reduce Fe(III) to Fe(II) at the cell surface of leaf cells. The *AtFRO7* gene is known to contribute to delivery of iron to chloroplasts while mitochondrial family members *AtFRO3* and *AtFRO8* genes are hypothesized to influence mitochondrial metal ion homeostasis. Recent research showed that *AtFRO4* and *AtFRO5* genes are more likely to function to reduce Cu^{2+} to Cu^{+} at the root surface rather than iron (Bernal et al., 2012).

Other than those in *Arabidopsis*, many *FRO* genes were also cloned and characterized in other species, such as pea (Waters et al., 2002), tomato (Li et al., 2004) and potato (Legay et al.,

2012). In pea, the *PsFRO1* gene also encodes a Fe(III)-chelate reductase and its expression was correlated with Fe(III)-chelate reductase activity and induced by iron deficiency. Moreover, *PsFRO1* transcripts were detected in roots, leaves and nodules suggesting *PsFRO1* may play a role in iron distribution within the plant rather than only iron uptake (Waters et al., 2002). The *LeFRO1* encoding a Fe(III)-chelate reductase protein was isolated from tomato (Li et al., 2004). Expression of *LeFRO1* in yeast increased Fe(III)-chelate reductase activity. *LeFRO1* protein was targeted on the plasma membrane and was detected in various tissues including roots, leaves, cotyledons, flowers, and young fruits. The expression level of *LeFRO1* in roots was highly related to iron status. In potato, the expression of an EST, 94% homologous to *LeFRO1*, was induced dramatically in roots under the iron deficient condition (Legay et al., 2012).

***Iron-regulated transporter* (*IRT*) gene family**

The *IRT* genes encode the iron transporter proteins that are essential for iron uptake and transport in plants (Vert et al., 2001, 2002). The *IRT1*, *IRT2* and *IRT3* genes isolated from *Arabidopsis* are members of the ZIP metal transporter family. The *AtIRT1* gene was first identified from *Arabidopsis* by functional complementation of an iron uptake-deficiency mutant (*fet3/fet4*) in yeast (Eide et al., 1996). *AtIRT1*, expressed in the external cell layers of the root, was specifically induced in response to iron starvation. The *IRT1* knock-out *Arabidopsis* mutation displayed chlorotic leaves, severe growth defect and even seedling lethality (Henriquies et al., 2002). The *AtIRT2* gene, another important member of the ZIP family, is a homolog of the *AtIRT1* gene. Both the *AtIRT1* and *AtIRT2* genes are divalent cation transporters; however, only *AtIRT1* is required for iron homeostasis under the iron deficient condition because *IRT2*-insertion mutant (*irt2*) plants did not show the symptom of iron deficiency and overexpression of *AtIRT2* in *IRT1* defective mutant (*irt1-1*) plants failed to restore the wild-type phenotype (Vert et al.,

2001). Expression of *AtIRT2* was enhanced in roots of an *AtIRT1* defective mutant as an altered response to iron deficiency (Henriques et al., 2002). Recent research proposed that *AtIRT2* does not play a significant role in iron uptake from the soil, but may be involved in intracellular Fe trafficking and co-regulation with *FRO2* and *IRT1* (Vert et al., 2009). The *AtIRT3* gene, which is a homolog of *AtIRT1* and *AtIRT2*, also plays an important role in transport of divalent metal cations. Grotz et al. (1998) proposed that *AtIRT3* shares more sequence similarity to *AtZIP4* and more likely plays a role in Zn transport from soil to plants as its expression level was increased by zinc deficiency. Such an up-regulation of *AtIRT3* in response to the zinc deficient condition was also reported by Talke et al. (2006) and Lin et al. (2009). Additionally, the *AtIRT3* gene appeared to also be involved in iron uptake and transport in plants. Shanmugam et al. (2011) reported that overexpression of the *AtIRT3* gene in the *irt1-1* mutant rescued the growth defect of *irt1-1* under iron deficiency. Unlike *AtIRT1* and *AtIRT2* expressing in root tissues only, GUS staining indicated that the *IRT3* promoter was constitutively expressed in leaves, root tips, flowers, stamens, siliques and seeds (Lin et al., 2009).

The *IRT* orthologs were found to be up-regulated by iron deficiency in other species including tomato (Eckhardt et al., 2001), tobacco (Hodoshima et al., 2007), cucumber (Waters et al., 2007), peanut (Ding et al., 2010), potato (Legay et al., 2012), and apple (Li et al., 2006). In tomato, *LeIRT1* and *LeIRT2* expressed in both iron-sufficient and iron-deficient roots, with *LeIRT1* showing induction under iron deficiency (Eckhardt et al., 2001). Qu et al. (2005) found that the *LeIRT2* transgenic plants of *Malus robusta* had enhanced iron deficiency tolerance indicated by higher leaf chlorophyll content and net photosynthetic rate. In potato, the expression level of *IRT1* that is a homolog of *LeIRT1* was relative low under the iron sufficient condition and significantly increased under the iron deficient condition in roots (Legay et al., 2012). In

woody plants, the expression level of *MxIRT1* was strongly enhanced in the root of *Malus xiaojinensis* under the iron limited condition. Besides, *MxIRT1* could complement iron uptake activity in a yeast (*Saccharoomyces cerevisiae*) mutant strain DEY1453 (*fet3fet4*) (Li et al., 2006). In peanut, the *AhIRT1* gene could restore the growth of yeast mutant *fet3fet4* under the iron deficient condition and its expression was induced by iron deficiency in peanuts (Ding et al., 2010). A more recent study demonstrated that the transgenic tobacco plants overexpressing peanut *AhIRT1* accumulated more Fe and showed tolerance to iron deficiency in calcareous soils (Xiong et al., 2014).

Iron deficiency inducible transcription factor *basic helix-loop-helix* (*bHLH*) gene family

The overexpression of *IRT1* and *FRO2* in plants has revealed post-transcriptional regulation. *IRT1* mRNA was detected in the root and shoot of 35S-*IRT1* plants regardless of iron status; however, *IRT1* protein was only detected in iron-deficient roots (Connolly et al., 2002). Likewise, 35S-*FRO2* plants showed increased *FRO*2 mRNA level, but Fe(III) chelate reductase activity elevated only when plants were iron deficient (Connolly et al., 2003). The mechanism of this regulation is currently not well known.

The tomato *fer* (T3238*fer*) mutant and the cloning of the corresponding gene, *FER*, have offered the first clues as to how iron deficiency responses are regulated by plants (Ling et al., 2002). The *FER* gene encodes a basic helix-loop-helix (*bHLH*) transcription factor that is a large family of transcription factors involved in gene regulation. The *FER* mRNA was detected in the root epidermis, the outer cortical layer of root tips, and in the vascular cylinder in the mature root-hair zone. The *fer* mutant failed to induce *LeIRT1* expression under the iron deficient condition, indicating the direct role of *LeFER* in regulating the *IRT1* gene in tomato. In addition,

FER expression was suppressed by iron sufficiency at post-transcriptional level (Brumbarova et al., 2005).

An ortholog of *LeFER* named *AtFIT1* (*FER*-Like *Iron Deficiency-Induced Transcription Factor*, also known as *bHLH29* or *FRU*) is required for induction of iron mobilization genes in *Arabidopsis*. The *AtFIT1* gene regulates iron deficiency inducible genes with known or putative functions in iron homeostasis, including the *AtFRO* and *AtIRT* genes (Colangelo and Guerinot, 2004; Jakoby et al., 2004; Yuan et al., 2005). The expression of *AtFIT1* is detected in the root epidermal cells of *Arabidopsis* and is enhanced under the iron deficient condition. The tomato *fer* mutant expressing *AtFIT1* has restored iron deficiency responses and has survived under the iron deficient condition indicating *AtFIT1* may have a function similar to *LeFER* (Yuan et al., 2005). Under the iron deficient condition, in *Arabidopsis fit1* mutants that are chlorotic and defective, *AtFRO2* mRNA was not detectable, suggesting that *AtFIT1* regulates *AtFRO2* at the level of mRNA accumulation. Eventhough *AtIRT1* mRNA was still detectable, *AtIRT* protein is not detectable, which indicated that *AtFIT1* controls *AtIRT1* at the level of protein accumulation (Colangelo and Guerinot, 2004). Further study demonstrated that with the co-expression of another two *bHLH* transcription factors, forming *AtFIT1*/*AtbHLH38* and *AtFIT1/AtbHLH39* complexes, *AtFRO2* and *AtIRT1* could be constitutively expressed even under the iron sufficient condition (Yuan et al., 2008). In addition, another two *bHLH* transcription factors (*AtbHLH100* and *AtbHLH101*) within the same subgroup of *AtbHLH38* and *AtbHLH39*, were also strongly induced by iron deficiency in the root and leaf of *Arabidopsis* (Wang et al., 2007). Sivitz et al. (2012) found that *AtIRT1* and *AtFRO2* were not up-regulated in the *bhlh100/bhlh101* double mutant that showed severe reduced growth and chorosis grown under iron deficiency. They also proposed that rather than the *AtFIT1* target genes, *AtbHLH100* and *AtbHLH101* likely regulate

genes involved in the distribution of iron within plants and *AtbHLH100* and *AtbHLH101* play a *FIT*-independent regulation role on iron deficiency responses. In disagreement, Wang et al. (2013) reported that both *AtbHLH100* and *AtbHLH101* could interact with *AtFIT1* according to the yeast two-hybrid analysis and bimolecular fluorescence complementation assay. Besides, they also concluded that *AtbHLH38*, *AtbHLH39*, *AtbHLH100*, and *AtbHLH101* function redundantly in regulation of iron deficiency responses and uptake with different significance (*AtbHLH39* > *AtbHLH101* > *AtbHLH38* > *AtbHLH100*).

In *Arabidopsis*, in addition to *AtFIT1* acting as a master regulator in the iron deficiency response, *POPEYE* (*AtPYE*, also known as *AtbHLH047*) was found to be pericycle specific and was also responding to iron deficiency (Long et al., 2010). *AtPYE* plays a role in maintaining iron homeostasis by regulating the expression of known iron homeostasis genes, such as *AtIRT1*, *AtIRT2*, and *AtFRO3* and other genes involved in stress responses according to microarray data. In addition, *AtPYE* interacts with its homologs, including IAA–Leu Resistant3 (*AtILR3*, also known as *AtbHLH105*) or *AtbHLH115* that is involved in metal ion homeostasis to regulate downstream targets. In other species, Legay et al. (2012) proposed that in potato, the expression of *FER*-like transcription factor that share 90% identities with the *LeFER* gene was also influenced by iron status. Besides, a strong positive correlation between expression of *FER*-like transcription factor and *IRT1* gene was observed. In *Malus xiaojinesis*, three *bHLH* genes (*MxbHLH01*, *MxIRO2* and *MxFIT)* were isolated and characterized. All three *bHLH* genes were localized to the nucleus (Xu et al., 2011; Yin et al., 2013, 2014). The expression of *MxbHLH01* was restricted to the root and up-regulated under the iron deficient condition. Besides, *MxbHLH01* might interact with other proteins to regulate genes in response to iron deficiency (Xu et al., 2011). The *MxIRO2* gene was induced by iron deficiency in roots and leaves. It might

form a heterodimer or multimer with other transcription factors to control the expression of genes related to iron absorption (Yin et al., 2013). The *MxFIT* gene was up-regulated in roots under iron deficiency at both mRNA and protein levels, while almost no expression was detected in leaves irrespective of iron supply. The transgenic *Arabidopsis* plants with *MxFIT* had increased *AtIRT1* and *AtFRO2* transcripts in roots under the iron deficient condition, showing a stronger resistance to iron deficiency (Yin et al., 2014).

Poplar, a model tree species for molecular and biotechnology research

The genus *Populus,* belonging to the family *Salicaceae*, includes 30-40 species that are classified into five sections according to leaf and flower characters. Due to a dioecious (rarely monoecious) breeding system, poplar could be propagated vegetatively. Poplar is widely used in paper (pulp production), energy (biofuel), forest (wood) and agforest (shelterbelt) industries. In the research, poplar has been a model tree species for either applied or basic research because of its rapid growth, well-developed micropropagation and transformation system, and great genetic diversities (Tuskan, et al., 2004; Jansson and Douglas, 2007). With 19 chromosomes and a relatively smaller genome size of ~ 500 Mbp, *Populus trichocarpa* was selected for genome sequencing (Tuskan et al., 2006). A total of 41,427 genes are predicted in poplar nuclear genome according to *Populus trichocarpa Poptr2_0* submitted by US DOE Joint Genome Institute (http://www.ncbi.nlm.nih.gov/genome/98) and released in 2006 and then modified in 2013. This genome information has been used by researchers worldwide in various areas, such as comparative genomics, molecular biology, and genetics. (Tuskan, et al., 2004; Jansson and Douglas, 2007; Polle and Douglas, 2010). Therefore, poplar is ideal for the study of iron uptake and transport and its response to metal deficiency stress in woody species.

References

Abadia, J. 1992. Leaf responses to Fe deficiency: a review. J. Plant Nutri. 15:1699-1713

Abadia, J., Vazquez, S., Rellan-Alvarez, R., EI-Jendoubi, H., Abadia, A., Alvarez-Fernandez, A. and López-Millán, A.F. 2011. Towards a knowledge-based correction of iron chlorosis. Plant Physiol. Biochem. 49:471-482

Andaluz, S., López-Millán A.F., De las Rivas, J., Aro, E.M., Abadia, J. and Abadia, A. 2006. Proteomic profiles of thylakoid membranes and changes in response to iron deficiency. Photosynth. Res. 89:141-155

Belkhodja, R., Morales, F., Quilez, R., López-Millán, A.F., Abadia, A. and Abadia, J. 1998. Iron deficiency causes changes in chlorophyll fluorescence due to the reduction in the dark of the Photosystem II acceptor. Photosynth. Res. 56:265-276

Bernal, M., Casero, D., Singh, V., Wilson, G.T., Grande, A., Yang, H., Dodani, S.C., Pellegrini, M., Huijser, P., Connolly, E.L., Merchant, S.S. and Krämer, U. 2012. Transcriptome sequencing identifies SPL7-regulated Cu acquisition genes *FRO4/FRO5* and the Cu dependence of Fe homeostasis in *Arabidopsis*. Plant Cell 24:738-761

Bertamini, M., Nedunchezhian, N. and Borghi, B. 2001. Effect of iron deficiency induced changes on photosynthetic pigments, ribulose-1,5-bisphosohate carboxylase and photosystem activities in field grown grapevine (*Vitis Vinifera* L. cv. Pinot Noir) leaves. Photosynthetica 39:59-65

Bienfait, H.F. 1985. Regulated redox processes at the plasmalemma of plant root cells and their function in iron uptake. J. Bioenerg. Biomembr. 17:73-83

Bienfait, H.F., Bino, R.J., van der Bliek, A.M., Duivenvoorden, J.F. and Fontaine, J.M. 1983. Characterization of ferric reducing activity in roots of Fe-deficient *Phaseolus vulgaris*. Physiol. Plant. 59:196-202

Boukhalfa, H. and Crumbliss, A.L. 2002. Chemical aspects of siderophore mediated iron transport. Biometals 15:325-339

Briat, J.F., Fobis-Loisy, I., Grignon, N. Lobréaux, S., Pascal, N., Savino,G., Thoiron, S., Wirén, N. and Wuytswinkel, O.V. 1995. Cellular and molecular aspects of iron metabolism in plants. Biol. Cell 84:69-81

Buckhout, T.J., Bell, P.F., Luster, D.G. and Chaney, R.L. 1989. Iron-stress induced redox activity in tomato (*Lycopersicum esculentum* Mill.) is localized on the plasma membrane. Plant Physiol. 90:151-156

Cheng, L., Wang, F., Shou, H., Huang, F., Zheng, L., He, F., Li, J., Zhao, F., Ueno, D., Ma, J.F. and Wu, P. 2007. Mutation in nicotianamine aminotransferase stimulated the Fe(II) acquisition system and led to iron accumulation in rice. Plant Physiol. 145:1647-1657

Colangelo, E.P. and Guerinot, M.L. 2004. The essential basic helix-loop-helix protein *FIT1* is required for the iron deficiency response. Plant Cell 16:3400-3412

Colombo, C., Palumbo, G., He, J-Z., Pinton, R. and Cesco, S. 2014. Review on iron availability in soil: interaction of Fe minerals, plants, and microbes. J. Soils Sediments 14:538-548

Connolly, E.L., Campbell, N., Grotz, N., Prichard, C.L. and Guerinot, M.L. 2003. Overexpression of the *FRO2* iron reductase confers tolerance to growth on low iron and uncovers post-transcriptional control. Plant Physiol. 133:1102-1110

Connolly, E.L., Fett, J.P. and Guerinot, M.L. 2002. Expression of the *IRT1* metal transporter is controlled by metals at the levels of transcript and protein accumulation. Plant Cell 14:1347-1357

Cornell, R.M. and Schwertmann, U. 2003. Iron oxides: structure, properties, reactions. Occurrence and uses. 2nd Ed., Wiley-VCH, Weinheim.

Curie, C., Cassin, G., Couch, D., Divol, F., Higuchi, K., Jean, M.L., Misson, J., Schikora, A., Czernic, P. and Mari, S. 2009. Metal movement within the plant: contribution of nicotianamine and *yellow stripe 1-like* transporters. Ann. Bot. (Lond) 103:1-11

Curie, C., Panaviene, Z., Loulergue, C., Dellaporta, S.L., Briat, J.F. and Walker, E.L. 2001. Maize *yellow stripe1* encodes a membrane protein directly involved in Fe(III) uptake. Nature 409:346-349

De la Guardia, M.D. and Alcántara, E. 2002. A comparison of ferric-chelate reductase and chlorophyll and growth ratios as indices of selection of quince, pear and olive genotypes under iron deficiency stress. Plant Soil 241:49-56

Ding, H., Duan, L., Li, J., Yan, H., Zhao, M., Zhang, F. and Li, W. 2010. Cloning and functional anaylsis of the peanut iron transporter *AhIRT1* during iron deficiency stress and intercropping with maize. J. Plant Physiol. 167:996-1002

Dinneny, J.R., Long, T.A., Wang, J.Y., Jung, J.W., Mace, D., Pointer, S., Barron, C., Brady, S.M., Schiefelbein, J. and Benfey P.N. 2008. Cell identity mediates the response of *Arabidopsis* roots to abiotic stress. Science 320:942-45

Eckhardt, U., Marques, A.M. and Buckhout, T.J. 2001. Two iron-regulated cation transporters from tomato complement metal uptake-deficient yeast mutants. Plant Mol. Biol. 45:437-448

Eide, D., Broderius, M., Fett, J. and Guerinot, M.L. 1996. A novel iron-regulated metal transporter from plants identified by functional expression in yeast. Proc. Natl. Acad. Sci. USA 93:5624-5628

Ellsworth, J.W., Jolley, V.D., Nuland, D.S. and Blaylock, A.D. 1997. Screening for resistance to iron deficiency chlorosis in dry bean using iron reduction capacity. J. Plant Nutr. 20:1489-1502.

Feng, H., An, F., Zhang, S., Ji, Z., Ling, H.Q. and Zuo, J. 2006. Light-regulated, tissue-specific, and cell differentiation-specific expression of the *Arabidopsis* Fe(III)-chelate reductase gene *AtFRO6.* Plant Physiol. 140:1345-1354

González-Vallejo, E.B., Morales, F., Cistué, L. Abadia, A. and Abadia J. 2000. Iron deficiency decreases the Fe(III)-chelate reducing activity of leaf protoplasts. Plant Physiol. 122:337-344

Grotz, N., Fox, T., Connolly, E., Park, W., Guerinot, M.L. and Eide, D. 1998. Identification of a family of zinc transporter genes from *Arabidopsis* that respond to zinc deficiency. Proc. Natl. Acad. Sci. USA 95:7220-7224

Guerinot, M.L. 2000. The ZIP family of metal transporters. Biochim. Biophy. Acta 1465:190-198

Guerinot, M.L. and Yi, Y. 1994. Iron: Nutritious, noxious, and not readily available. Plant Physiol. 104:815-820

Henriques, R., Jasik, J., Klein, M., Martinoia, E., Feller, U., Schell, J., Pais, M.S. and Koncz, C. 2002. Knock-out of *Arabidopsis* metal transporter gene *IRT1* results in iron-deficiency accompanied by cell differentiation defects. Plant Mol. Biol. 50:587-597

Hodoshima. H., Enomoto, Y., Shoji, K., Shimada, H., Goto, F. and Yoshihara, T. 2007. Differential regulation of cadmium-inducible expression of iron-deficiency-responsive genes in tobacco and barley. Physiologia Plantarum 129:622-634

Holden, M.J., Luster, D.G., Chaney, R.L., Buckout, T.J. and Robinson, C. 1991. Fe^{3+}-chelate reductase activity of plasma membranes isolated from tomato (*Lycopersicon esculentum* Mill.) roots: comparison of enzymes from Fe-deficient and Fe-sufficient roots. Plant Physiol. 97: 537-544.

Jain, A., Wilson, G.T. and Connolly, E.L. 2014. The diverse roles of *FRO* family metalloreductases in iron and copper homeostasis. Front. Plant Sci. 5:100

Jakoby, M., Wang, H.Y., Reidt, W., Weisshaar, B. and Bauer, P. 2004. FRU(bHLH029) is required for induction of iron mobilization genes in *Arabidopsis thaliana*. FEBS Lett. 577:528-34

Jansson, S. and Douglas, C. 2007. *Populus*: a model system for plant biology. Annu. Rev. Plant Biol. 58:435-458

Jeong, J. and Connolly, E.L. 2009. Iron uptake mechanisms in plants: Functions of the *FRO* family of ferric reductases. Plant Sci. 176:709-714

Jolley, V.D., Fairbanks, D.J., Stevens, W.B., Terry, R.E. and Orf, J.H. 1992. Root iron reduction capacity for genotypic evaluation of iron efficiency in soybean. J. Plant Nutr. 15:1679-1690.

Kim, S.A. and Guerinot, M.L. 2007. Mining iron: iron uptake and transport in plants. FEBS Lett. 581:2273-2280

Legay, S., Guignard, C., Ziebel, J. and Evers, D. 2012. Iron uptake and homeostasis related genes in potato cultivated in vitro under iron deficiency and overload. Plant Physiol. Biochem. 60:180-189

Li, L., Cai, Q., Yu, D. and Guo, C. 2011. Overexpression of *AtFRO6* in transgenic tobacco enhances ferric chelate reductase activity in leaves and increases tolerance to iron-deficiency chlorosis. Mol. Biol. Rep. 38:3605-3613

Li, L., Cheng, X. and Ling, H.Q. 2004. Isolation and characterization of Fe(III)-chelate reductase gene *LeFRO1* in tomato. Plant Mol. Biol. 54:125-136

Li, P., Qi, J.L., Wang, L., Huang, Q.N., Han, Z.H. and Yin, L.P. 2006. Functional expression of *MxIRT1*, from Malus xiaojinensis, complements an iron uptake deficient yeast mutant for plasma membrane targeting via membrane vesicles trafficking process. Plant Sci. 171:52-59

Lin, Y.F, Liang, H.M., Yang, S.Y., Boch, A., Clemens, S., Chen, C.C., Wu, J.F., Huang, J.L. and Yeh, K.C. 2009. *Arabidopsis IRT3* is a zinc-regulated and plasma membrane localized zinc/iron transporter. New Phytol. 2182:392-404

Lindsay, W.L. 1988. Solubility and redox equilibria of iron compounds in soils. In: Stucki, J.W., eds. Iron in soils and clay minerals. Reidel Publ. NATO, Dordrecht, pp 37-60

Ling, H.Q., Bauer, P., Bereczky, Z., Keller, B. and Ganal, M.W. 2002. The tomato fer gene encoding a bHLH protein controls iron-uptake responses in roots. Proc. Natl. Acad. Sci. USA 99:13938-13943

Long, T.A., Tsukagoshi, H., Busch, W., Lahner, B., Salt, D.E. and Benfey, P.N. 2010. The bHLH transcription factor POPEYE regulates response to iron deficiency in *Arabidopsis* roots Plant Cell 22:2219-2236

Malkin, R. and Niyogi, K. 2000. Photosynthesis. In: Buchanan, B. B., Gruissem, W., and Jones, R., eds. Biochemistry and Molecular Biology of Plants. American Society of Plant Physiologists, Rockville, MD, pp. 575-577

Marschner, H. 1995. Mineral nutrition of plants. Academic Press, Boston

Mengel, K. 1994. Iron availability in plants tissues-iron chlorosis on calcareous soils. Plant Soil 165:275-283

Morales, F., Abadia, A., Belkhodja, R., and Abadia, J. 1994. Iron deficiency-induced changes in the photosynthetic pigment composition of field-grown pear (*Pyrus communis* L.) leaves. Plant Cell Environ. 17:1153-1160

Mori, S. 1999. Iron acquisition by plants. Curr. Opin. Plant Biol. 2:250-253

Morrissey, J. and Guerinot, M.L. 2009. Iron uptake and transport in plants: the good, the bad, and the ionome. Chem. Rev. 109:4553-4567

Mukherjee, I., Campbell, N.H., Ash, J.S. and Connolly, E.L. 2006. Expression profiling of the *Arabidopsis* ferric chelate reductase (*FRO*) gene family reveals differential regulation by iron and copper. Planta 223:1178-1190

Naumann, B., Stauber, E.J., Busch, A., Sommer, F. and Hippler, M. 2005. N-terminal processing of Lhca3 is a key step in remodeling of the photosystem I-light-harvesting complex under iron deficiency in Chlamydomonas reinhardtii. J. Biol. Chem. 280:20431-20441.

Polle, A. and Douglas, C. 2010. The molecular physiology of poplars: paving the way for knowledge-based biomass production. Plant Biol. 12:239-241

Pushnik,J.C., Miller,G.W. and Manwaring, J.H. 1984. The role of iron in higher plant chlorophyll biosynthesis, maintenance and chloroplast biogenesis. J. Plant Nutri.7:733-757

Qu. S.C., Huang, X.D., Zhang, Z., Yao, Q.H., Tao, J.M., Qiao, Y.S. and Zhang, J.Y. 2005. *Agrobacterium*-mediated transformation of *Malus robusta* with tomato iron transporter gene. J. Plant Physiol. Mol. Biol. 31:235-240

Robinson, N.J., Procter, C.M., Connolly, E.L. and Guerinot, M.L. 1999. A ferric-chelate reductase for iron uptake from soils. Nature 397:694-697

Römheld, V. 1987. Different strategies for iron acquisition in higher plants. Physiol. Plant 70:231-234

Römheld, V. and Marschner, H. 1986. Evidence for a specific uptake system for iron phytosiderophores in roots of grasses. Plant Physiol. 80:175-180

Santi, S., Cesco, S., Varanini, Z. and Pinton, R. 2005. Two plasma membrane H^+-ATPase genes are differentially expressed in iron-deficient cucumber plants. Plant Physiol. Biochem. 43:287-92

Santi, S., and Schmidt, W. 2008. Laser microdissection-assisted analysis of the functional fate of iron deficiency-induced root hairs in cucumber. J. Exp. Bot. 59:697-704

Schmidt, W. 1999. Mechanisms and regulation of reduction-based iron uptake in plants. New Phytol. 141:1-26

Shanmugam, V., Lo, J., Wu, C., Wang, S., Lai, C., Connolly, E.L., Huang, L. and Yeh, K. 2011. Differential expression and regulation of iron-regulated metal transporters in *Arabidopsis halleri* and *Arabidopsis thaliana* - the role in zinc tolerance. New Phytol. 190:125-137

Sivitz, A.B., Hermand, V., Curie, C. and Vert, G. 2012. *Arabidopsis bHLH100* and *bHLH101* control iron homeostasis via a *FIT*-independent pathway. PLoS ONE 7: e44843

Spiller, S. and Terry, N. 1980. Limiting factors in photosynthesis II. Iron stress diminishes photochemical capacity by reducing the number of photosynthetic units. Plant Physiol. 65:121-125

Tagliavini, M. and Rombolà, A.D. 2001. Iron deficiency and chlorosis in orchard and vineyard ecosystems. Eur. J. Agron. 15:71-92

Takagi, S. 1976. Naturally occurring iron-chelating compounds in oat- and rice-root washing. I. Activity measurement and preliminary characterization. Soil Sci. Plant Nutri. 22:423-433

Talke, I.N., Hanikenne, M. and Kramer, U. 2006. Zinc-dependent global transcriptional control, transcriptional deregulation, and higher gene copy number for genes in metal homeostasis of the hyperaccumulator *Arabidopsis halleri*. Plant Physiol.142:148-167

Terry, N. 1983. Limiting factors in photosynthesis. IV. Iron stress-mediated changes in light harvesting and electron transport capacity and its effects on photosynthesis in vivo. Plant Physiol. 71:855-860

Thomine, S. and Vert, G. 2013. Iron transport in plants: better be safe than sorry. Curr. Opin. In Plant Bio. 16:322-327

Tuskan, G., Difazio, S., Jansson, S., et al. 2006. The genome of black cottonwood, *Populus trichocarpa* (Torr. & Gray). Science 313:1596-1604

Tuskan, G., DiFazio, S. and Teichmann, T. 2004. Poplar genomics is getting popular: the impact of the poplar genome project on tree research. Plant Biology 6:2-4

Vasconcelos, M., Eckert, H., Arahama, V., Graef, G., Grusak, M.A. and Clemente, T. 2006. Molecular and phenotypic characterization of transgenic soybean expressing the *Arabidopsis* ferric chelate reductase gene, *FRO2*. Planta 224:1116-1128

Vert, G., Barberon, M., Zelazny, E., Seguela, M., Briat, J.F. and Curie, C. 2009. *Arabidopsis IRT2* cooperates with the high-affinity iron uptake system to maintain iron homeostasis in root epidermal calls. Planta 229:1171-1179

Vert, G., Briat, J.F. and Curie, C. 2001. *Arabidopsis IRT2* gene encodes a root-periphery iron transporter. Plant J. 26:181-189

Vert, G., Grotz, N., Dedaladechamp, F., Gaymard, F., Guerinot, M.L., Briat, J.F. and Curie, C. 2002. *IRT1*, an *Arabidopsis* transporter essential for iron uptake from soil and for plant growth. Plant Cell 14:1223-1233

Wang, H.Y., Klatte, M., Jakoby, M., Baumlein, H., Weisshaar, B. and Bauer, P. 2007. Iron deficiency-mediated stress regulation of four subgroup Ib *bHLH* genes in *Arabidopsis thaliana*. Planta 226:897-908

Wang, L., Cui, Y., Liu, Y., Fan, H., Du, J., Huang, Z., Yuan, Y., Wu, H. and Ling, H.Q. 2013. Requirement and Functional Redundancy of Ib subgroup *bHLH* proteins for iron deficiency responses and uptake in *Arabidopsis thaliana*. Mol. Plant 6:503-513

Waters, B.M., Blevins, D.G. and Eide, D.J. 2002. Characterization of *FRO1*, a pea ferric-chelate reductase involved in root iron acquisition. Plant Physiol. 129:85-94

Waters, B.M. and Sankaran, R.P. 2011. Moving micronutrients from the soil to the seeds: Genes and physiological processes from a biofortification perspective. Plant Sci. 180:562-574

Waters, B.M., Lucena, C., Romera, F.J., Jester, G.G., Wynn, A.N., Rojas, C.L., Alcantara, E. and Perez-Vicente, R. 2007. Ethylene involvement in the regulation of the H(+)-ATPase *CsHA1* gene and of the new isolated ferric reductase *CsFRO1* and iron transporter *CsIRT1* genes in cucumber plants. Plant Physiol. Biochem. 45:293-301

Wu, H., Li, L., Du, J., Yuan, Y., Cheng, X. and Ling, H.Q. 2005. Molecular and biochemical characterization of the Fe(III) chelate reductase gene family in *Arabidopsis thaliana*. Plant Cell Physiol. 46:1505-1514

Xiong, H., Guo, X., Kobayashi, T., Kakei, Y., Nakanishi, H., Nozoye, T., Zhang, L., Shen, H., Qiu, W., Nishizawa, N.K. and Zuo, Y. 2014. Expression of peanut iron regulated transporter 1 in tobacco and rice plants confers improved iron nutrition. Plant Physiol. Biochem. 80:83-89

Xu, H.M., Wang, Y., Chen, F., Zhang, X.Z. and Han, Z.H. 2011. Isolation and characterization of the iron-regulated MxbHLH01 gene in *Malus xiaojinensis*. Plant Mol. Biol. Report 29:936-942

Yin, L., Wang, Y., Yuan, M., Zhang, X., Pan, H., Xu, X. and Han, Z. 2013. Molecular cloning, polyclonal antibody preparation, and characterization of a functional iron-related transcription factor *IRO2* from *Malus xiaojinensis*. Plant Physiol. Biochem. 67:63-70

Yin, L., Wang, Y., Yuan, M., Zhang, X., Xu, X. and Han, Z. 2014. Characterization of *MxFIT*, an iron deficiency induced transcriptional factor in *Malus xiaojinensis*. Plant Physiol. Biochem. 75:89-95

Yuan, Y, Wu, H., Wang, N., Li, J., Zhao, W., Du, J., Wang, D., Ling, H.Q. 2008. *FIT* interacts with *AtbHLH38* and *AtbHLH39* in regulating iron uptake gene expression for iron homeostasis in *Arabidopsis*. Cell Res. 18:385-397

Yuan, Y., Zhang, J., Wang, D.W. and Ling, H.Q. 2005. *AtbHLH29* of *Arabidopsis thaliana* is a functional ortholog of tomato *FER* involved in controlling iron acquisition in strategy I plants. Cell Res. 15:613-621

CHAPTER III. PHYSIOLOGICAL ANALYSIS OF IRON CHLOROSIS IN *POPULUS TREMULA* L. 'ERECTA'

Abstract

Two trees of *Populus tremula* L. 'Erecta' grown close to each other have contrasting phenotypes. One tree grows normally with green leaves during the growing season (PtG). The other tree has interveinal chlorotic leaves (PtY). Leaf chlorosis with green veins indicated that the chlorosis might be caused by iron deficiency. Soil tests revealed that the soil at the tree site is slightly alkaline with no significant variations in mineral elements around the trees. Leaf analysis showed that differences in physiological parameters including leaf dry weight, content of chlorophyll and carotenoids, Chl a/b ratio, and content of Zn and Fe were significant between PtG and PtY trees. Ferric reductase activity in the root revealed that PtG and PtY had a similar ferric reduction capacity and PtY showed more sensitivity to changes in pH. A hydroponic system was established for the iron deficiency treatment. Leaf analysis of the hydroponic plants showed differences in chlorophyll, carotenoid, and Chl a/b ratio between PtG and PtY under the iron deficient condition; however, no significant difference in leaf dry weight was found. Under iron deficiency, a significant increase in Zn in both trees was detected and Cu content was lower in PtG than in PtY. A significant decrease in Fe content was observed in both PtG and PtY trees and Fe content was significantly lower in PtY than in PtG, suggesting that the contrasting phenotypes of PtG and PtY might be due to their different tolerance to iron deficiency.

Introduction

Leaf chlorosis refers to yellowing of healthy leaves due to abnormal chlorophyll synthesis. Chlorophyll is the site of photosynthesis, therefore, leaf chlorosis will cause reduced plant growth and yield. In fruit trees, chlorotic plants often produce smaller fruits with poor

quality and severe chlorosis may cause tree death. Plant chlorosis can be induced by the deficiency of certain nutrients, such as iron (Fe), zinc (Zn), and nitrogen (N). There are two major reasons that may cause plant nutrient deficiency: lack of nutrients in the soil and the low availability of nutrients to the plant. A few causes may trigger inability of a plant to uptake nutrients from the soil, including root injury, compact soil, waterlogging, and high soil pH (alkaline soil) (Schuster, 2008). Different nutrient deficiencies result in different chlorosis symptoms. For example, old and mature leaf chlorosis may be caused by nitrogen deficiency, interveinal chlorosis can be caused by either iron or zinc deficiency and leaf marginal chlorosis may be caused by calcium deficiency (Taiz and Zeiger, 2010). Nutrient deficiency can be diagnosed by visual symptoms; however, a leaf or soil test is often used to distinguish various symptoms of nutrient deficiency and to interpret how the nutrient deficiency occurred.

Two clonal trees of *Populus tremula* L. 'Erecta' with contrasting phenotypes were found on the North Dakota State University (NDSU) campus. According to the interveinal chlorosis symptom, we have hypothesized that leaf chlorosis of the trees is caused by iron deficiency. The tree with green leaves might be a natural mutant tolerant to iron chlorosis, while the tree with chlorotic leaves could be a wild type that is sensitive to iron deficiency. In this study, soil and leaf analyses were conducted to investigate the physiological differences that may contribute to the contrasting phenotype. A tissue culture system and a hydroponic system for the two genotypes were established to facilitate research on their responses to iron deficient and sufficient conditions.

Materials and methods

Plant materials

Upright European aspen (*Populus tremula* L. 'Erecta') was used in the study. Two trees of 'Erecta' grown close to each other (3 meters apart) on the NDSU campus have contrasting phenotypes. One tree grows normally with green leaves during the growing season (PtG). The other tree has leaves with interveinal chlorosis (PtY) (Figure 3.1a-b).

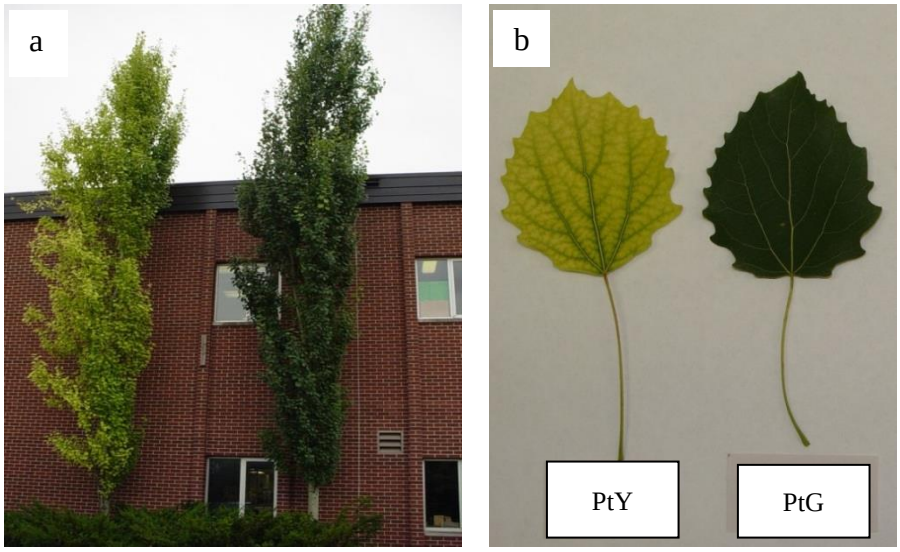

Figure 3.1. Two trees of *Populus tremula* L. 'Erecta' with contrasting leaf phenotypes as grown in the field.

Establishment of a tissue culture system

Dormant apical buds were collected from PtG and PtY in August, 2009. Buds were washed with running tap water overnight. The bud scales were excised and subsequently surface sterilized in 70% ethanol (v/v) for one min, followed by 12% Clorox bleach (v/v) (0.6% sodium hypochlorite) for 10 min and rinsed four times with sterile distilled water. Surface sterilized buds were inserted in MS (Murashige and Skoog, 1962) basal medium supplemented with MS vitamins, 3% sucrose, and 0.65% agar in a 100 ml baby-food jar with 25 ml medium. The

medium pH was adjusted to 5.8 before autoclaving. Additionally, thidiazuron (TDZ) at 1.0 μM was added to the medium for bud dormancy relief and shoot initiation. To control contamination, 1 ml PPM (Plant Preservative Mixture, PCT, Inc., Jefferson Place, Washington DC) was added per liter of medium. Cultures were placed in the culture room at 25 ± 2°C under cool-white fluorescent light at 36 μmol m^{-2} s^{-1} with a 16/8 h photoperiod. All experiments in this study were performed under these conditions unless otherwise noted. After initiation, three basal media, MS, Woody Plant Medium (WPM) (Lloyd and McCown, 1980) and Driver and Kuniyuki Walnut (DKW) (Driver and Kuniyuki, 1984), supplemented with BA at 0, 1.25, 2.5, 5.0 μM were tested for shoot proliferation. MS and DKW media were supplemented with MS vitamins, 3% sucrose, 0.65% agar and the pH was adjusted to 5.8 before autoclaving. WPM medium was supplemented with 2.0% sucrose, 0.65% agar and the pH was adjusted to 5.2 before autoclaving. Twenty-five milliliter of medium was poured into each of the 100 ml baby-food jars. In vitro shoots (1-1.5 cm long) were inserted into the medium for shoot proliferation. Each treatment had three jars with 3–4 shoot explants in each jar. The number of explants forming new shoots and the number of responding explants forming more than five new shoots were recorded. Proliferated shoots (>2.5 cm long) were excised and placed vertically into rooting medium. Five media (MS, ½ MS, DKW, ½ DKW, and WPM) containing 0.5 μM NAA were compared for in vitro rooting. Each treatment had five magenta boxes with three shoots per box. All rooting cultures were kept in the culture room. After 4 weeks, rooting percentage and the number of shoots forming more than five roots were recorded. The experiment was conducted as a completely randomized design (CRD) and repeated three times.

Establishment of a hydroponic culture system

A hydroponic system was set up in the culture room to control the growth condition of plants, as shown in Figure 3.2. The growth conditions were 25 ± 2°C, cool-white fluorescent light at 36 μmol m^{-2} s^{-1}, and a 16/8 h photoperiod. The hydroponic system was comprised of black plastic containers (42 × 34 × 13 cm) with 30-hole PVC plate covers, hydroponic nutritional solution, and air pumps. Black containers were used to prevent the growth of algae and light destruction of hydroponic solutions. The PVC plate cover was placed on the top of the container and 1 cm away from the surface of hydroponic solution that prepared according to Hoagland and Arnon (1939). Each container contained seven liters of hydroponic solution. The hydroponic solutions were aerated with an air pump (TOPFIN Aquarium Air Pump, Model: AIR-8000) and air stones (Blue Ribbon® Blu-Mist™ 12'' Air Stone, Model: 206) and were refreshed every week. In vitro plants with roots being trimmed to 1-2 mm long were transplanted into the hydroponic system. Each hole of a plate cover contained one individual plantlet. The container was then covered by plastic film to maintain the moisture. For acclimation, film was gradually removed from the container after one week.

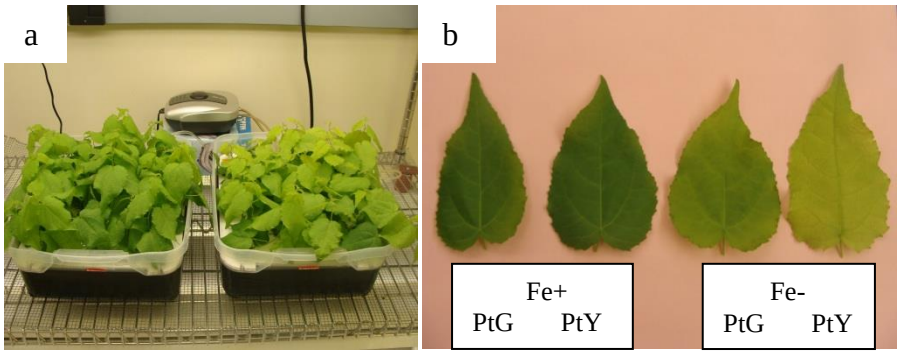

Figure 3.2. Acclimated in vitro plants of *Populus tremula* L. 'Erecta' grown in a hydroponic system under iron sufficient (Fe+) or iron deficient (Fe-) conditions.

Field soil test

Soil samples were collected from three sites of the tree-growing area in three depths (0-12, 12-24, and 24-48 inches) in June, 2012. After being air dried, samples were subjected to tests in the Soil Testing lab at NDSU. Soil pH, calcium carbonate equivalent (CCE), and mineral elements (Zn, Fe and Cu) were determined. Each samples had two runs as two replicates.

Leaf test

Sample collection

For the field-grown trees, leaves were collected in mid-May, late-June, and mid-August, representing samples from the early (E), mid (M), and late (L) stages of a growing season. Leaf sampling was repeated in 2011 and 2012. Leaves in the middle portion of the current-year branches that were located outside the tree crown were collected (3-5 branches each tree). All collected leaves were cut to small pieces (1-2 cm^2), well mixed, and divided into three samples (replicates) for leaf tests.

The hydroponic system was used to evaluate the physiological responses of PtG and PtY to iron deficiency. The iron deficient treatment was performed by adding 200 µM ferrozine [3-(2-pyridyl)-5,6-diphenyl-1,2,4-triazine sulphonate] (HACH Chemical Co., Ames, IA) into iron-free hydroponic solution. Plants grown under full strength of hydroponic solution containing 30 µM Fe(II)-EDTA was considered as the iron sufficient treatment. Leaves were collected from the middle portion of the 28-day-old hydroponic plant. Each treatment had five individual plants and was repeated three times.

Leaf dry matter content

Leaf dry matter content (DMC) was calculated as dry weight using the equation: DMC=DW/FW×100%, where DW is dry leaf weight and FW is fresh leaf weight. Leaf fresh

weight was recorded immediately after leaves were removed from the tree and leaf dry weight was recorded after leaves were oven-dried at 65 °C for 2 days.

Chlorophyll content

Leaf chlorophyll a (chl a), chlorophyll b (chl b), and carotenoids (xanthophylls and β-carotene) were determined in this study. Chlorophyll was extracted from leaves according to the method of Lichtenthaler (1987). In brief, fresh leaves were ground into powder in liquid nitrogen using pestle and mortar. About 0.2 g leaf powder was transferred to a 2.0 ml centrifuge tube containing 1.8 ml of 80% acetone and then vortexed for 10 s. The sample tube was placed in a 4°C refrigerator for >12 h and centrifuged at 10,000 rpm for 8 min. The absorbance of the mixture of 20 µl extraction (supernatant) and 980 µl of 80% acetone was measured at 470 nm, 646.8 nm, and 663.2 nm using a BECKMAN DU-600 spectrophotometer (Beckman Coulter Inc. CA). The 80% acetone was used as a blank (reference) for the spectrophotometer. The content of chlorophyll in the cuvette (test cont.) was calculated as described by Lichtenthaler (1987): Chl a = 12.25A663.2-2.79A646.8; Chl b = 21.50A646.8-5.10A663.2; Chl a+b=7.15A663.2+18.71A646.8; Carotenoids = (1000A470-1.82Chl a-85.02Chl b)/198. The final content of chlorophyll was expressed in mg/kg fresh leaf using the equation: Final content = test cont.×1000×1.8/20/fresh leaf weight.

Leaf mineral element content

The dried leaf powders were sent to the NDSU Cereal Science lab for the analysis of mineral elements. A standard HNO_3-H_2O_2 digestion method was employed as described by Alcock (1987). Mineral element contents were measured by AAS (Atomic Absorption Spectrometry) on a Varian SpectrAA150 (Varian Canada, Inc., Mississauga, Ontario, Canada) as described by Thavarajah et al. (2009).

Ferric reductase activity

Ferric reductase activity (FRA) in the hydroponic plants under iron sufficient and deficient conditions was determined. Plants were grown in the iron sufficient solution [30µM Fe(III)-EDTA] or in the iron deficient solution [1µM Fe(III)-EDTA] for 28 days before the sampling. All roots and leaves in the middle port of the plant were collected separately. Each treatment had three replicates with 3-4 individual plants per replicate.

Ferric reductase activity in the root or leaf was measured based on the intensity of the purple Fe(II)-ferrozine complex according to Gibbs (1976) and Yi and Guerinot (1996). A standard curve was developed using a serial dilution of Fe(II)-EDTA. In brief, a serial amount of Fe(II)-EDTA (30 µM) from 0 to 50 µl in increments of 5 were added into the assay solution containing 0.1 mM Fe(III)-EDTA and 0.3 mM ferrozine with pH 5.5 or 8.0. The total volume of the reaction was 40 ml. After 30 min, reaction solutions were subjected to the absorbance measurement at 562 nm (A_{562}) using a SPECTRONIC 20D+ spectrophotometer (Thermo Electron Scientific Instruments LLC, Madison, WI, UAS). Each solution was read three times. The average of three reads was used to calculate the linear regression line. Harvested roots and leaves were rinsed with ddH_2O three times and blotted dry with a paper tower. Each root or leaf sample was divided into two subsamples and weighed. One set of subsamples was submerged in 40 ml assay solution at pH 5.5, while the other set was submerged in 40 ml assay solution at pH 8.0. The mixtures (leaf or root tissue + assay solution) were shaken in the dark at 70 rpm for 30 min. Leaf or root tissues were removed from the reaction solution. The absorbance of the assay solution was measured three times at 562 nm using a SPECTRONIC 20D+ spectrophotometer. An aliquot of the assay solution that had no roots or leaves was used as blank. The amount of

Fe(II) produced was calculated using the standard curve. The result was expressed in mol Fe(II)-EDTA produced per g fresh weight (FW).

Statistics

Data obtained from all experiments were presented as the means ± SE of three replicates and subjected to analysis of variance (ANOVA) using the GLM procedure of SAS software Version 9.1 (SAS Institute 2004).

Results

Tissue culture of *Populus tremula* L. 'Erecta'

A tissue culture system of *P. tremula* L.'Erecta' was established (Figure 3.3). A significant effect of both medium and BA on shoot proliferation was observed. The best combination of medium and BA for shoot proliferation was MS with 2.5 μM BA, in which 97.2% of explants formed new shoots and 77.1% of responding explants developed more than five shoots (Figure 3.3 a) (Table 3.1).

In vitro shoots greater than 2.5 cm in length were transferred to the rooting medium. The medium type had no significant effect on the rooting rate, but showed significant effect on the percentage of responding shoots forming more than five roots (Table 3.2). All shoots in ½ DKW medium supplemented with 0.5 μM NAA produced roots, followed by DKW, ½ MS, WPM, and MS with the rooting rate of 94.4%, 93.6%, 80%, and 54%, respectively. It was noted that lowering medium salt concentration increased the number of shoots with more than five roots produced. Around 80% of shoots produced more than five roots per responding shoot in ½ DKW and ½ MS media, while only 0, 24.1%, and 16.7% of responding shoots had more than five roots developed in full strength DKW, MS, and WPM media, respectively. In addition, roots were

induced 2 weeks earlier in the ½ strength medium compared to the full strength medium. The best medium for rooting was ½ strength MS with 0.5 µM NAA (Figure 3.3 b-c).

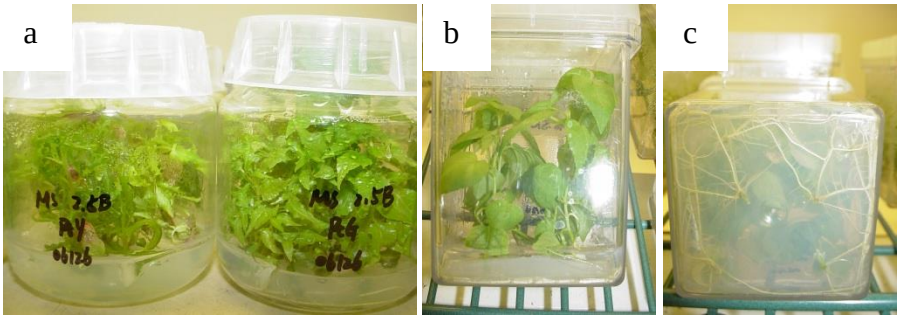

Figure 3.3. In vitro plants of *Populus tremula* L. 'Erecta' used in this study. a: shoots were proliferated in MS medium with 2.5 µM BA; b-c: in vitro shoots were rooted in ½ strength MS medium with 0.5 µM NAA.

Table 3.1. Effects of medium and BA on shoot proliferation rate (SPR) and percentage of explants having more than five new shoots (PEMFS) *of Populus tremula* L.'Erecta' [z].

Medium	SPR (%)	PEMFS (%)
MS	10.7	0
MS + 1.25 µM BA	95.6	60.9
MS + 2.5 µM BA	97.2	77.1
MS + 5.0 µM BA	73.8	56.3
DKW	2.6	0
DKW + 1.25 µM BA	71.3	37.5
DKW + 2.5 µM BA	47.4	25.7
DKW + 5.0 µM BA	41.8	25
WPM	5.1	0
WPM + 1.25 µM BA	70.9	48.4
WPM + 2.5 µM BA	86.3	27.1
WPM + 5.0 µM BA	80.6	10.7

[z] Data are presented as means of three replicates.

Table 3.2. Effects of medium on in vitro rooting rate (IRR) and percentage of shoots forming more than five roots (PSMFR) of *Populus tremula* L.'Erecta' [z].

Basal medium	IRR (%)	PSMFR (%)
½ DKW	100	78.6
DKW	94.4	0
½ MS	93.6	86.9
MS	54	24.1
WPM	80	16.7

[z] Data are presented as means of three replicates.

A hydroponic culture system for *Populus tremula* L. 'Erecta'

All plants were surviving after two weeks of the acclimation process. Plants showed significant growth in the third week and the root system was completely recovered. An average of 6-8 expanded leaves were seen on each plant. Leaves were showing yellow only after one week of culture in the iron deficient hydroponic solution containing 200 µM ferrozine (Figure 3.2).

Soil test

Soil pH and calcium carbonate equivalent

The pH in the soil where PtG and PtY were grown was 7.42 - 7.88, indicating that the soil was slightly alkaline based on the soil classification of the United States Department of Agriculture Natural Resources Conservation Services (Soil survey division staff, 2011). No significant changes in pH among three layers (depth) of the soil were observed, but the soil of site 2 showed a slightly lower pH than the other two soil sites (Table 3.3).

The soil CCE showed variations in sites and layers (depths) (Table 3.3). The soil in site 2 showed the lowest CCE% value. The CCE value was similar between layers 1 and 2 (0-24"), but

significantly lower in layer 3 (24-48"). Significant differences in CCE were also observed among three sites in layer 2.

Table 3.3. The pH and CCE of the field soil in three sites and three soil layers[z].

	pH			CCE (%)		
	soil depth (inches)					
	0-12	12-24	24-48	0-12	12-24	24-48
Site 1	7.61	7.87	7.56	5.75	6.70	4.95
Site 2	7.58	7.51	7.42	4.70	4.80	1.07
Site 3	7.63	7.85	7.58	5.80	8.35	2.85

[z] Data are presented as means of two replicates.

Soil mineral element contents

Variations in the mineral element content were observed at different sites and in different layers of the soil (Figure 3.4). Different elements showed different patterns of distribution in the soil. The top layer of soil (0-12″) contained significantly higher Zn than the other two layers of soils; however, the deep layer of soil (24-48″) showed higher Fe content than other layers. Compared to other sites, site 2, particularly in the top 2 layers (0-24″), contained significantly higher concentrations of all three elements. The Zn concentration at site 2 reached 40.4 mg/kg DW (dry weight), while it was only 1.61 mg/kg DW at site 3. The Fe concentration at site 2 was also relatively higher than the other two sites in the top two layers (0-24″). The other two sites (1 and 3) showed similar Fe concentration in layer 1 (14.60 and 13.75 mg/kg soil) and layer 2 (11.55 and 12.20 mg/kg soil).

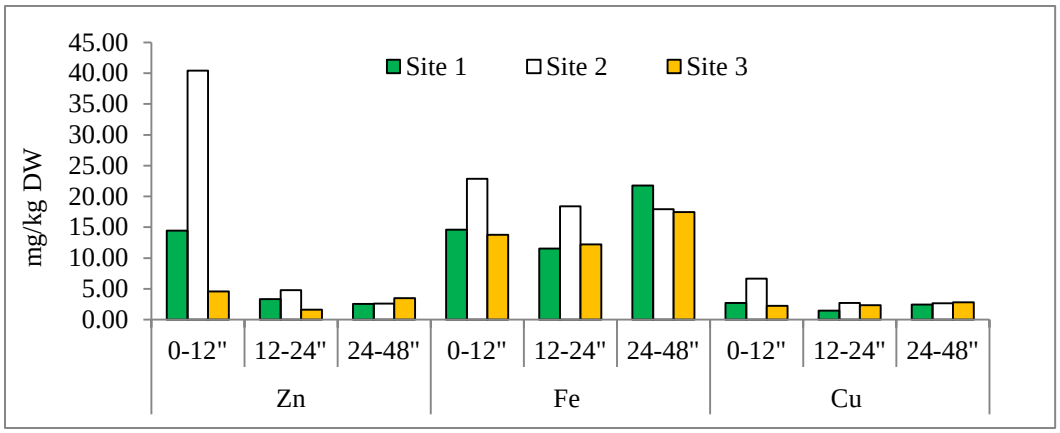

Figure 3.4. Mineral element contents in the soil collected from three sites and three soil layers. Data is presented as means of two replicates.

Leaf test of the field-grown trees

Leaf dry matter content

Leaf dry matter content (DMC) was from 23.30 to 44.95% for PtY and from 35.72 to 50.53% for PtG tree (Figure 3.5). The DMC of PtG and PtY sharply increased in the early and middle growing stages and maintained the same level in the late growing stage. Even though there is a slight difference, the pattern of DMC showed consistence among three years. ANOVA analysis revealed that the DMC was significantly different between PtG and PtY ($p < 0.001$) (Table 3.4). Compared to PtY, PtG had a significantly higher DMC in the whole growing season in two years (2011-2012), which indicated that PtG accumulated more biomass than PtY.

Leaf chlorophyll content

Total chlorophyll (a+b) content showed a significant difference in PtG and PtY (Figure 3.6) across years. PtG had relatively constant chlorophyll content in the whole growing season of both 2011 and 2012. In PtY, the chlorophyll content first increased in the middle growing stage and then decreased in the late growing stage of 2011, and it decreased from the early to the late growing stage in 2012. A similar pattern of change for carotenoids content in three stages of a

growing season was observed (Figure 3.7). The Chl a/b ratio in PtG was stable ranging 2.86-3.10 in the whole study. In PtY, the Chl a/b ratio was significantly increased in the middle (2012) and late growing stages (2011 and 2012), ranging 3.13-4.15 (Figure 3.6). ANOVA showed that the contents of chlorophyll and carotenoids and the Chl a/b ratio were significantly different in PtG and PtY (Table 3.4). Significantly higher contents of chlorophyll and carotenoids and significantly lower Chl a/b ratio were observed in PtG compared to PtY.

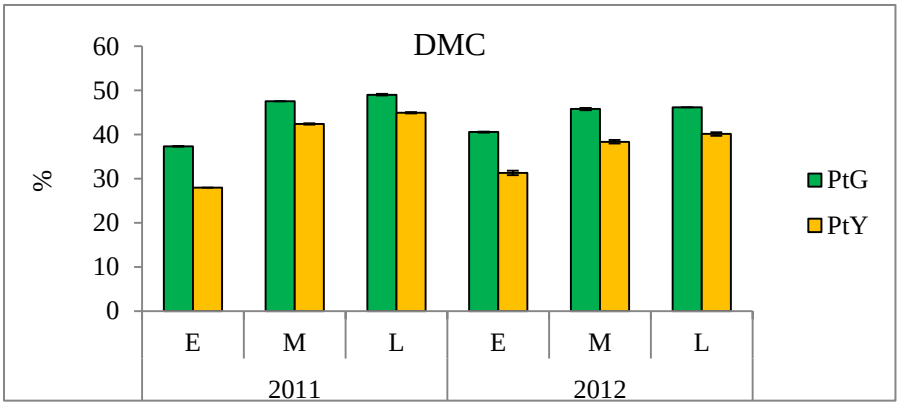

Figure 3.5. Leaf dry matter content (DMC) of the field-grown PtG and PtY trees in three stages of a growing season in year 2011 and 2012. E, M and L stand for the early, middle, and late stages of growing season, respectively. Values are means of three replicates and standard errors are indicated as a vertical line of the top of each bar.

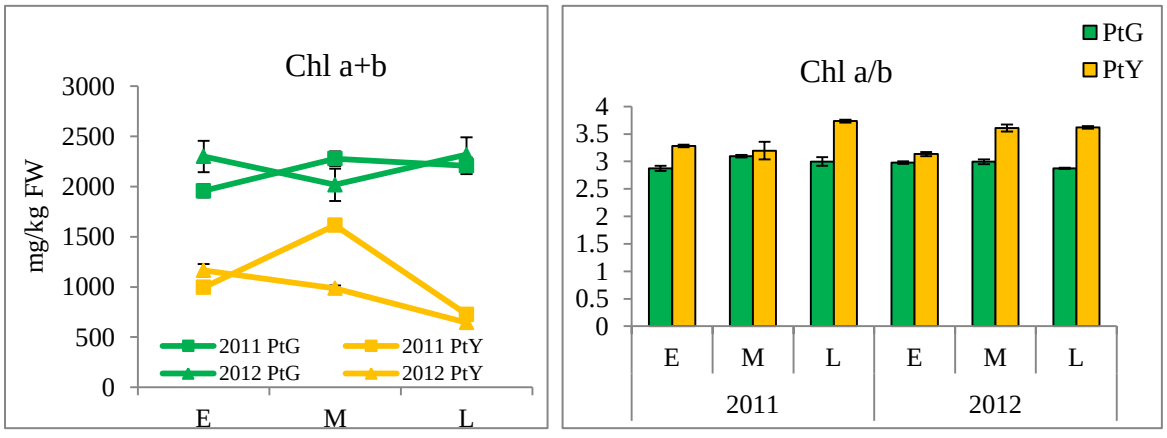

Figure 3.6. Chlorophyll content and Chl a/b ratio of the field-grown PtG and PtY in three stages of a growing season in year 2011 and 2012. E, M and L stand for the early, middle, and late stages of growing season, respectively. Values are means of three replicates and standard errors are indicated as a vertical line of the top of each bar.

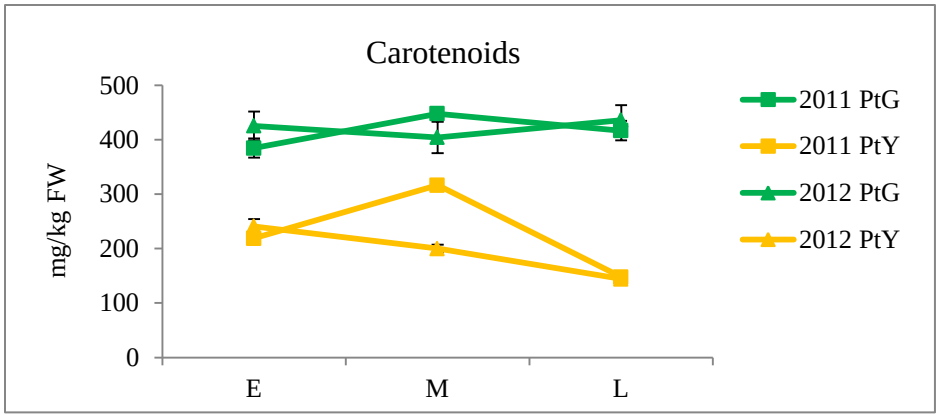

Figure 3.7. Carotenoid content of the field-grown PtG and PtY in three stages of a growing season in year 2011 and 2012. E, M and L stand for the early, middle, and late stages of a growing season, respectively. Values are means of three replicates and standard errors are indicated as a vertical line of the top of each bar.

Leaf mineral element content

As shown in Figure 3.8, Zn content significantly increased from the early to middle and late growing stage in both years (2011 and 2012). In PtY, Zn content peaked in the middle growing stage in 2011 and in the late growing stage in 2012. The Fe content was continuously increasing during the growing season in 2011. In 2012, Fe content decreased in the late growing stage. The Cu content reached its peak in the middle growing stage and then dramatically decreased in the late growing stage. PtG had the same pattern of mineral element content change in three stages of a growing season of both years. According to the ANOVA analysis, the Zn and Fe content were significantly different between PtG and PtY at the level of 0.05 and 0.001, respectively. Compared to PtY, PtG showed a significantly higher content of Zn across the growing stages and years. A significant difference in Fe content between PtG and PtY was found in the early growing stage of 2011 and the middle and late growing stage of 2012. No significant difference in Cu content was found between PtG and PtY.

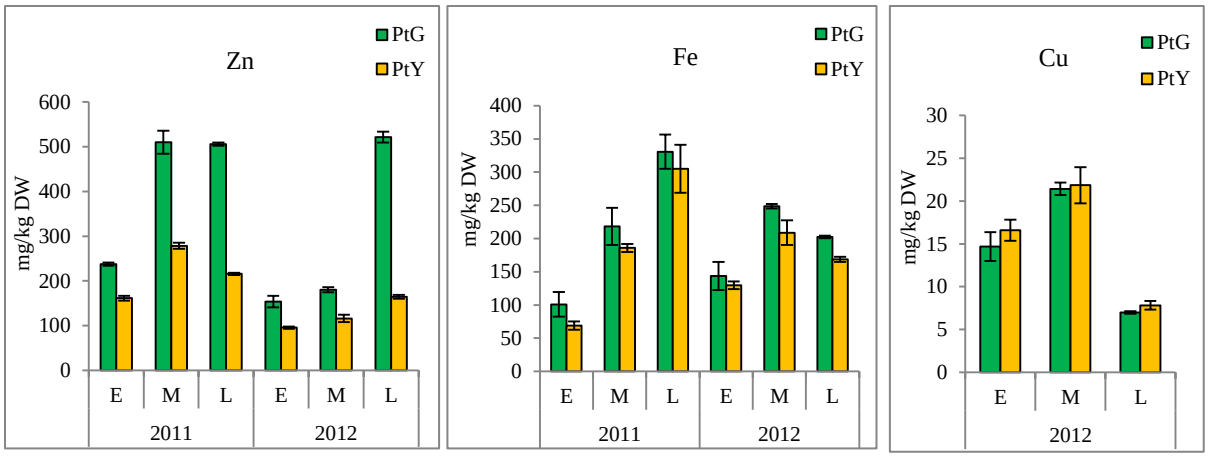

Figure 3.8. Mineral element (Fe, Zn and Cu) content of the field-grown PtG and PtY in three stages of a growing season in year 2011 and 2012. E, M and L stands for the early, middle, and late stages of a growing season, respectively. Values are means of three replicates and standard errors are indicated as a vertical line of the top of each bar.

Table 3.4. Analysis of variance (ANOVA) of physiological parameters of the field-grown PtG and PtY trees in three stages of a growing season in year 2011 and 2012 [z].

	DMC	Chl a+b	Chl a/b	Caro	Fe	Zn
Genotype	***	***	***	***	*	***
Stage	***	*	**	**	***	***
Genotype × Stage	***	**	**	**	ns	***
Year	***	ns	ns	ns	ns	***
Year × Genotype	***	ns	ns	ns	ns	*
Year × Stage	***	**	ns	**	***	***
Year × Genotype × Stage	*	ns	**	ns	ns	***

[z] Data are presented as means ±SE (n=3)
DMC: leaf dry matter content; Chl: chlorophyll; Caro, carotenoids.
*, **, ***: the significant differences at p< 0.05, 0.01, and 0.001, respectively.
ns; nonsignificant differences at p<0.05.

Leaf test of the hydroponic trees responding to iron deficiency

Leaf dry matter content

The leaf dry matter content (DMC) of PtG and PtY grown in the hydroponic system under iron sufficient or deficient conditions showed no significant difference (Table 3.5), suggesting that the DMC was not affected by iron status in a short period of iron deficiency in the hydroponic culture.

Leaf chlorophyll content

The chlorophyll (a+b) and carotenoids were significantly reduced by iron deficiency in the hydroponic PtG and PtY plants (Table 3.5). The Chl a/b ratio was not affected by the iron status. Under the iron sufficient condition, no significant differences in chlorophyll and carotenoids were found between PtG and PtY. However, under the iron deficient condition, PtG accumulated a notably higher content of chlorophyll and carotenoids than PtY. The Chl a/b ratio was higher in PtY than in PtG under both iron sufficient and deficient conditions.

Table 3.5. Leaf analysis of the hydroponic PtG and PtY plants under either the iron sufficient or deficient condition [z].

	Fe sufficiency		Fe deficiency	
	PtG	PtY	PtG	PtY
DMC (%)	14.40 ± 0.41	15.19 ± 0.61	14.50 ± 0.21	14.25 ± 0.16
Chl (a+b) (mg/kg)	2096.05 ± 22.64	2042.15 ± 7.70	1820.02 ± 28.29	1504.11 ± 40.95
Chl a/b ratio	2.33 ± 0.02	2.56 ± 0.04	2.25 ± 0.12	2.56 ± 0.03
Carotenoids (mg/kg)	377.65 ± 8.00	326.86 ± 9.77	285.96 ± 18.93	207.10 ± 5.24

[z] Data are presented as means±SE of three replicates.

Leaf mineral element content

The analysis of mineral elements in the leaf showed that under iron deficiency, Fe content significantly decreased and Zn content significantly increased, while no significant change was detected in Cu content (Figure 3.9). PtG accumulated more Fe and Zn than that of PtY under iron deficiency. Under iron sufficiency, no difference in Fe was found between PtG and PtY; however, more Zn and Cu accumulated in PtY than in PtG.

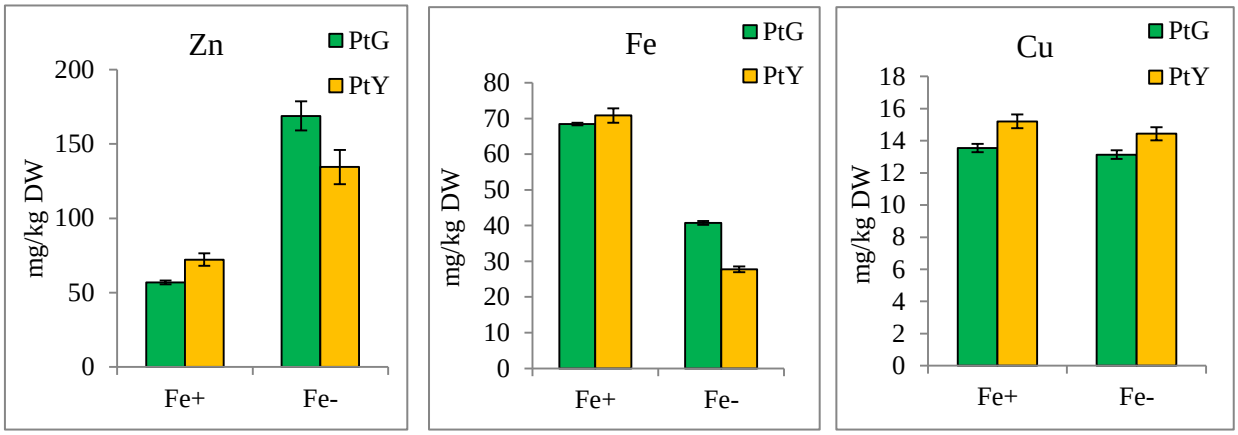

Figure 3.9. Contents of mineral element (Fe, Zn and Cu) in PtG and PtY grown in the hydroponic system under iron sufficient (Fe+) or iron deficient (Fe-) conditions. Values are means of three replicates and standard errors are indicated as a vertical line on the top of each bar.

Ferric reductase activity

Ferric reductase activity (FRA) was measured in PtG and PtY grown in the Fe(III)-EDTA solution at different pH. High pH (pH 8.0) significantly reduced the root FRA in PtYand had no effect on the root FRA in PtG under the iron sufficient condition. High pH significantly reduced the leaf FRA in PtG under both iron deficiency and sufficiency and increased the leaf FRA in PtY under iron sufficiency. Under low pH (5.5), iron deficiency decreased the root FRA in PtY and increased the leaf FRA in both PtG and PtY. Interestingly, at pH 8.0, iron deficiency showed

no effect on the leaf FRA, but increased the root FRA in both PtG and PtY. Notably, PtG showed a significantly lower root FRA at pH 5.5 and the root FRA increased with an increase of pH under the iron sufficient condition. PtY had a significantly higher leaf FRA than PtG under either iron sufficient or deficient conditions.

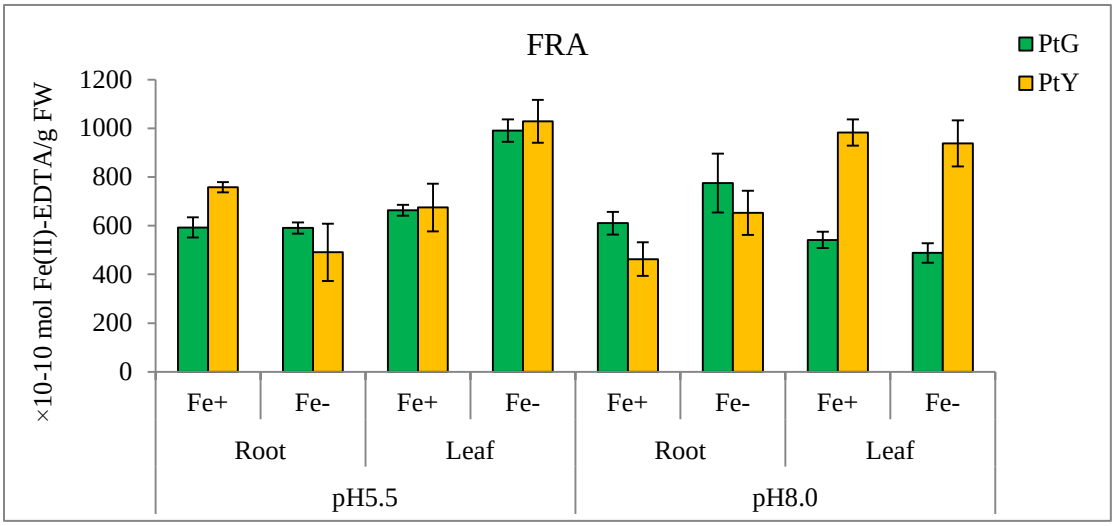

Figure 3.10. Ferric reductase activity (FRA) in PtG and PtY plants grown in the hydroponic system under iron sufficient (Fe+) or deficient (Fe-) conditions. FRA was measured by the amount of Fe(II) produced per gram fresh weight of root or leaf tissue in the assay solution with pH 5.5 or pH 8.0. Values are means of three replicates and standard errors are indicated as a vertical line on the top of each bar.

Discussion

The objective of the study was to investigate the physiological causes of leaf chlorosis in *Populus tremula* L. 'Erecta' trees. In the very early growing stage, no visible difference in leaf color was found between PtG and PtY. However, the leaves of the PtY tree soon turnd yellow with veins remaining green and the leaves on the PtG tree remained green during the whole growing season (Figure 3.1a-b). The chlorosis symptom is the result of a physiological disorder caused by deficiency of certain elements, such as Mn, K, Zn, Fe, Mg, S, and N (Taiz and Zeiger, 2010). In general, iron chlorosis appears first on young or terminal leaves and progresses to older

and lower leaves with eventual bleaching of the new growth under severe conditions (Whiting et al., 2011). In this study, analyses of the soil and leaves were conducted to diagnose possible reasons for chlorotic symptoms on the PtY tree.

Soil analysis can reveal the chemical and physical characteristics in the soil. In this study, we evaluated the pH, calcium carbonate equivalent (CCE), and the content of Zn, Fe, and Cu in the field where PtG and PtY trees were grown. Soil pH directly affects the potential availability of minerals including some beneficial nutrients and some toxic elements to plants because the solubility of a few minerals is affected by soil pH (Fageria and Barbosa, 2008; Kang et al., 2011; Anugoolprasert et al., 2012). Most minerals are more soluble or available in acid soil than in alkaline soil; therefore plant nutritional deficiencies are often avoided in soil of pH 5.5 - 6.5. The CCE value can indicate the amount of lime needed to neutralize soil acidity. In the field where PtG and PtY were grown, the soil pH was slightly alkaline (pH 7.4-7.8) (Table 3.3) and the low CCE (1.07%-8.35%) in the soil also indicated the alkaline feature of the soil. A relatively high pH and low lime requirement suggested that this soil is not ideal for dissolving micronutrients, such as Fe, Zn, and Cu. The soil test also showed that Zn content had a wide range from 1.61 to 40.40 mg/kg and the contents of Fe and Cu were ranged from 11.55 to 22.85 mg/kg and from 1.46 to 6.68 mg/kg, respectively (Figure 3.4). The mineral contents of Zn, Fe, and Cu appear to be lower than those recommended by Agricola's prediction of ideal soils for plant growth (http://www.soilminerals.com/IdealSoilII.htm). No significant difference in mineral content was observed between site 1 and site 3 except that Zn in top layer at site 1 was higher (14.45 mg/kg) than site 3 (4.60 mg/kg). Therefore, it can be concluded that there were no significant differences in the field conditions of PtG and PtY trees in this study.

Leaf tests were also conducted to investigate the cause of the contrasting phenotype of PtG and PtY. As shown in Figures 3.5, 3.6, and 3.7, PtG showed a significantly higher level in dry matter content (DMC), chlorophyll (a+b), and carotenoid content than PtY across all stages and years. In addition, the Chl a/b ratio in PtG was constant (~3.0), but varied in PtY (3.13-4.15). This indicates that the synthesis of chlorophyll in PtY might be negatively affected. Chlorophyll is an important biomolecule that allows plants to absorb energy from light for photosynthesis. The Chl a/b ratio is positively correlated with the ratio of PSII cores to light harvesting chlorophyll-protein complexes (LHCII) (Terashima and Hikosaka, 1995). The lower chlorophyll content and the higher Chl a/b ratio may result in decreased photosynthesis, which can interpret the low DMC in PtY. It was reported that deficiency of nitrogen, sulfur, zinc, or iron could influence the photosynthetic apparatus by affecting the synthesis of protein complexes in photosynthetic reactions (Abadia, 1992; Ciompi et al., 1996; Tsonev and Lidon, 2012; D'Hooghe et al., 2013). The chlorophyll synthesis was directly affected by the deficiency of N, Mg, and Fe (Lin and Stocking, 1978; Terry and Abadia, 1986; Abadia, 1992; Abadia and Abadia, 1993; Morales et al., 1994; Ciompi et al., 1996; Laing et al., 2000). Zinc could be indirectly involved in chlorophyll formation by regulating cytoplasmic concentrations of other nutrients (Kosesakal and Unal, 2009). The content of Zn, Fe, and Cu in the field-grown plants indicated that PtG had a significantly higher content of Zn and Fe than PtY (Figure 3.8). This may explain why the PtY tree had a lower content of chlorophyll.

Tissue culture and the hydroponic culture system provided a controlled environment for plant growth and development; therefore they are ideal systems for inducing chlorosis symptoms under the nutrient deficient condition. A tissue culture system was developed here to proliferate PtG and PtY plants used for the hydroponic culture. Multiple copies of PtG and PtY were grown

in a hydroponic system with or without Fe(II)-EDTA to induce iron chlorosis symptoms. Ferric chelate reductase is involved in root iron uptake and chloroplast iron acquisition (Chaney et al., 1972; Welch et al., 1993; Jeong et al., 2008; Takanori and Nishizawa, 2012). The activity of ferric chelate reductase at the plasma membrane of root epidermal cells increases when iron is deficient (Bienfait, 1985; Welch et al., 1993). By contrast, iron deficiency decreases the ferric-chelate reducing activity in leaf mesophyll protoplasts (Gonzalez-Vallejo et al., 2000). A different result was reported by Li et al. (2011) , where ferric reductase was not changed in root tissues regardless of the Fe(III)-EDTA amount, but slightly decreased in leaf tissues under the Fe(III)-EDTA sufficient condition in tobacco. Our results showed the ferric reductase activity was not changed in the root of PtG regardless of iron status and was significantly induced by iron deficiency in the leaf of both PtG and PtY under pH 5.5. Conversely, under pH 8.0 (close to the soil pH where PtG and PtY were grown), ferric reductase activity in leaves was not changed by iron status, but in roots it was slightly induced by iron deficiency.

The dry matter content, chlorophyll, and mineral element contents were also determined in hydroponically-grown PtG and PtY. No significant difference in DMC was found between PtG and PtY regardless of iron supply. The chlorophyll and carotenoid contents were significantly decreased under the iron deficient condition, which is consistent with the result of Morales et al. (2000) (Table 3.5). The iron deficiency showed no effect on the Chl a/b ratio in hydroponic plants. It is not surprising that Fe content was significantly decreased under the iron deficient condition. However, acquisition of other ions is also affected by iron deficiency. Welch et al. (1993) reported that the concentrations of a few divalent cations, such as Cu, Mn, and Mg, increased in the shoot of iron deficient pea seedlings. Cohen et al. (1998) presented that iron deficiency might facilitate the transport of heavy-metal divalent cations, such as Cd and Zn.

Martinez-Cuenca et al. (2013) also reported that Zn and Mn content was significant increased under the iron deficient condition in woody plants. In this study, Zn content was significantly increased in *Populus tremula* under iron deficiency; however, Cu content was not affected by iron status. Meanwhile, we also observed that PtY accumulated less Zn and Fe and more Cu than PtG under iron deficiency, indicating that the capability of PtY to uptake some divalent cations might be inhibited by certain factors.

In conclusion, the leaf and soil test revealed that iron deficiency existed in the field and PtG and PtY trees were undergoing nutrient deficiency mainly due to the high soil pH. The lower content of dry matter, chlorophyll, carotenoid, Zn, and Fe in PtY tree indicates that PtY is more susceptible to iron chlorosis than PtG. The hydroponic culture further verified that PtY was more sensitive to iron deficiency. Thus, we predicted that the contrasting phenotypes of PtG and PtY were caused by their different sensitivity/tolerance to iron deficiency.

References

Abadia, J. 1992. Leaf responses to Fe deficiency. J. Plant Nutr. 15(10):1699-1713

Abadia, J. and Abadia, A. 1993. Iron and plant pigments. In: Barton LL and Hemming BC (eds) Iron Chelation in Plants and Soil Microorganisms, pp 327-344. Academic Press, San Diego, California.

Alcock, N.W. 1987. A hydrogen-peroxide digestion system for tissue trace-metal analysis. Biol. Trace Elem. Res. 13:363-370

Anugoolprasert, O., Kinoshita, S., Naito, H., Shimizu, M. and Ehara, H. 2012. Effect of low pH on the growth, physiological characteristics and nutrient absorption of Sago Palm in a hydroponic System. Plant Prod. Sci. 15:125-131

Bienfait, H.F. 1985. Regulated redox processes at the plasmalemma of plant root cells and their function in iron uptake. J. Bioenerg. Biomembr. 17:73-83

Chaney, R.L., Brown. J.C. and Tiffin, L.O. 1972. Obligatory reduction of ferric chelates in iron uptake by soybean. Plant Physiol. 50:208-213

Ciompi, S., Gentili, E., Guidi, L. and Soldatini, G.F. 1996. The effect of nitrogen deficiency on leaf gas exchange and chlorophyll fluorescence parameters in sunflower. Plant Sci. 118:177-184

Cohen, C.K., Fox., T.C., Garvin, D.F. and Kochian, L.V. 1998. The role of iron-deficiency stress responses in stimulating heavy-metal transport in plants. Plant Physiol. 116:1063-1072

D'Hooghe, P. Escanmez, S., Trouverie, J. and Avice, J. 2013. Sulphur limitation provokes physiological and leaf proteome changes in oilseed rape that lead to perturbation of sulphur, carbon and oxidative metabolisms. BMC Plant Biol. 13:23

Fageria, N.K. and Barbosa, M.P. 2008. Influence of pH on productivity, nutrient use efficiency by dry bean, and soil phosphorus availability in a non-tillage system. Commun. Soil Sci. Plant Anal. 39:1016-1025

Gibbs, C.R. 1976. Characterization and application of ferrozine iron reagent as a ferrous iron indicator. Anal. Chem. 48:1197-1201

González-Vallejo, E.B., Morales, F., Cistué, L. Abadia, A. and Abadia J. 2000. Iron deficiency decreases the Fe(III)-chelate reducing activity of leaf protoplasts. Plant Physiol. 122:337-344

Hoagland, D.R. and Arnon, D.I. 1939. The water culture method for growing plants without soil. Calif. Agr. Expt. Sta. Circ. 347

Institute SAS. 2004. SAS/STAT 9.1 user's guide. SAS Institute Inc, Cary, NC

Jeong, J., Cohu, C., Kerkeb, L., Pilon, M., Connolly, E.L. and Guerinot, M.L. 2008. Chloroplast Fe(III) chelate reductase activity is essential for seedling viability under iron limiting conditions. Proc. Natl. Acad. Sci. USA 105:10619-10624.

Kang, Y.I., Park, J.M., Kim, S.H., Kang, N.J., Park, K.S., Lee, S.Y. and Jeong, B.R. 2011. Effects of root zone pH and nutrient concentration on the growth and nutrient uptake of tomato seedlings. J. Plant Nutr. 34:640-652

Kosesakal, T. and Unal, M. 2009. Role of zinc deficiency in photosynthetic pigments and peroxidase activity of tomato seedlings. IUFS J. Biol. 68:113-120

Laing, W., Greer, D., Sun, O., Beets, P, Lowe, A. and Payn, T. 2000. Physiological impacts of Mg deficiency in *Pinus radiate*: growth and photosynthesis. New Phytol. 146:47-57

Li, L., Cai, Q., Yu, D. and Guo, C. 2011. Overexpression of *AtFRO6* in transgenic tobacco enhances ferric chelate reductase activity in leaves and increases tolerance to iron-deficiency chlorosis. Mol. Biol. Rep. 38:3605-3613

Lichtenthaler, H.K. 1987. Chlorophylls and carotenoids: pigments of photosynthetic membranes. Methods Enzymol. 148:350-382

Lin, C.H. and Stocking, C.R. 1978. Influence of leaf age, light, dark and iron deficiency on polyribosome levels in maize leaves. Plant Cell Physiol. 19:461-470

Lloyd, G. and McCown, B. 1980. Commercially-feasible micropropagation of mountain laurel, Kalmia latifolia, by use of shoot-tip culture. Proc. Int. Plant Prop. Soc. 30:421-427

Martinez-Cuenca, M., Quiñones, A., Iglesias, D. J., Forner-Giner, M. Á., Primo-Millo, E. and Legaz, F. 2013. Effect of higher levels of zinc and manganese ions on strategy I responses to iron deficiency in citrus. Plant Soil 373:943-953

Morales, F., Abadia, A., Belkhodja, R. and Abadia, J. 1994. Iron deficiency-induced changes in the photosynthetic pigment composition of field-grown pear (*Pyrus communis* L) leaves. Plant Cell Environ. 17:1153-1160

Murashige, T. and Skoog, F. 1962. A revised medium for rapid growth and bioassays with tobacco tissue culture. Physiol. Plant 15:473-497

Schuster, J. 2008. Focus on Plant Problems-Chlorosis. University of Illinois. Retrieved 2008-12-22

Soil Survey Division Staff. "Soil survey manual.1993. Chapter 3, selected chemical properties". Soil Conservation Service. U.S. Department of Agriculture Handbook 18. Retrieved 2011-03-12

Taiz, L. and Zeiger, E. 2010. Plant Physiology. 5th edition. Sinauer Associates. Sunderland, MA.

Takanori, K. and Nishizawa, N.K. 2012. Iron uptake, translocation, and regulation in higher plants. Annu. Rev. Plant Biol. 63:131-152

Terashima, I. and Hikosaka, K. 1995. Comparative ecophysiology of leaf and canopy photosynthesis. Plant, Cell Environ. 18:111-1128

Terry, N. and Abadia, J. 1986. Function of iron in chloroplasts. J. Plant Nutr. 9:609-646

Thavarajah, D., Thavarajah, P., Sarker, A. and Vandenberg, A. 2009. Lentils (*Lens culinaris* Medikus Subspeices *culinaris*): A whole food for increased iron and zinc intake. J. Agri. Food Chem. 57:5413-5419

Tsonev, T. and Lidon, F. 2012. Zinc in plants-an overview. Emir. J. Food Agric. 24:322-333

Welch, R.M., Norvell, W.A., Schaefer, S.C., Shaff, J.E. and Kochian, L.V. 1993. Induction of iron (III) and copper (II) reduction in pea (*Pisum sativum* L.) roots by Fe and Cu status: does the root-cell plasmalemma Fe(III)-chelate reductase perform a general role in regulating cation uptake? Planta 190:555-561

Whiting, D., Card, A., Wilson, C. and Reeder, J. 2011. CMG GardenNotes#223, Iron chlorosis. Colorado State University Extension. Revised April 2011

Yi, Y. and Guerinot, M.L. 1996. Genetic evidence that induction of root Fe(III) chelate reductase activity is necessary for iron uptake under iron deficiency. Plant J. 10(5):835-844

CHAPTER IV. CLONING AND CHARACTERIZATION OF THE *IRON-REGULATED TRANSPORTER* (*IRT*) GENES IN *POPULUS*

Abstract

Iron-Regulated Transporters (IRTs) play an important role in uptake and transport of iron and other metals in plants. In this research, two *IRT* genes (*PtIRT1* and *PtIRT3*) and the promoter region of the *PtIRT1* gene were cloned from the iron chlorosis sensitive (PtY) and resistant (PtG) trees of *Populus tremula* L. 'Erecta'. Nucleotide sequence analysis showed no significant difference between PtG and PtY. The predicted proteins of the *PtIRT* genes contain a conserved ZIP domain with eight transmembrane (TM) regions. A ZIP signature sequence was located in the fourth TM domain. Phylogenetic analysis revealed that *PtIRT1* was clustered with tomato and tobacco *IRT* genes that are highly responsible to iron deficiency. The *PtIRT3* gene was clustered with *AtIRT3* gene that was related to zinc and iron transport in plants. Tissue-specific expression analysis indicated that *PtIRT1* only expressed in root tissues, while *PtIRT3* constitutively expressed in the whole plant. However, the histochemical staining of transgenic tobacco with the GUS gene deriven by the native promoter of *PtIRT1* revealed that this promoter is not root specific. Under the iron deficient condition, the expression of *PtIRT1* was dramatically increased and a significantly higher transcript level was detected in PtG than in PtY. Iron deficiency was also enhancing the expression of *PtIRT3* in PtG. Differently, zinc deficiency down-regulated the expression level of *PtIRT1* and *PtIRT3* in both PtG and PtY; however, the expression of *PtIRT1* was recovered at six days after zinc deficiency treatment in PtY. It was found that zinc was significantly accumulated under the iron deficient condition, whereas the zinc deficiency showed no significant effect on Fe accumulation. The Fe content in transgenic poplar lines overexpressing *PtIRT1* and *PtIRT3* did not increase under either the iron sufficient

or deficient condition even though the gene expression level was enhanced by iron deficiency. The results suggest that *PtIRT1* might play a role in Fe uptake and contribute to the contrasting phenotypes of PtG and PtY, but its expression might be regulated through certain transcriptional factors that affect the function of its promoter.

Introduction

Iron (Fe), an essential plant nutrient, is involved in biosynthesis and functional maintenance of chlorophyll in plants (Abadia, 1992). Iron is an important component of Fe-S and heme proteins families that are involved in biological electron transfer in respiration and photosynthesis processes (Briat and Lobreaux, 1997). Meanwhile, iron is an essential nutrient for human beings and iron deficiency leads to the major human nutritional disorder of anemia, particularly in populations of children and women **(**http://www.who.int/nutrition/topics/ida/en/index.html**).**

In plants, iron deficiency causes a decrease of chlorophyll content and alteration in chlorophyll structure, resulting in plant chlorosis. Iron is sufficient in most soils; however, most iron, particularly in calcareous or alkaline soils, predominantly exists in the ferric form [Fe(III)] that is not available for plant uptake (Guerinot and Yi, 1994). The mechanism of iron acquisition by plants can be distinctly classified into two strategies. Non-graminaceous species, known as Strategy I plants, acquire Fe from the soil by transport of soluble Fe(II) that is reduced by ferric reductase. Graminaceous species, also called Strategy II plants, release iron-chelating mugineic acid family phytosiderophores (MAs) to the root surface to chelate Fe(III). The complexes of Fe(III)-MAs are then transported into roots via *YS1* (*Yellow stripe 1*) and *YSL* (*Yellow stripe 1-like*) transporters (Takagi, 1976; Römheld and Marschner, 1986; Römheld, 1987; Guerinot and Yi, 1994; Mori, 1999; Curie et al., 2001, 2009).

It has been well documented that iron uptake and transport in Strategy I plants involves two processes. One is an iron reduction process in which Fe(III) is reduced to Fe(II). This process is regulated by the genes in the *FRO* (*Ferric Reductase Oxidase*) family. The other is an Fe-transport movement that is controlled by the *IRT* (*Iron-Regulated Transporter*) genes belonging to the ZIP (zinc-regulated transporter, iron-regulated transporter-like protein) family (Guerinot, 2000; Morrissey and Guerinot, 2009; Jeong and Connolly, 2009; Water and Sankaran, 2011; Kobayashi and Nishizawa, 2012). Briefly, Strategy I plants increase the solubility of ferric ions on the root surface by excretion of proton and phenolic compounds from roots to the rhizosphere (Olsen et al., 1981; Santi, et al., 2005; Santi and Schmidt., 2009; Cesco et al., 2010). The acquirable ferrous ion is then formed by a redox reaction using ferric-chelate reductase on the root surface (Robinson et al., 1999; Wu et al., 2005; Mukherijee et al., 2006). The *IRT* transporter protein on the plasma membrane of the root epidermis/exodermis helps ferrous ion cross the membrane to the root symplast (Eide et al., 1996; Guerinot, 2000; Vert et al., 2001, 2002; Connolly et al., 2002).

The *IRT* genes, members of the ZIP metal transporter family, play an important role in iron uptake and transport in plants. Three *IRT* genes were identified from *Arabidopsis*. The *AtIRT1* was first identified by functional complementation of an iron uptake-deficiency mutant (*fet3/fet4*) in yeast; *AtIRT2* and *AtIRT3* were found and named according to their similarity to *AtIRT1* (Eide et al., 1996). *AtIRT1* and *AtIRT2* are divalent cation transporters and their expressions are specially induced in the root of iron deficient plants (Vert et al., 2001); however, only *AtIRT1* is required for iron homeostasis under the iron deficient condition because *IRT2*-insertion mutant (*irt2*) plants did not show the symptom of iron deficiency and overexpression of *AtIRT2* in *IRT1* defective mutant (*irt1-1*) plants failed to restore the wild-type phenotype

(Varotto et al., 2002; Vert et al., 2009). Recent research confirmed that *AtIRT2* does not play a significant role in iron uptake from the soil, but may be involved in intracellular Fe trafficking and co-regulation with *FRO2* and *IRT1* (Vert et al., 2009). It was further proved that *AtIRT1* expressed in the external cell layers of the root, specifically in response to iron starvation since almost no *AtIRT1* protein was detected after plants were returned to the iron sufficient condition (Connolly et al., 2002). Expression of *AtIRT2* was enhanced in the root of the *AtIRT1* defective mutant as an altered response to iron deficiency (Henriques et al., 2002). *AtIRT3* appeared to be also involved in iron uptake and transport in plants. Shanmugam et al. (2011) reported that overexpression of *AtIRT3* in the *irt1-1* mutant rescued the growth defect of *irt1-1* under iron deficiency. However, the *AtIRT3* gene may play an important role in transport of other divalent metal cations, particularly for zinc, and their homeostasis in the plant. Grotz et al. (1998) proposed that *AtIRT3* has more sequence similarity to *AtZIP4* and its mRNA was induced in zinc-limited plants. *AtIRT3* might play a role in Zn transport from the soil to the plant as its expression was increased by zinc deficiency. Such an up-regulation of *AtIRT3* in response to the zinc deficient condition was also reported by Talke et al. (2006) and Lin et al. (2009).

The *IRT* orthologs were found to be up-regulated by iron deficiency in other species including tomato (Eckhardt et al., 2001), tobacco (Hodoshima et al., 2007), cucumber (Waters et al., 2007), peanut (Ding et al., 2010), potato (Legay et al., 2012), and apple (Li et al., 2006). Unlike in *Arabidopsis*, expression of *LeIRT1* and *LeIRT2* in tomato was observed in both iron sufficient and deficient roots, with *LeIRT1* showing induction under iron deficiency (Eckhardt et al., 2001). Qu et al. (2005) reported that the transgenic *Malus robusta* overexpressing *LeIRT2* had increased iron deficiency tolerance. In potato, the expression of *IRT1* was dramatically increased under the iron deficient condition in roots (Legay et al., 2012). The *MxIRT1* gene in

Malus xiaojinensis was strongly enhanced in iron deficiency roots. Furthermore, *MxIRT1* could complement iron uptake activity in a yeast (*Saccharoomyces cerevisiae*) mutant strain DEY1453 (*fet3fet4*) (Li et al., 2006). In peanut, the *AhIRT1* gene could restore the growth of yeast mutant *fet3fet4* under the iron deficient condition and its expression was induced by iron deficiency in peanuts (Ding et al., 2010). A more recent study demonstrated that the transgenic tobacco plants overexpressing peanut *AhIRT1* accumulated more Fe and showed tolerance to iron deficiency in calcareous soils (Xiong et al., 2014).

Plants may be injured because of the oxidative stress caused by excessive Fe. The excessive Fe could promote the Fenton reaction, an iron-catalyzed reaction where hydrogen peroxide produces hydroxide and the highly reactive hydroxyl radical, which is harmful for plants (Marschner, 1995; Winterbourn, 1995). Barberon et al. (2011) reported that transgenic plants overexpressing *AtIRT1* overaccumulated some metals including iron, zinc, manganese, and cobalt, causing the oxidative stress that resulted in reduced biomass and root elongation. Plants have ways to protect themselves from iron toxicity, such as reduction of iron uptake by degrading IRT1 protein (Connolly et al., 2002) or formation of the non-toxic iron storage protein ferritin (Ravet et al., 2009; Briat et al., 2010). In *AtIRT1*-transgenic *Arabidopsis*, the *AtIRT1* protein was only detected in the root under iron deficiency, resulting in no enhancement of iron uptake when iron was sufficient. Research by Shin et al. (2013) found that *AtIRT1* was degraded by *IDF1* (*IRT1 DEGRADATION FACTOR1*) under the iron sufficient condition to inhibit the overtransport of iron in *Arabidopsis*.

Poplar is a model tree species for basic research. With the completed genome sequence of *Populus trichocarpa* available (Tuskan et al., 2006), multiple information resources and tools are ready for studying different traits using genomic approaches. Therefore, poplar is an ideal

species in which to study iron uptake and transport and response to metal deficiency stress in woody species. However, functional analysis of the *IRT* genes in woody species is rarely reported. In this study, two *IRT* genes and their promoter regions were isolated from *Populus tremula*. Sequence analysis was performed and a phylogenetic tree was constructed to characterize the features of the *PtIRT* genes. The expression profile of *PtIRTs* in both chlorotic (PtY) and normal (PtG) genotypes of *P. tremula* 'Erecta' was analyzed. Functions of the two *PtIRT* genes were analyzed by overexpressing them in another poplar species. Gene promoters of *PtIRT1* were isolated and its function was also investigated in transgenic tobacco plants.

Materials and methods

Plant materials and growth conditions

Iron deficiency sensitive (PtY) and tolerant (PtG) genotypes of European aspen (*Populus tremula* L. 'Erecta') were used in this study. An in vitro culture system was developed (Huang and Dai, 2011) and a hydroponic culture system has been set up, as described in Chapter III Material and Methods (page 34).

For the iron or zinc sufficient treatment, plants were grown in full strength Hoagland's solution containing 30 μM Fe(II)-ethylenediaminetetraacetic acid (EDTA) and 0.7 μM zinc sulfate heptahydrate ($ZnSO_4 \cdot 7H_2O$). For the iron deficient treatment, Fe(II)-EDTA was removed from Hoagland's solution and 200 μM ferrozine was added. For the zinc deficient treatment, $ZnSO_4 \cdot 7H_2O$ was removed from Hoagland's solution.

DNA/RNA extraction and cDNA preparation

Genomic DNA of PtG and PtY was extracted from leaf tissues according to the method of Lodhi et al. (1994) with some modifications that included washing ethanol-precipitated DNA with 70% ethanol in a slow moving shaker for 3-5 h before being dissolved in TE buffer and

treated with both RNase A (10 mg/ml) and Proteinase K (1 mg/ml) for another 60 min at 37 °C. The DNA concentration was determined using a NanoDrop ND-1000 Spectrophotometer (Thermo Fisher Scientific Inc., Waltham, MA, USA) and stored at 4 °C until use.

Total RNA was isolated using the QIAGEN RNeasy Plant Mini Kit (QIAGEN Inc, Valencia, CA, USA) according to the manufacturer's instructions. RNA was isolated from three biological replicates in each treatment. Prior to cDNA synthesis, the RNA was quantified using a NanoDrop ND-100 spectrophotometer (Thermo Fisher Scientific Inc., Waltham, MA, USA) and agarose gel electrophoresis. A total of 1 µg RNA was treated with gDNA wipeout buffer to eliminate possible contaminating genomic DNA and then subjected to reverse transcription with RT primer mix (oligo-dT and random primers) and unique QIAGEN Omniscript and Sensiscript reverse transcriptases according to the manufacturer's instructions of the QuantiTect Reverse Transcription Kit (QIAGEN Inc, Valencia, CA, USA).

Isolation and sequence analysis of the *PtIRT* genes

The sequence of the open reading frame (ORF) region of the *PtIRT* genes was retrieved using a homologous cloning method. To identify the *IRT* homologous genes in *P. tremula*, the ZIP domain amino acid sequences of the *Arabidopsis IRT1* gene (GeneID: 827713) were used as a query to BLASTP the whole genome sequence of *Populus trichocarpa* (taxid: 3694) in NCBI (http://blast.ncbi.nlm.nih.gov/Blast.cgi). Candidate genes, which are considered as the orthologs of the *AtIRT1* gene, were used as references to design primers for gene cloning using the PrimerSelect module of DNASTAR Lasergene® software package (DNASTAR, Inc., Madison, WI, USA). All primers are listed in Table 4.1. For gene cloning, PtG and PtY plants were transferred to the iron deficient hydroponic system for two weeks before leaf and root samples were collected. The PCR was performed according to the instruction of Elongase® Enzyme Mix

(Invitrogen™, Carlsbad, CA, USA). Target PCR products were purified using the QIAquick Gel Extraction Kit (QIAGEN Inc, Valencia, CA, USA). The purified PCR products were then cloned into the pGEM-T easy vector (Promega, Madison, WI, USA). Plasmid DNA was extracted from the white colonies grown on indicator plates containing X-gal and IPTG, using PerfectPrep™ Spin Mini Kit (5 PRIME Inc., Gaithersburg, MD, USA) and sent for sequencing at Iowa State University DNA Facility (Ames, IA, USA).

The gene structure was predicted by alignment of the cloned genomic DNA sequence and the corresponding cDNA sequence using Splign software at NCBI website (http://www.ncbi.nlm.nih.gov/sutils/splign/splign.cgi). The domain of putative proteins was analyzed using SMART online (http://smart.embl-heidelberg.de/). The prediction of transmembrane regions and orientation was performed using online TMpred (http://www.ch.embnet.org/software/TMPRED_form.html). The predicted amino acid sequences of the *PtIRT* genes and the *IRT* genes from other species were used to decipher their exact relationship. Phylogenetic analysis was conducted by the MegAlign module of DNASTAR Lasergene® software package. The phylogenetic tree was visualized with software FigTree v1.4.0.

Amplification of 5'-flanking sequences of the *PtIRT* genes

The putative promoter region of the *PtIRTs* gene was identified from the upstream genome sequence of the corresponding *PtIRT* genes in *Populus trichocarpa* (taxid: 3694) using online software TSSP (http://linux1.softberry.com/berry.phtml?topic=tssp&group=programs&subgroup=promoter). Primer design, DNA fragment isolation, cloning, and sequencing were performed as described above.

Table 4.1. List of primers used in different experiments.

Primer name	Sequence (5'-3')	Application
PtIRT1-F3	TAGCTAGAGAACCATCATCATCAAT	*PtIRT1*gene clone
PtIRT1-R3	GACTTGACAGATTCTTCCACGAG	
PtIRT3-F1	GAAGCAATCTCTAAATCAATGTCAA	*PtIRT3* gene clone
PtIRT3-R1	AACCACTAAGCTCAAGCCCAGACT	
PtIRT1-F6	AAATCCATGGCACAAGTTCC	Semi-quantitative RT-PCR for *PtIRT1*
PtIRT1-R6	GAGAGGCCTATCACAACT	
PtIRT3-F4	CATTCTCTTGGGCAGGAT	Semi-quantitative RT-PCR for *PtIRT3*
PtIRT3-R4	CCAGAAAGGGCCAAAACGAG	
PtAct1-F7	ATGGTTGGAATGGGGCAGAAG	Semi-quantitative RT-PCR internal control
PtAct1-R7	CGAAGGATGGCGTGTGGA	*PtAct1*
PtIRT1-F50	TCTCGGAGCCTCAAACAACACT	Real-time quantitative PCR for *PtIRT1*
PtIRT1-R50	AAAAATGCCATGACTGCCTTCTT	
PtIRT3-F31	GCGCACGCAGCACACCATAG	Real-time quantitative PCR for *PtIRT3*
PtIRT3-R53	GACCGTGCTCGTGCCCAGAT	
PtTIF5α -F	GACGGTATTTTAGCTATGGAATTG	Real-time quantitative PCR reference
PtTIF5α-R	CTGATAACACAAGTTCCCTGC	*PtTIF5α*
PtIRT1-ProF1	ATCCAATGTCTTACGCCTCAAT	*PtIRT1* promoter region clone
PtIRT1-ProR3	AGAAGAGGTGCACTTACCCC	
PtIRT1-ProF2	GTATCT*aagctt*AAAATCCAATGTCTTACGCCTCA	Subclone of *PtIRT1* gene promoter region
PtIRT1-ProR2	CATAGA*tctaga*TGATGATGATGGTTCTCTAG	clone

Evaluation of tissue-specific expression of the *PtIRT* genes by semi-quantitative RT-PCR

To determine the tissue-specific expression of the *PtIRT* genes, samples of the root tip, root, phloem, xylem, mature leaf, young leaf, and shoot tip were collected from PtG and PtY plants grown in the iron sufficient or deficient solution for six days. The transcripts were detected using semi-quantitative RT-PCR. Primers corresponding to the *PtIRT* gene and the *Populus* actin gene (accession no. XM_002298674.1) were designed by the module PrimerSelect of DNASTAR Lasergene® software package (Table 4.1). Prior to RT-PCR, the quality of cDNA was assessed by PCR using *actin*-specific primers designed to span introns to detect genomic DNA contamination. PCR amplification was carried out in a 16 µl reaction solution that consisted of 1.0 µl (5 ng) cDNA template, 0.375 µM of each primer, 0.2 mM dNTP, 1.5 mM $MgCl_2$, 1× GoTaq® Flexi buffer, and 5 U *Taq* DNA Polymerase. The amplification conditions were: denaturing for 30 seconds at 94 °C (3 min before the first cycle), annealing for 40 seconds at 56 °C, and extension for 50 seconds at 72 °C (5 min after the final cycle) for 30 cycles. PCR products were separated in a 2% agarose gel at 110 volts (V) for 30 min. The gel was visualized under UV light and images were captured using a AlphaImager® Gel Documentation System (ProteinSimple Inc., Santa Clara, California, USA).

Quantitative expression of the *PtIRT* genes responding to iron or zinc deficiency by real-time quantitative PCR

The expression of the *PtIRT* genes in the root of PtG and PtY plants responding to iron or zinc deficiency was quantified using an ABI 7900HT Sequence Detection System (Applied Biosystems, Foster City, CA, USA). Samples for RNA extraction were collected from PtG and PtY plants after they were transferred to the iron or zinc deficient solution for 0, 0.5, 1, 3, and 6 days. Each treatment had three biological replicates with 10 individual plants per replicate.

Gene specific primers were designed based on the sequences of the *PtIRT* genes and *PtTIF5α* (accession no: CV251327.1) was used as the internal control gene (Table 4.1). Amplification conditions were: (1) incubation at 95 °C for 5 min; (2) cDNA amplification for 35 cycles at 95 °C for 15 s, 56 °C for 20 s, and 72 °C for 30 s. To evaluate amplification specificity, melting curve analysis was performed at the end of each PCR run according to the manufacturer's recommendation. The melting curve temperature profile was generated through the cycle of 95 °C for 1 min, 60 °C for 1 min, and heating to 95°C in 20 min. Each sample had two technical replicates. Real-time PCR data were exported from ABI 7900 software version SDS v2.2 for calculation of mean threshold (Ct) values and standard deviations (SD).

The absolute quantity of the target gene was determined according to the methods of Peirson et al. (2003) and Larionov et al. (2005). In brief, the artificial plasmid DNA template containing the real-time PCR amplicons of the gene was constructed using pGEM-T easy vector. The purified plasmid DNA was diluted at a 1:10 ratio from 10^{-2} ng/µl to 10^{-6} ng/µl. The standard curve was generated by the Absolute Quantification of ABI 7900 HT Fast Real-Time system according to the manufacture's instructions. The copy number of each ng of plasmid DNA was calculated based on the method at http://cels.uri.edu/gsc/cndna.html. The copy number of the target gene were recorded automatically based on the equation of the regression line fitted to the standard curve. The amplification efficiency was calculated based on the slope of the standard curve at http://www.thermoscientificbio.com/webtools/qpcrefficiency/. The gene expression level data was finally presented as the ratio of copy number of *PtIRTs* to that of *PtTIF5α*.

Expression vector construction and plant transformation

The full coding region of the *PtIRT* gene was inserted to the pCAMBIA S1300 vector (Figure 4.1-4.2) to construct the gene expression vector Suppro*::PtIRT*. Another expression

vector PtIRT1-pro*::GUS* was also constructed by replacing the CaMV35S promoter with the native *PtIRT* promoter in pBI121 plasmid (Figure 4.3). Three vectors, Suppro*::PtIRT*, PtIRT1-pro*::GUS*, and CaMV35S::*GUS* were transformed into *Agrobacterium tumefaciens* strain EHA105 using the freeze-thaw method (Weigel and Glazebrook, 2006). The *hpt* gene coding hygromycin phosphotransferase is the selective marker for vector Suppro*::PtIRT* and NPTII coding neomycin phosphotransferase II is the selective marker for the other two vectors.

The Suppro*::PtIRT* genes were transferred to two other poplar species, *P. tremula* × *P. alba* '717' and *P. canescens* × *P. grandidentata* 'Cl6' using an *Agrobacterium*-mediated method based on Dai et al. (2003) and Han et al. (2000). The PtIRT1-pro*::GUS* and CaMV35S*::GUS* cassettes were transferred to tobacco plants as described by Horsch et al. (1985) and Gallois and Marinho (1995). The media used for poplar and tobacco transformation are listed in Table 4.2.

Gene transfer was confirmed by PCR using insertion-specific primers according to the method of Dai et al. (2003). Transgenic lines were proliferated in vitro and grown in the hydroponic culture system. Expression of the *PtIRT* genes in the transgenic plants responding to iron deficiency was evaluated using semi-quantitative PCR as described above.

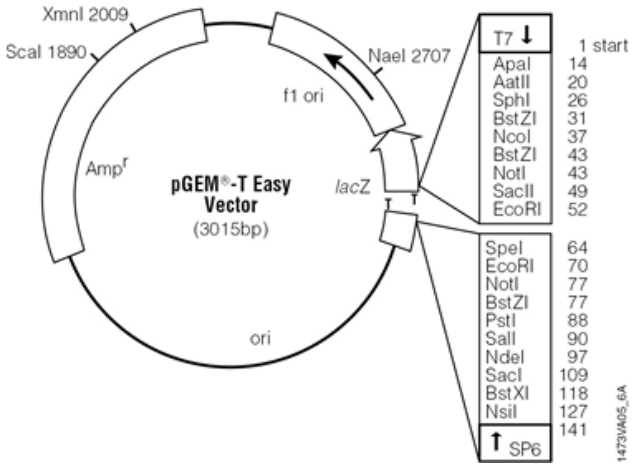

Figure 4.1. Schematic representation of pGEM-T easy vector.

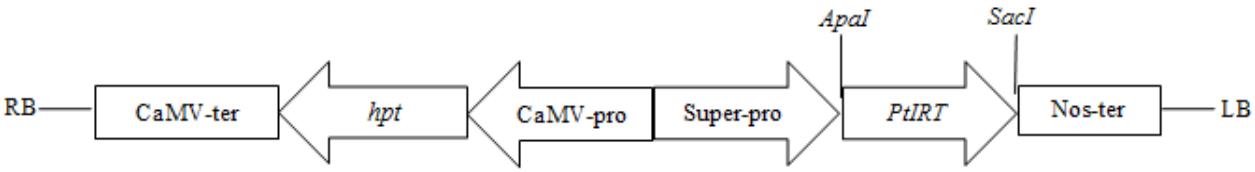

Figure 4.2. Schematic representation of the Suppro*::PtIRT* vector. RB and LB: T-DNA right and left borders, respectively; CaMV-pro: CaMV 35S promoter from cauliflower mosaic virus; *hpt*: hygromycin phosphotransferase gene; CaMV-ter: CaMV-Poly A terminator; Super-pro: a trimer of the octopine synthase transcriptional activating element affixed to the mannopine synthase 2' transcriptional activating element plus minimal promoter; Nos-ter: nopaline synthase terminator; and *PtIRT*: IRT genes cloned from *Populus tremula* L. 'Erecta'.

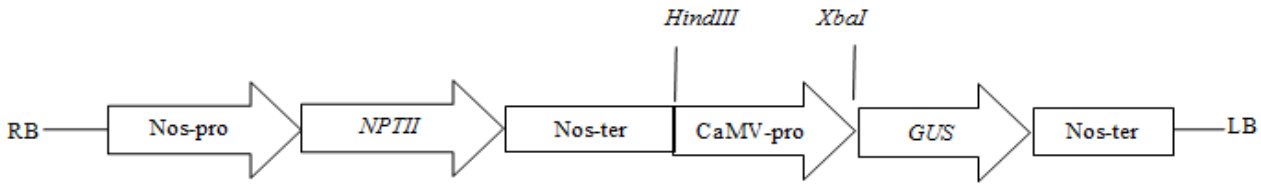

Figure 4.3. Schematic representation of the pBI121 vector. RB and LB: T-DNA right and left borders, respectively; Nos-pro: nopaline synthase promoter; NPTII: neomycin phosphotransferase II gene; Nos-ter: nopaline synthase terminator; CaMV-pro: CaMV 35S promoter from cauliflower mosaic virus; CaMV-ter: CaMV-Poly A terminator; and GUS: β-glucuronidase.

GUS histochemical and GUS activity assay

The activity of the GUS enzyme (β-glucuronidase) in transgenic tobacco tissues was determined to evaluate the function of the *PtIRT* promoter. A GUS staining method was used to stain leaves and roots of transgenic tobaccos containing the gene cassette of PtIRT1-pro*::GUS* or CaMV35S*::GUS* according to Jefferson et al. (1987). Briefly, fresh leaf and root tissues collected from three transgenic plants of each gene vector and three non-transgenic plants (WT) were cut to small pieces and incubated in GUS staining buffer (100 mM $NaPO_4$ buffer, pH 7.0, 2 mM X-Gluc, 0.5 mM $K_3Fe(CN)_6$, 0.5 mM $K_4Fe(CN)_6$, 0.1% Triton X-100 and 10 mM

Table 4.2. Medium used in plant transformation and proliferation.

Explant	Medium type	Basal medium	Hormones& antibiotic	Time required (Days)	Conditions
717	Co-cultivation	MS	5 µM 2iP; 10 µM NAA 100 µM acetosyringone	2-3	Dark, 25 ± 2°C
	Callus induction	MS	5 µM 2iP; 10 µM NAA 5 µM hygromycin	28-30	Dark, 25 ± 2°C
	Shoot induction	MS	0.2 µM TDZ; 5 µM hygromycin	28-30	16/8 h photoperiod, 25 ± 2°C
	Rooting	½ MS	0.5 µM NAA; 5 µM hygromycin	28-30	16/8 h photoperiod, 25 ± 2°C
Cl6	Co-cultivation	WPM	10 µM BA; 5 µM NAA 100 µM acetosyringone	2-3	Dark, 25 ± 2°C
	Callus induction	WPM	10 µM BA; 5 µM NAA 100 µM acetosyringone	28-30	Dark, 25 ± 2°C
	Shoot induction	WPM	0.05 µM TDZ; 5 µM hygromycin	28-30	16/8 h photoperiod, 25 ± 2°C
	Rooting	½ MS	0.5 µM NAA; 5 µM hygromycin	28-30	16/8 h photoperiod, 25 ± 2°C
Tobacco	Co-cultivation	MS	5 µM BA; 100 µM kanamycin	2-3	16/8 h photoperiod, 25 ± 2°C
	Shoot induction	MS	5 µM BA; 100 µM kanamycin	28-30	16/8 h photoperiod, 25 ± 2°C
	Rooting	½ MS	0.5 µM NAA; 100 µM kanamycin	28-30	16/8 h photoperiod, 25 ± 2°C

Na_2EDTA) at 37 °C for 8-12 h. Stained tissues were washed with 75% ethanol for several times to remove the chlorophyll and other pigments. Tissue staining was detected and photographed under a stereomicroscope.

For the GUS activity assay, transgenic and WT tobacco plants were grown in the iron sufficient or deficient Hoagland's solution. After six days, fresh leaves and roots were collected and immediately stored in a -80°C freezer. Quantification of GUS activity was performed using 4-methylumbelliferyl-b-glucuronide (4-MUG) as described by Jefferson et al. (1987) with a few modifications. Protein was extracted from 50 mg tissues ground in liquid nitrogen in the extraction buffer (50 mM sodium phosphate buffer pH 7.0, 0.1 % β-mercaptoethanol, 10 mM Na_2EDTA, 0.1% sodium lauroyl sarcosine, and 0.1% Triton X-100). The protein concentration was determined using Qubit Protein Assay Kit (Life Technologies, Grand Island, NY, USA) with a Qubit® 2.0 Fluorometer (Life Technologies, Grand Island, NY USA) following the manufacture's instruction. A total of 20 µl protein solution was mixed with GUS assay buffer (2 mM 4-MUG in the protein extraction buffer). The fluorescence was measured using a Gemini EM microplate reader (Molecular Devices, LLC, Sunnyvale, CA, USA) every 2 min within a 60 min duration under excitation at 365 nm and emission at 455 nm with a slit width of 10 nm. GUS activity was represented by the change of fluorescence per min per g protein (ΔFn/min/g protein).

Leaf test

Transgenic aspen plants were grown in the hydroponic culture system. Treatments of iron sufficiency or deficiency were conducted as described above. Leaves were collected from plants nine days after the treatment. All leaf samples were oven-dried at 65°C for 2 days and subjected

to leaf tests in the North Dakota State University Cereal Science lab according to the method of Thavarajah et al. (2009).

Results

Identification of the *PtIRT* genes in *Populus*

The *IRT* family is part of subfamily I of a larger superfamily of ZIP that includes three *IRT* genes and 12 ZIP genes in *Arabidopsis* (Guerinot, 2000). In an attempt to screen the ZIP family members in the *Populus trichocarpa* genome, the ZIP family domain derived from *AtIRT1* (accession no: NP_567590) was used as a query in a BLASTP search in NCBI. A total of 18 poplar protein sequences showed high similarity (E value $<10^{-5}$) to *AtIRT1*. The domain information analyzed using SMART online is presented in Table 4.3. The number of amino acids in the ZIP domains varied from 278 to 362. Six of 18 putative proteins have less than 278 amino acids. Of the six proteins, five putative proteins showed partially high similarity to the ZIP domain (shadowed as yellow) and one putative protein (shadowed as blue) was predicted as a member of ZIP subfamily II that is comprised of eight ZIP genes from non-plant species. Thus, only 12 putative proteins were considered as candidate genes belong to the ZIP family in *Populus trichocarpa*.

A phylogenetic tree was constructed by aligning putative *Populus* ZIP genes with other genes listed in Table 4.3 using Cluster W method (Figure 4.4). Two proteins (XP_002322355.1 and XP_002322353.1) were clustered with most of the *IRT* genes of Strategy II plants. Another two proteins (XP_002315981.1 and XP_002311421.1) were clustered with the *IRT* genes of rice (*Oryza sativa*) that belongs to the Strategy I plant group. One protein (XP_002324173.1) was clustered with *AtIRT3*. Thus, two proteins (XP_002322355.1 and XP_002324173.1) were selected as the references to design specific primers to clone *PtIRTs* from PtG and PtY trees.

Table 4.3. Putative protein information of the *IRT* genes and ZIP family genes.

	Predicted protein domain region			
	Signal peptide	Pfam: ZIP (PF02535)	No. of amino acids	Protein designation
LeIRT1 (AAF97509)	1-25	45-349	351	Iron regulated transporter1
LeIRT2 (AAF97510)	1-25	45-349	353	Iron regulated transporter2
AtIRT1 (NP_567590)	1-20	41-336	340	Fe(II) transport protein 1
AtIRT2 (NP_001031670)	1-23	44-347	351	Fe(II) transport protein 2
AtIRT3 (NP_564766)	1-17	61-422	426	Iron regulated transporter 3
MxIRT1 (AAO17059)	1-29	51-361	365	Root iron transporter protein
OsIRT1 (BAB85123)	1-33	59-371	375	Iron regulated metal transporter
OsIRT2 (BAD18964)	1-25	52-367	371	Iron regulated transporter-like protein
OsFe3+ (AAP92124)	1-33	59-371	375	Iron transporter Fe^{3}
CsIRT1 (AAT01414)	1-23	43-347	351	Iron regulated transporter
NtIRT1 (BAF48330)	1-24	44-352	356	Iron transporter protein
PsIRT1 (AAC17441)	1-27	44-345	349	Root iron transporter protein
AtZIP1 (AAC24197)	1-28	48-352	356	Putative zinc transporter
AtZIP2 (AAC24198)	1-29	61-350	354	Putative zinc transporter
AtZIP3 (AAC24199)	1-25	51-336	340	Putative zinc transporter
AtZIP4 (AAB65480)	-	25-371	375	Putative zinc transporter
AtZIP5 (AAL38432)	1-26	45-357	361	Similar to Fe(II) transport protein
AtZIP6 (AAL38433)	-	24-338	342	metal ion transmembrane transporter
AtZIP7 (AAL38434)	1-26	53-362	366	metal ion transmembrane transporter
AtZIP8 (AAL83293)	1-27	48-344	348	metal ion transmembrane transporter

Table 4.3. Putative protein information of the *IRT* genes and ZIP family genes (Continued).

AtZIP9 (AAL38435)	-	1-341	345	metal ion transmembrane transporter
AtZIP10 (AAL38436)	1-28	49-361	365	metal ion transmembrane transporter
AtZIP11 (AAL67935)	1-25	45-322	327	metal ion transmembrane transporter
AtZIP12 (AAL38437)	1-25	47-352	356	metal ion transmembrane transporter
XP_002322355.1	-	28-334	337	
XP_002315981.1	-	16-325	328	
XP_002322353.1	-	-	235	
XP_002307860.1	-	31-340	343	
XP_002315075.1	-	29-339	342	
XP_002307858.1	-	23-315	318	
XP_002312231.1	1-29	46-357	360	
XP_002326631.1	-	21-291	296	
XP_002338269.1	-	1-148	151	
XP_002313244.1	-	22-332	335	
XP_002299993.1	-	22-334	337	
XP_002307861.1	-	2-220	220	
XP_002324173.1	-	21-390	393	
XP_002311421.1	-	6-163	163	
XP_002313423.1	-	17-299	302	
XP_002332153.1	-	-	79	
XP_002300374.1	1-20	48-346	349	
XP_002336493.1	-	1-217	225	

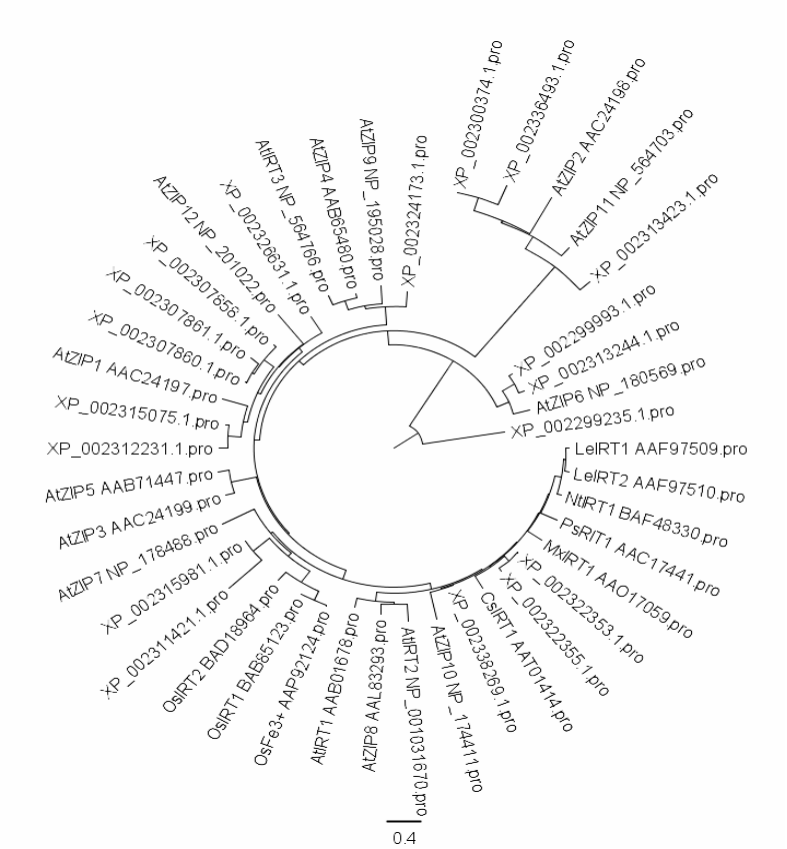

Figure 4.4. Phylogenetic tree of the ZIP family genes in *Populus* and other species. The corresponding sources are *Lycopersicon esculentum* (*Le*), *Nicotiana tabacum* (*Nt*), *Malus xiaojinensis* (*Mx*), *Pisum sativum* (*Ps*), *Cucumis sativus* (*Cs*), *Arabidopsis thaliana* (*At*), and *Oryza sativa* (*Os*). Bar lenght indicates the amount of genetic change.

Percent Identity

Divergence

	1	2	3	4	5	6	7	8	9	10	11	12	13		
1		71.4	42.9	67.0	67.3	66.1	64.1	67.7	53.8	53.8	63.5	66.9	45.8	**1**	AtIRT1
2	36.0		41.3	60.5	63.1	61.8	56.4	61.9	48.9	48.7	57.9	60.5	44.3	**2**	AtIRT2
3	101.0	106.6		43.0	44.4	43.9	43.1	44.7	39.7	39.5	44.7	42.3	68.4	**3**	AtIRT3
4	43.4	55.6	100.7		72.3	71.1	69.4	71.9	54.3	54.1	68.7	71.7	46.0	**4**	CsIRT1
5	42.9	50.5	96.0	34.7		91.1	72.3	89.4	54.3	53.0	72.0	76.8	47.7	**5**	LeIRT1
6	45.0	52.9	97.8	36.5	9.4		69.0	88.6	53.4	51.7	70.5	74.9	47.7	**6**	LeIRT2
7	48.6	64.1	100.3	39.2	34.6	39.9		72.0	53.5	51.1	67.8	73.6	44.9	**7**	MxIRT1
8	42.2	52.8	95.4	35.2	11.4	12.4	35.0		53.0	52.1	73.7	76.7	48.6	**8**	NtIRT1
9	70.1	83.0	112.5	69.1	69.1	71.2	71.1	72.3		77.8	55.2	55.2	42.7	**9**	OsIRT1
10	70.2	83.4	113.5	69.6	72.1	75.4	76.9	74.3	26.4		53.9	55.2	41.5	**10**	OsIRT2
11	49.7	60.9	95.2	40.4	35.0	37.4	41.9	32.4	67.0	69.9		70.2	48.3	**11**	PsIRT1
12	43.6	55.5	103.2	35.5	27.8	30.6	32.6	27.9	66.9	67.0	37.9		46.5	**12**	PtIRT1
13	91.9	96.4	40.9	91.2	86.2	86.2	94.6	83.6	101.7	106.1	84.5	89.7		**13**	PtIRT3
	1	**2**	**3**	**4**	**5**	**6**	**7**	**8**	**9**	**10**	**11**	**12**	**13**		

Figure 4.5. Amino acid similarity among the *IRT* genes calculated by ClustalW.

Cloning and sequence analysis of the *PtIRT* genes

Two *IRT* genes were cloned from PtG and PtY, named *PtIRT1* and *PtIRT3*, according to their similarity to *AtIRT* (Figure 4.5). The *PtIRT1* gene consists of three exons encoding a 357 amino acid protein with a predicted molecular weight (MW) of 37.8 KDa and a theoretical isoelectric point (pI) of 7.7. The *PtIRT3* gene has two exons encoding a 391amino acid protein with a predicted MW of 41.4 KDa and a pI of 6.4 (Figure 4.6). No difference was found in the nucleotide sequence of *PtIRTs* cloned from PtG and PtY. Indeed, an 845 bp fragment located upstream of the *PtIRT1* start codon was also cloned from PtG and PtY. The nucleotide sequence alignment indicated that the fragments from PtG and PtY are identical. The plant promoter prediction software TSSP (Using RegSite Plant DB, Softberry Inc.) found one promoter at position 395 and a TATA box at position 365.

According to the structure of other ZIP family members in *Arabidopsis* (Eide et al., 1996; Guerinot, 2000), *PtIRT1* and *PtIRT3* were predicted to possess the conserved ZIP domain (Pfam accession: PF02535) with eight potential transmembrane (TM) domains (Figure 4.7 and Figure 4.8). A signal peptide was predicted in *PtIRT1*, while no signal peptide was found in *PtIRT3*. A highly conserved region containing the ZIP signature sequence was located in TM domain IV in *PtIRT1* and *PtIRT3*. The histidine cluster proposed to be involved in the formation of a cytoplasmic heavy metal binding site is presented in *PtIRT1* and *PtIRT3* between TM domains III and IV (Eng et al., 1998; Roger et al., 2000). The region between TM domains III and IV was longer in *PtIRT1* than in *PtIRT3* and this region contains a potential metal-binding domain rich in histidine residues, suggesting that *PtIRT1* and *PtIRT3* may play different roles in metal transport in plants. These features of *PtIRT1* and *PtIRT3* indicate that *PtIRT* genes are members of the ZIP family.

PtIRT1 and *PtIRT3* have similarity of 42.3-76.7% and 41.5-68.4% to the *IRT1* and *IRT3* genes in other species, respectively (Figure 4.5). The *PtIRT1* gene has the highest similarity to *LeIRT1* (76.8%) and lowest similarity to *AtIRT3* (42.3%). It is noted that *PtIRT1* also has high similarity to *MxIRT1* (73.6%) which is an iron transporter cloned from a tree species (*Malus xiaojinensis*) and whose expression was strongly enhanced in roots under iron deficiency. The *PtIRT3* gene showed the highest similarity to *AtIRT3* (68.4%). Indeed, *PtIRT3* has an alanine-100 (A100) instead of aspartic acid-100 (D100) at the corresponding position in all tested *IRT1* and *IRT2* genes (indicated as $*$ in Figure 4.8). Besides, both *PtIRT1* and *PtIRT3* have relatively low similarity to *OsIRT1* and *OsIRT2* cloned from Strategy II plants.

A phylogenetic tree (Figure 4.9) constructed using the predicted amino acid sequences of the *IRT* genes revealed that *PtIRT1* was clustered with tomato and tobacco *IRT* genes that are highly responsive to iron deficiency (Eckhardt et al., 2001; Hodoshima et al., 2007), while *PtIRT3* was clustered with *AtIRT3* that is related to zinc and iron transport (Lin et al., 2009).

Figure 4.6. Comparison of gene structures of *PtIRT1* and *PtIRT3*.

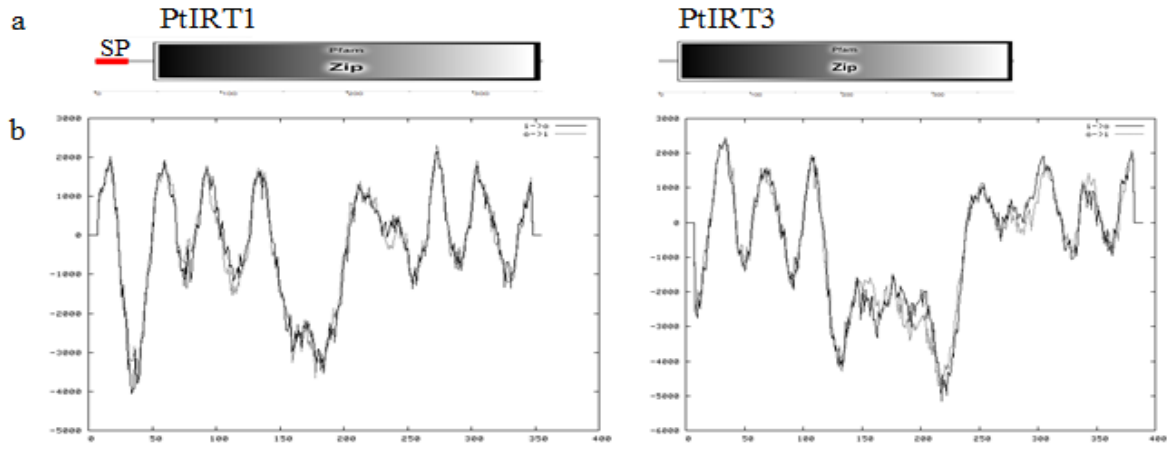

Figure 4.7. Prediction of protein domain and transmembrane regions of the *PtIRT* genes
a, Protein domain predicted by SMART. The red box indicates signal peptide (SP) detected by the SignalP v4.0 program. The gray box indicates a ZIP domain predicted by HMMER3.
b, Transmembrane (TM) prediction by TMpred.

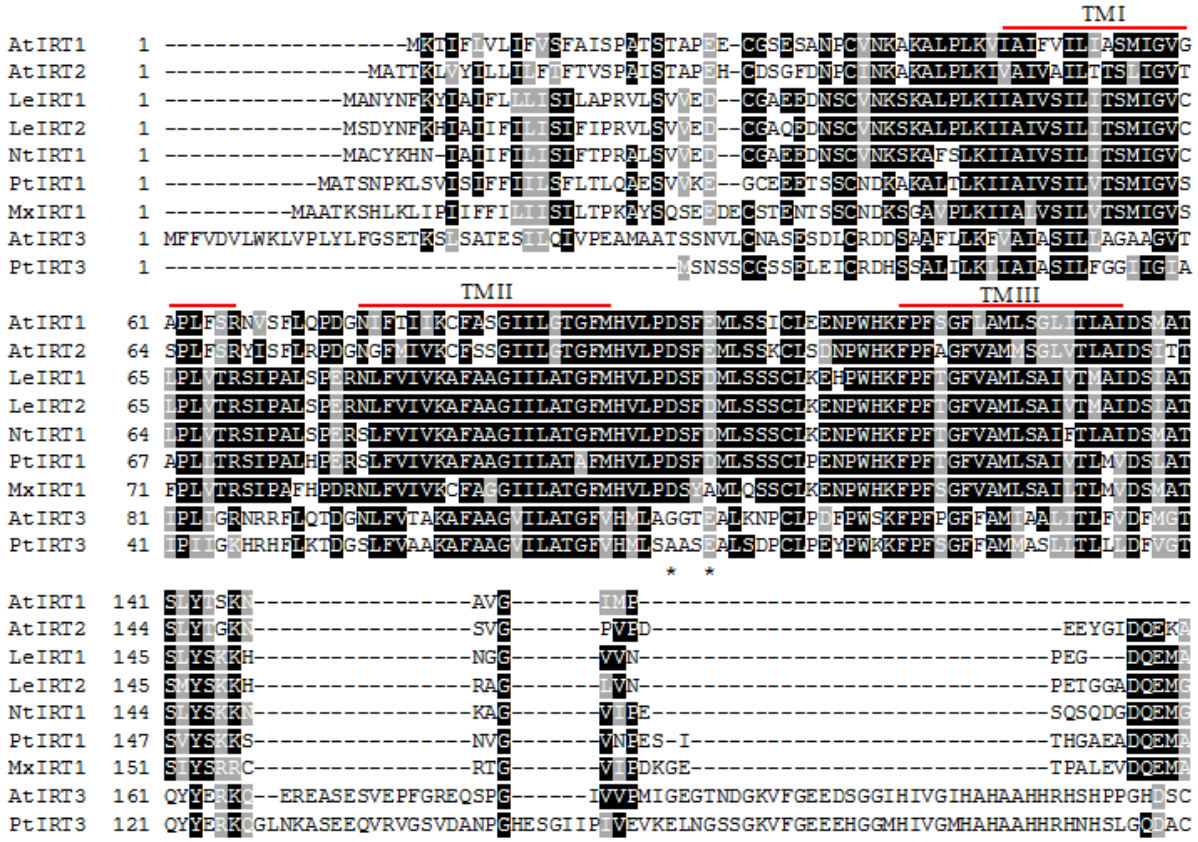

Figure 4.8. Amino acid alignment of deduced *PtIRT* genes with other reported *IRT* genes. Red lines indicate predicted transmembrane (TM) domains, and the green line indicates the signature of the ZIP family domain. The asterisk indicates the nucleotides associated with metal transport selectivity. Shaded areas represent identical residues (black) or similar residues (gray) found in most of the proteins.

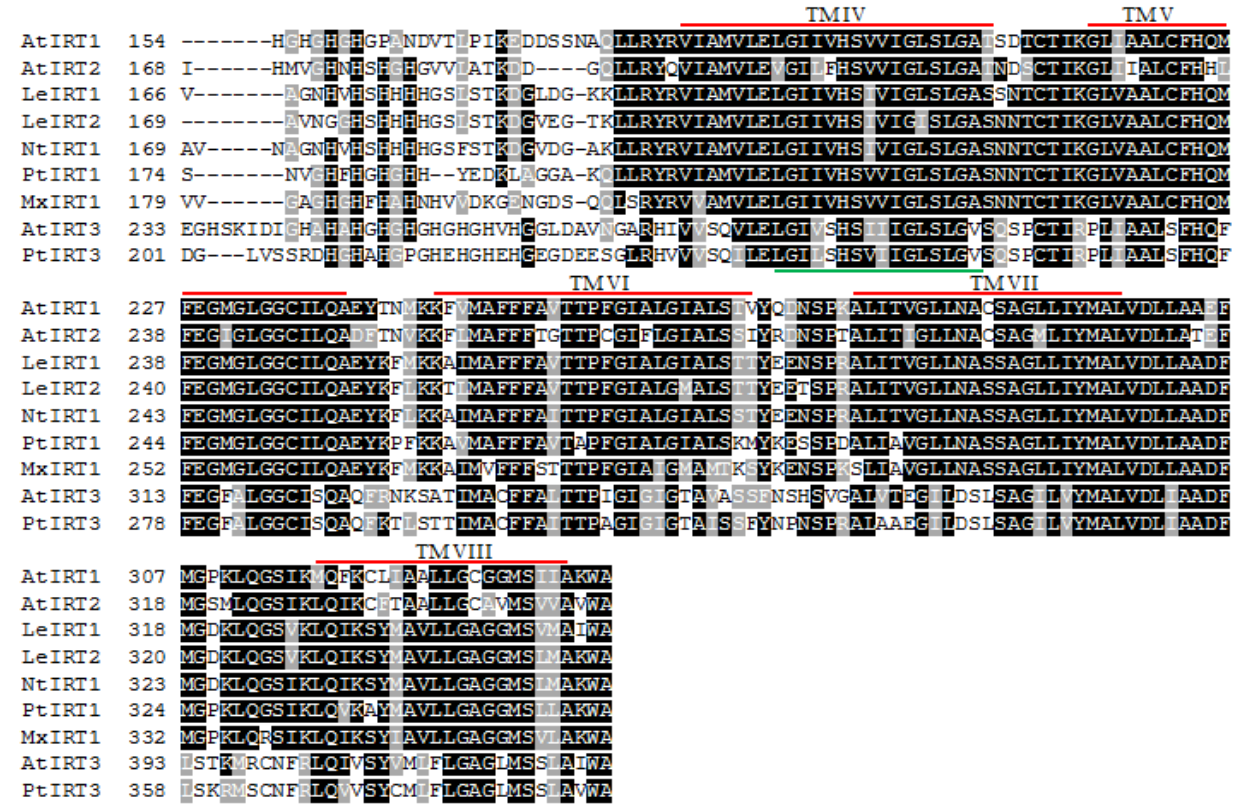

Figure 4.8. Amino acid alignment of deduced *PtIRT* genes with other reported *IRT* genes (continued). Red lines indicate predicted transmembrane (TM) domains, and the green line indicates the signature of the ZIP family domain. The asterisk indicates the nucleotides associated with metal transport selectivity. Shaded areas represent identical residues (black) or similar residues (gray) found in most of the proteins.

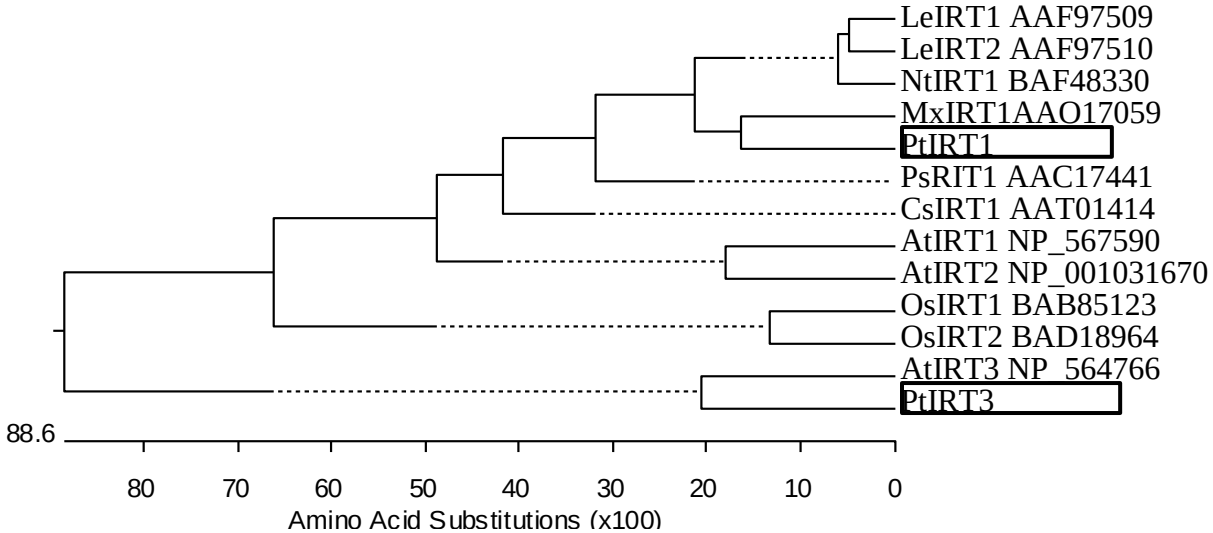

Figure 4.9. Phylogenetic analysis of the *PtIRT* genes and 11 additional *IRT* genes from various plant species. The two *PtIRT* genes are framed. The corresponding sources are *Lycopersicon esculentum* (*Le*), *Nicotiana tabacum* (*Nt*), *Malus xiaojinensis* (*Mx*), *Pisum sativum* (*Ps*), *Cucumis sativus* (*Cs*), *Arabidopsis thaliana* (*At*), and *Oryza sativa* (*Os*).

Tissue-specific expression of the *PtIRT* genes

The expression of *PtIRTs* were examined in various tissues including the root tip, root, phloem, xylem, mature leaf, young leaf, and shoot tip using semi-quantitative RT-PCR. As shown in Figure 4.10, *PtIRT1* expressed only in the root (root tip and other root tissues) and the expression was relatively higher in PtY than in PtG. The highest expression level of *PtIRT1* was observed in the root tip of PtY; however, *PtIRT3* expressed in all tested tissues of both PtG and PtY with a higher expression level was detected in the leaf compared to other tissues. Furthermore, the most abundant transcript of *PtIRT3* was observed in the mature leaf of PtG and the young leaf of PtY. Under the iron deficient condition, the *PtIRT1* gene still expressed in root tissues only and was up-regulated, while *PtIRT3* constitutively expressed in all tissues.

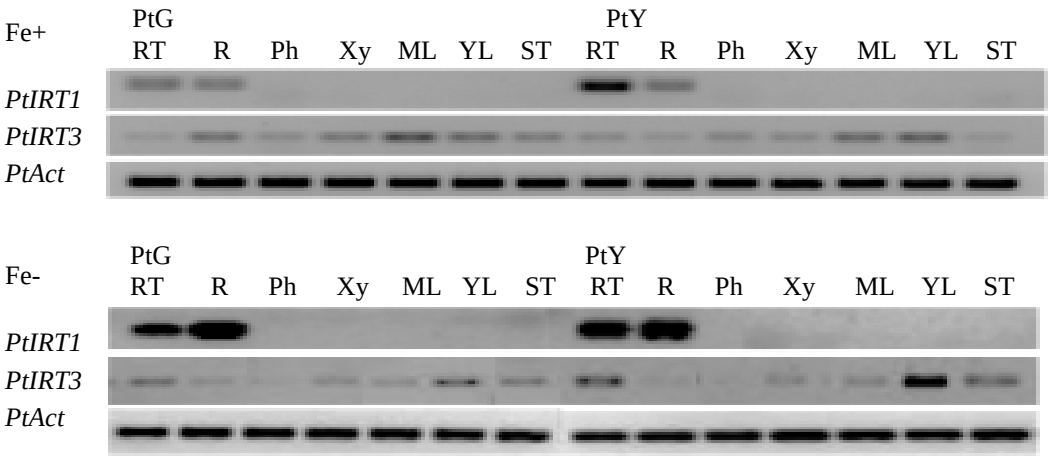

Figure 4.10. Expression of the *PtIRT* genes in different tissues of PtG and PtY under iron sufficient (Fe+) and deficient (Fe-) conditions. PtG: iron deficiency tolerant clone of *Populus tremula*; PtY: iron deficiency sensitive clone of *Populus tremula*; RT: root tips; R: roots; Ph: phloem; Xy: xylem; ML: mature leaf; YL: young leaf; ST: shoot tips.

Expression of the *PtIRT* genes responding to iron deficiency

The expression of two *PtIRT* genes responding to iron deficiency was determined using real-time quantitative PCR. The absolute quantity (the copy number) of the target gene was measured according to the standard curve method (Peirson et al., 2003; Larionov et al., 2005) (Figure 4.11a). The primer specificity was evaluated by the resulting melting curve. Results indicated that all real-time PCR primers generated single PCR products (Figure 4.11b-d). The amplification efficiency of *PtTIF5α* (internal control), *PtIRT1,* and *PtIRT3* primers were 87.75%, 89.37%, and 87.92%, respectively.

Under the iron deficient condition, the expression level of *PtIRT1* continuously increased along with the increase of the exposure time to iron deficiency, indicating that *PtIRT1* was up-regulated by iron deficiency (Figure 4.12). The *PtIRT1* gene in PtG and PtY showed a similar expression pattern; however, a significantly higher level of transcript was found in PtG one day after iron deficiency treatment. At day 6, the expression transcript was doubled in PtG. The expression of *PtIRT3* was gradually increasing after iron deficiency treatment in PtG. In PtY, the expression level of *PtIRT3* showed a fluctuate pattern and no significant increase was observed under iron deficiency. A significantly higher transcript level of *PtIRT3* was detected in PtG than that in PtY three days after iron deficiency treatment (Figure 4.12).

Expression of the *PtIRT* genes responding to zinc deficiency

As shown in Figure 4.13, the *PtIRT1* gene responded to zinc deficiency; however, a different expression pattern was found between PtG and PtY. In PtG, after zinc deficient treatment, the expression gradually increased from day 0 to day 1 and then significantly decreased. At day 6, the level of transcript was only half of that at day 0. In PtY, the expression of *PtIRT1* significantly decreased and then gradually increased one day after the zinc deficient

treatment. At day 6, the expression level went back to the level at day 0. Similarly, the expression of the *PtIRT3* gene was also down-regulated by zinc deficiency. In PtG, the expression sharply decreased at day 0.5 after the zinc deficiency treatment, then increased to the peak at day 1, and decreased again afterwards. In PtY, the expression was decreasing between day 0 and day 3 of the treatment, and then slightly increased at day 6. The expression level of *PtIRT*3 was higher in PtY than in PtG. Overall, the expression of the *PtIRT* genes was up-regulated by iron deficiency and down-regulated by zinc deficiency.

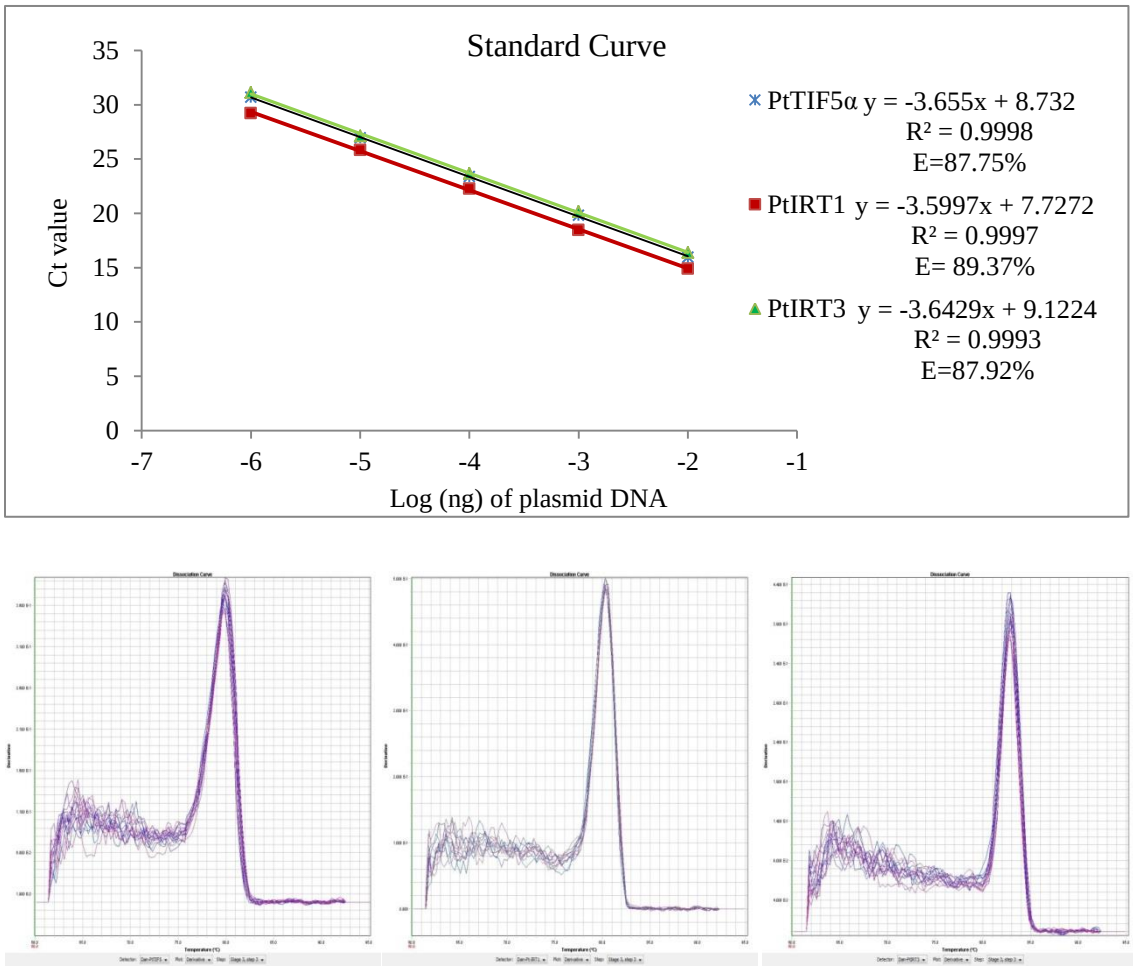

Figure 4.11. Standard curves and melting curves for real-time PCR assay. a, Standard curves were constructed for *PtTIF5α*, *PtIRT1*, and *PtIRT3*, respectively; E stands for the PCR efficiency; b-d, melting curves of PCR products using specific primers for amplification of *PtTIF5α*, *PtIRT1*, and *PtIRT3*, respectively.

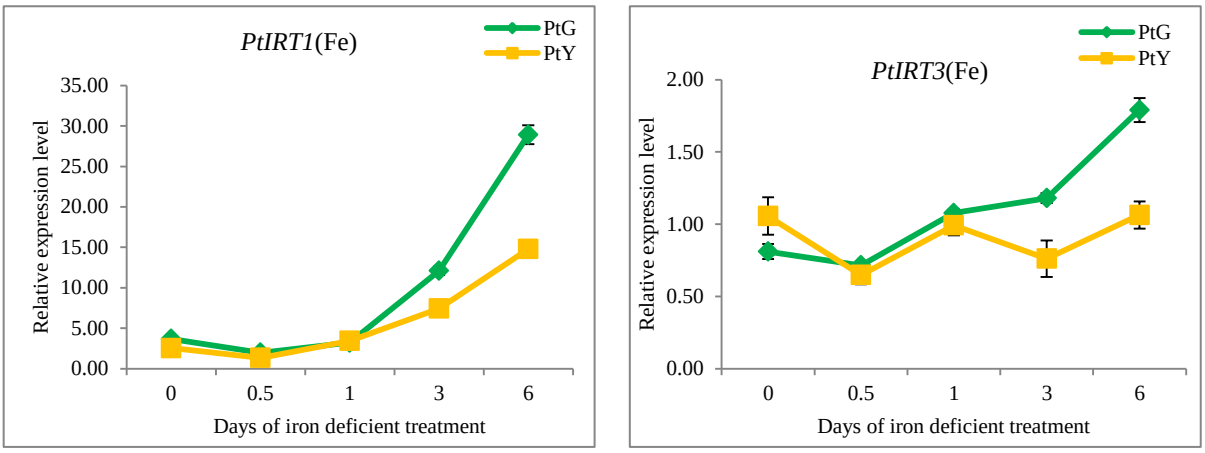

Figure 4.12. Relative expression levels of the *PtIRT* genes in root tissues of PtG and PtY responding to iron deficiency. The relative expression is quantified by real-time PCR and normalized to the *PtTIF5α* gene.

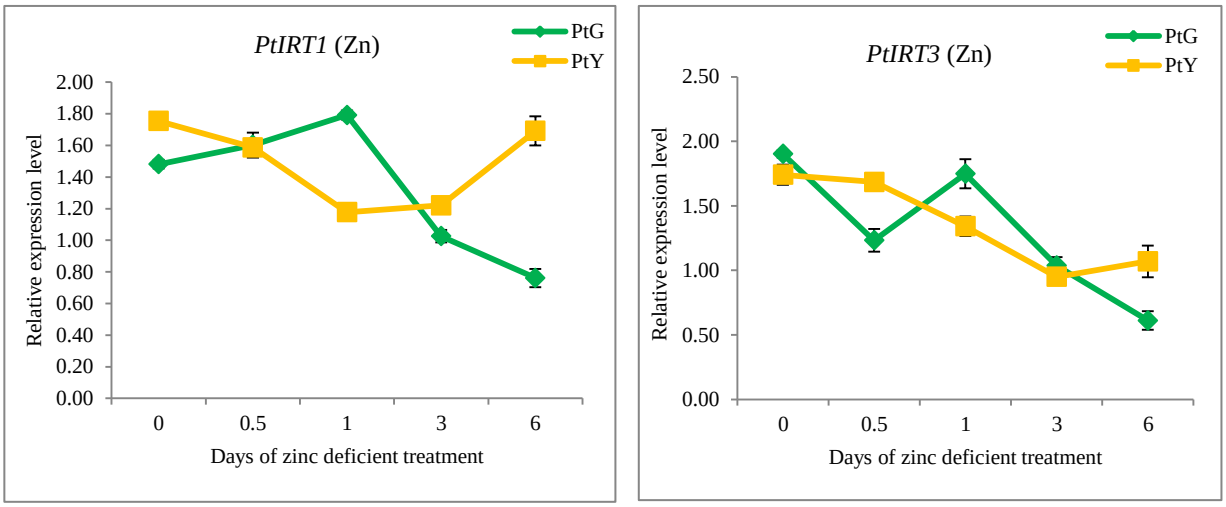

Figure 4.13. Relative expression levels of the *PtIRT* genes in root tissues of PtG and PtY responding to zinc deficiency. The relative expression is quantified by real-time PCR and normalized to the *PtTIF5α* gene.

Accumulation of mineral elements in the leaf of PtG and PtY after iron or zinc deficient treatment

The content of Mn, Fe, Zn, and Cu was determined in leaf tissues of PtG and PtY after iron or zinc deficient treatment. The element deficient treatment significantly decreased the

content of the responding element. As shown in Table 4.4, the leaf Fe content was significantly lower in the iron deficient treatment and the leaf Zn content was significantly lower in the zinc deficient treatment. The content of Cu did not significantly change regardless of iron or zinc supply. The iron deficiency treatment slightly reduced the Mn accumulation. Interestingly, iron deficiency dramatically increased the accumulation of Zn in leaves. The contents of Zn in iron deficient-treated leaves of PtG and PtY were 168.82 and 134.51 mg/kg DW, respectively, while only 56.90 and 72.22 mg/kg DW of Zn were accumulated in iron sufficient-treated PtG and PtY leaves. The zinc deficiency treatment showed no significant effect on the content of Mn and Fe. Comparisons of element contents between PtY and PtG showed that PtG accumulated significantly higher Fe (40.74 mg/kg DW) than that of PtY (27.76 mg/kg DW). PtG also had a higher content of Zn (168.82 mg/kg DW) than PtY (134.51 mg/kg DW) under the iron deficiency condition.

Table 4.4. The content of mineral elements in the leaves of PtG and PtY under iron or zinc sufficient (Fe+ or Zn+) and iron or zinc deficient (Fe- or Zn-) conditions[z].

		Fe+	Fe-	Zn+	Zn-
Mn	PtG	218.70±4.31	174.85±5.63	113.96±2.72	122.55±3.73
	PtY	232.38±7.20	195.56±9.87	112.63±1.22	112.32±1.19
Fe	PtG	68.43±0.38	40.74±0.55	68.27±2.02	63.34±2.59
	PtY	70.83±2.02	27.76±0.83	70.94±1.63	69.90±3.49
Zn	PtG	56.90±1.32	168.82±9.78	44.95±2.11	21.68±0.87
	PtY	72.22±4.24	134.51±11.46	41.24±0.53	21.29±0.19
Cu	PtG	13.55±0.26	13.13±0.26	11.97±0.18	11.44±0.31
	PtY	15.21±0.43	14.43±0.41	12.46±0.28	12.27±0.16

[z] The content of mineral elements is expressed as mean ±SE in mg/kg DW (leaf dry weight).

Evaluation of the spatial expression pattern of the *PtIRT1* gene

To determine if the root-specific expression of the *PtIRT1* gene was caused by the gene promoter specificity, the *PtIRT1* gene promoter was cloned from *P. tremula* 'Erecta', as an 845 bp fragment located upstream of the *PtIRT1* start codon (ATG). The cloned promoter was fused to a *GUS* gene to form a PtIRT1-pro*::GUS* reporter system. This system was transferred into tobacco using an *Agrobacterium*-mediated transformation method. Nine transgenic tobacco lines were obtained. Histochemical GUS staining revealed that six of nine plants were GUS-stained blue in both leaf and root tissues, indicating that the *PtIRT1* promoter was not root-specific (Figure 4.14). The activity of the GUS enzyme in leaf and root tissues was also determined. In the non-transgenic leaf and root tissues (WT), GUS activity was rarely detected. In the transgenic plants, the increase in fluorescence reached a linear phase after 10 min of the reaction (Figure 4.15); therefore, the change of fluorescence per min was calculated from 10 to 60 min of the reaction. The GUS activity in root tissues of the PtIRT1-pro*::GUS* and CaMV35S*::GUS* (control) lines were enhanced by the iron deficient condition except TL10. In leaf tissues, no substantial changes in the GUS activity were observed between iron sufficient and deficient conditions with the exception of TL7 in which iron deficiency enhanced the GUS activity (Table 4.5).

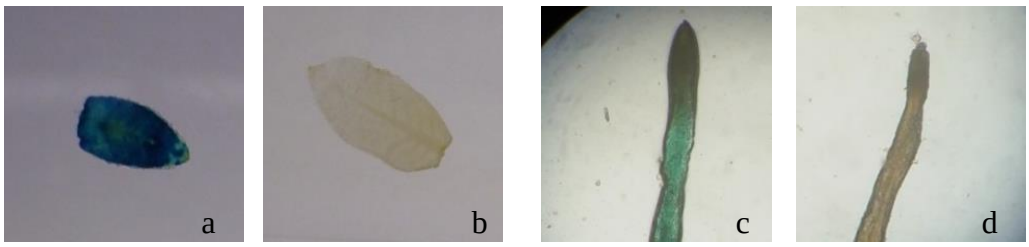

Figure 4.14. Histochemical staining of GUS in transgenic and wild type tobacco plants. a-b, leaf tissues of transgenic and wild type tobacco; c-d, root tissues of transgenic and wild type tobacco.

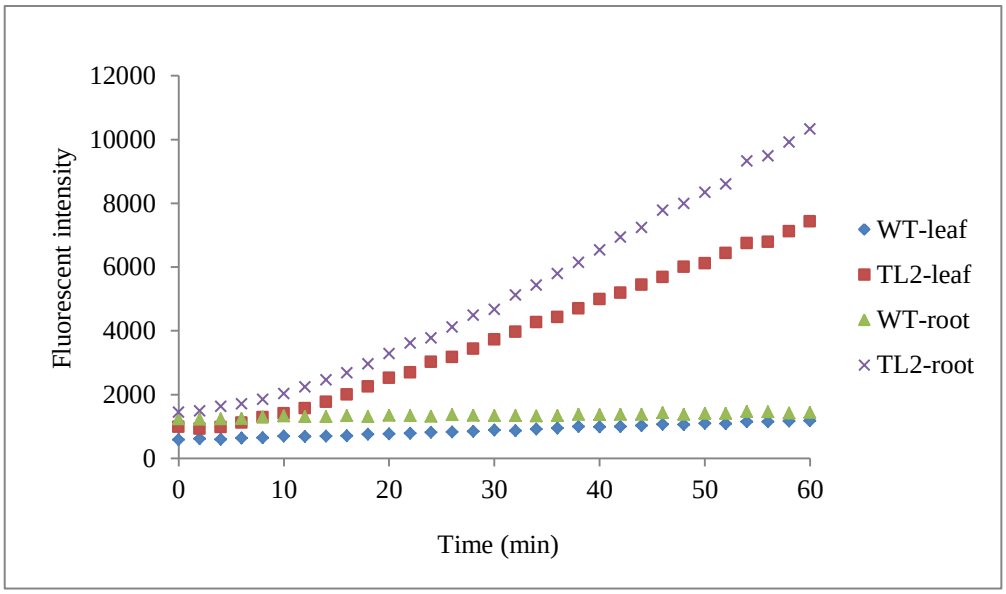

Figure 4.15 Time course of fluorescence of GUS quantitated in transgenic (TL2) and wild type (WT) tobacco.

Table 4.5. GUS activity measured by MUG fluorimetric assay in transgenic tobacco plants [z].

	Root		Leaf	
	Fe+	Fe-	Fe+	Fe-
35S	13.0-18.1	19.0-19.2	14.8-17.6	12.7-14.2
TL1	15.1-17.4	18.0-20.7	9.73-15	13.0-18.0
TL2	11.1-16.2	18.4-20.9	14.6-19.3	11.0-14.9
TL3	13.6-19.7	17.2-20.4	12.94-23.1	15.2-16.5
TL7	10.3-14.9	17.3-22.7	10.8-15.1	15.5-22.9
TL10	19.1-21.5	19.8-22.9	10.9-13.8	12.9-14.2
TL12	13.0-14.9	17.9-21.7	14.6-19.8	12.6-18.4

[z] The GUS activity is expressed as the change of fluorescence per min per g protein (ΔFn/min/g protein) from three biological replicates.

Overexpression of the *PtIRT* genes in aspen hybrids

PtIRT1 and *PtIRT3* were overexpressed in *P. tremula* × *P. alba* '717' and *P. canescens* × *P. grandidentata* 'Cl6' under control of the enhanced super promoter. Expression of the *PtIRT1* gene in transgenic aspen plants was also up-regulated by iron deficiency. In 'Cl 6' transgenic lines, *PtIRT1* showed a low expression level under the iron sufficient condition except for line 2 (Figure 4.16). In '717' transgenic lines, expression of *PtIRT1* was detected under both iron deficient and sufficient conditions. Iron deficiency significantly increased the transcript level in line 7 of '717'. Unlike *PtIRT1*, *PtIRT3* expressed at a lower level in transgenic plants and did not respond to iron deficiency.

Although the transgenic *PtIRT* genes expressed in the transgenic plants, the content of Fe and Zn in these plants was not significantly increased (Figure 4.17). The Fe content in both 'Cl 6' and '717' plants grown under the iron deficient condition was significantly lower than in plants under the iron sufficient condition; however, no significant difference was found in Fe content between transgenic and wild type lines under either iron sufficient or deficient conditions. The Zn content in both transgenic and wild type lines was not significantly affected by iron deficiency.

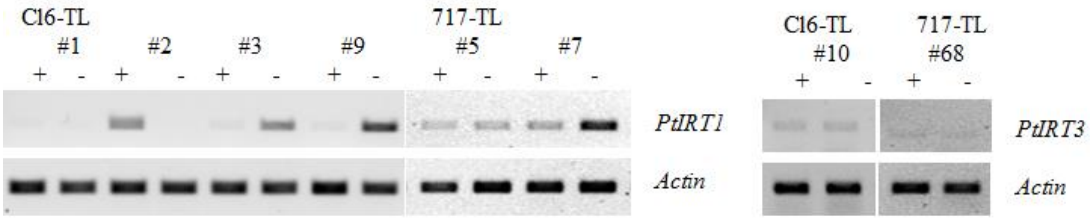

Figure 4.16. Expression of *PtIRT1* and *PtIRT3* in the roots of transgenic lines of aspen in response to iron deficiency. *Actin* gene expression served as an internal control; +, iron sufficient conditions; -, iron deficient conditions.

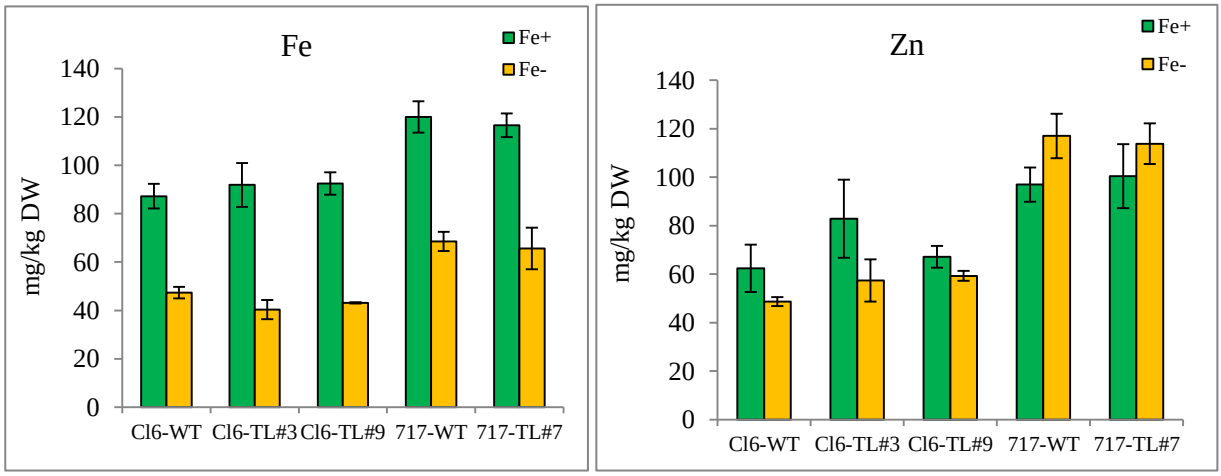

Figure 4.17. Fe and Zn content in leaves of transgenic plants overexpressing *PtIRT1* under iron sufficient (+) and iron deficient (-) conditions.

Discussion

Iron plays a crucial role in biosynthesis and maintenance of chlorophyll structure and function (Abadia, 1992); therefore, iron is directly related to plant growth and development. Iron uptake and transport in plants influence iron accumulation in plant organs, such as leaves, grains, and fruits, which are essential food sources for humans and animals. The *IRT* (*Iron-Regulated Transporter*) genes have been well researched for their roles in iron absorption and transport in many plant species (Eide et al., 1996; Vert et al., 2002); however, very limited research has been done on perennial woody species. In this study, two *IRT* genes were isolated from *Populus tremula* L. 'Erecta', a tree species in the genus *Populus*. Putative amino acid sequence analysis showed that the *PtIRT* genes had important features of ZIP metal transporters, such as highly conserved ZIP TM domains and a histidine-rich cluster between TM domains III and IV (Guerinot, 2000). Phylogenetic analysis showed that *PtIRT1* was most closely related to *LeIRT1*, *LeIRT2*, and *NtIRT1* genes (Figure 4.9). Eckhardt et al. (2001) reported that *LeIRT1* transcripts were exclusively detected in roots of both iron deficient and sufficient tomato plants and its expression was strongly enhanced under iron deficiency. Hodoshima et al. (2007) reported that

NtIRT1 in tobacco was significantly induced by iron deficiency in root tissues. In this study, expression of *PtIRT1* was exclusively observed in the root of *P. tremula* (Figure 4.10). Gene promoters play key roles in tissue-specific expression (Hochheimer and Tjian, 2003). The native promoter of the *PtIRT1* gene was fused with the GUS report gene (PtIRT1-pro*::GUS*) to determine if the root-specific expression of the *PtIRT1* gene was driven by its promoter itself. Histochemical GUS staining of the PtIRT1-pro*::GUS* transgenic tobacco plants showed that the expression of the GUS gene driven by the *PtIRT1* promoter was not root-specific (Figure 4.14); however, the activity of the GUS enzyme in transgenic tobacco roots was significantly enhanced by iron deficiency compared to that in the leaf or that in the root under the iron sufficient condition (Table 4.5). It is known that the spatial and temporal expression of a gene is controlled by a promoter (Thomas and Chiang, 2006; Heintzman and Ren, 2007; Juven-Gershon and Kadonaga, 2010). Generally, a promoter contains a core region that is required for accurate initiation of transcription, proximal regulatory elements that have a specific transcription factor binding site, and distal regulatory elements including enhancers and silencers (Maston et al., 2006). The enhancers particularly play an important role in regulation of tissue-specific gene expression (Ong and Corces, 2011), however, enhancers sometimes may locate up to 1 Mbp away from the regulated gene in both directions or even on a different chromosome (Spilianakis, et al., 2005; Maston et al., 2006; Pennacchio, et al., 2013). Obviously, the isolated 845 bp fragment from the upstream portion of the *PtIRT1* gene contains the core region and the iron deficiency responding transcription factor binding site; whereas, other elements related to the root-specific expression of the gene may not be included in the promoter region of the *PtIRT1* gene.

Unlike *PtIRT1* that only expressed in the root, *PtIRT3* expressed in the root, stem (phloem and xylem), and leaf (Figure 4.10). *PtIRT3* was clustered into a subgroup of *AtIRT3* (Figure 4.9). Lin et al. (2009) demonstrated that *AtIRT3* is a plasma membrane-localized transporter of zinc/iron in yeast (*Saccharomyces cerevisiae*). Indeed, its expression in the root and shoot of *Arabidopsis halleri* was induced by the deficiency of iron or zinc. Although the sequence of *AtIRT3* is similar to *AtIRT1* and *AtIRT2,* the position of some amino acids may change the selectivity of metal transporters (Rogers et al., 2000). For example, the amino acid residues D100 and E103 in *AtIRT1* were functional for Fe, Mn, and Zn transport; however, when the D100 was replaced by A100, *AtIRT1* was only functional for Zn transport. If the E103 was replaced by A103, *AtIRT1* would lose Zn transport ability. This indicated that A100 and E103 are two important signal amino acids for Zn transport. It was shown that A100 and E103 were present in the predicted amino acid sequence of *PtIRT3* (Figure 4.8), suggesting that *PtIRT3* may play a role in Zn uptake and transport in poplar plants.

The expression of the *PtIRT1* and *PtIRT3* genes responding to the iron and zinc deficiency in the iron deficiency sensitive (PtY) and resistant (PtG) *Populus. tremula* genotypes was conducted in this study. Results showed both *PtIRT1* and *PtIRT3* were responsive to iron and zinc deficiency (Figure 4.12 and 4.13), which suggests that *PtIRT1* and *PtIRT3* are involved in iron and zinc homeostasis in poplar trees. The *PtIRT1* gene was clearly up-regulated by iron deficiency in poplar trees. More transcripts of *PtIRT1* accumulated in PtG than in PtY under iron deficiency. Leaf tests also showed that Fe content was higher in PtG than in PtY under iron deficiency (Table 4.4); however, overexpression of the *PtIRT1* gene in other poplar species showed no increase in Fe content under either iron sufficient or deficient conditions (Figure 4.17). A similar finding was reported by Connolly et al. (2002) in that transgenic *Arabidopsis*

with *AtIRT1* did not increase Fe content. Up-regulation of the *PtIRT3* gene explains why zinc was accumulated in plants under iron deficiency (Table 4.4), but zinc deficiency had no effect on iron accumulation, which showed consistence with other reports (Lin et al 2009; Shamugam et al 2011; Legay et al. 2012). It is noted that the expression of *PtIRT3* was reduced in poplar plants under the zinc deficient condition; however, *AtIRT3* was induced by zinc deficiency in *Arabidopsis* plants (Lin et al., 2009). Such a difference might be caused by the difference between woody and herbaceous plants. It is not uncommon to observe species-specific expression of genes. *Populus* and *Arabidopsis* are two model species for woody perennial and herbaceous annual species. They have distinct growth and development habits. Differences in gene expression between poplar and other herbaceous plants have been documented (Quesada et al. 2008; Yang et al. 2009). These gene expression differences may contribute to the observed differences in anatomy structure, body size, growth habit, and the growing environment between *Populus* and *Arabidopsis*. Although *Populus* (*P. trichocarpa*) has almost 90% of predicted genes homologous to *A. thaliana* genes (Tuskan et al. 2006), difference in the quantitative expression pattern of the orthologs was still observed between these two species (Quesada et al. 2008). *Populus* may have different regulations for these similar genes rather than distinct differences in gene functions. This variation in gene regulation may have resulted in developmental and morphological diversity (Kirst et al. 2003; Quesada et al. 2008).

References

Abadia, J. 1992. Leaf responses to Fe deficiency: a review. J. Plant Nutri. 15:1699-1713

Barberon, M., Zelazny, E., Robert, S., Conéjéro, G., Curie, C., Friml, J. and Vert, G. 2011. Monoubiquitin-dependent endocytosis of the iron-regulated transporter 1 (IRT1) transporter controls iron uptake in plants. Proc. Natl. Acad. Sci. USA 108: E450-E458

Briat, J.F. and Lobreaux, S. 1997. Iron transport and storage in plants. Trends Plant Sci. 2:187-193

Briat, J.F., Ravet, K., Arnaud, N., Duc, C., Boucherez, J., Touraine, B., Cellier, F. and Gaymard, F. 2010. New insights into ferritin synthesis and function highlight a link between iron homeostasis and oxidative stress in plants, Ann. Bot. 105:811-822

Cesco, S., Neumann, G., Tomasi, N., Pinton, R. and Weisskopf, L. 2010. Release of plant-borne flavonoids into the rhizosphere and their role in plant nutrition. Plant Soil 329:1-25

Connolly, E.L., Fett, J.P. and Guerinot, M.L**.** 2002. Expression of the *IRT1* metal transporter is controlled by metals at the levels of transcript and protein accumulation. Plant Cell 14:1347-1357

Curie, C., Cassin, G., Couch, D., Divol, F., Higuchi, K., Jean, M.L., Misson, J., Schikora, A., Czernic, P. and Mari, S. 2009. Metal movement within the plant: contribution of nicotianamine and yellow stripe 1-like transporters. Ann. Bot. (Lond) 103:1-11

Curie, C., Panaviene, Z., Loulergue, C., Dellaporta, S.L., Briat, J.F. and Walker, E.L. 2001. Maize yellow stripe1 encodes a membrane protein directly involved in Fe(III) uptake. Nature 409:346-349

Dai, W., Cheng, Z.M. and Sargent, W. 2003. Plant regeneration and *Agrobacterium*-mediated transformation of two elite aspen hybrid clones from in vitro leaf tissues. In Vitro Cell Dev. Biol. Plant 39:6-11

Ding, H., Duan, L., Li, J., Yan, H., Zhao, M., Zhang, F. and Li, W. 2010. Cloning and functional anaylsis of the peanut iron transporter *AhIRT1* during iron deficiency stress and intercropping with maize. J. Plant Physiol. 167:996-1002

Eckhardt, U., Marques, A.M. and Buckhout, T.J. 2001. Two iron-regulated cation transporters from tomato complement metal uptake-deficient yeast mutants. Plant Mol. Biol. 45:437-448

Eide, D., Broderius, M., Fett, J. and Guerinot, M.L. 1996. A novel iron-regulated metal transporter from plants identified by functional expression in yeast. Proc. Natl. Acad. Sci. USA 93:5624-5628

Eng, B.H., Guiernot, M.L., Eide, D. and Saier, M.H. 1998. Sequence analysis and phylogenetic characterization of the ZIP family of metal ion transport proteins. J. Membr. Biol. 166:1-7

Gallois, P. and Marinho, P. 1995. Leaf disc transformation using *Agrobacterium* tumefaciens-expression of heterologous genes in tobacco. In: Jones H (ed.), Methods in Molecular Biology (pp 39-48) Humana Press, NY

Grotz, N., Fox, T., Connolly, E., Park, W., Guerinot, M.L. and Eide, D. 1998. Identification of a family of zinc transporter genes from *Arabidopsis* that respond to zinc deficiency. Proc. Natl. Acad. Sci. USA 95:7220-7224

Guerinot, M.L. 2000. The ZIP family of metal transporters. Biochim Biophy Acta 1465:190-198

Guerinot, M.L. and Yi, Y. 1994. Iron: Nutritious, noxious, and not readily available. Plant Physiol. 104:815-820

Han, K.H., Meilan, R., Ma, C. and Strauss, S.H. 2000. An *Agrobacterium tumefaciens* transformation protocol effective on a variety of cottonwood hybrids (genus *Populus*). Plant Cell Rep. 19:315-320

Heintzman, N.D. and Ren, B. 2007. The gateway to transcription: identifying, characterizing and understanding promoters in the eukaryotic genome. Cell Mol. Life Sci. 64:386-400

Henriques, R., Jasik, J., Klein, M., Martinoia, E., Feller, U., Schell, J., Pais, M.S. and Koncz, C. 2002. Knock-out of *Arabidopsis* metal transporter gene *IRT1* results in iron-deficiency accompanied by cell differentiation defects. Plant Mol. Biol. 50:587-597

Hochheimer, A. and Tjian, R. 2003. Diversified transcription initiation complexes expand promoter selectivity and tissue-specific gene expression. Genes Dev. 17:1309-1320

Hodoshima. H., Enomoto, Y., Shoji, K., Shimada, H., Goto, F. and Yoshihara, T. 2007. Differential regulation of cadmium-inducible expression of iron-deficiency-responsive genes in tobacco and barley. Physiologia Plantarum 129:622-634

Horsch, R.B., Fry, J.E., Hoffmann, N.L., Eichholtz, D., Rogers, S.G. and Fraley, R.T. 1985. A simple and general method for transferring genes into plants. Science 227:1229-1231

Huang, D. and Dai, W. 2011. Direct regeneration from in vitro leaf and petiole tissues of *Populus tremula* 'Erecta'. Plant Cell Tiss. Organ. Cult. 107:169-174

Jefferson, R.A., Kavanagh, T.A. and Bevan, M.W. 1987. GUS fusions: betaglucuronidase as a sensitive and versatile gene fusion marker in higher plants. EMBO J. 6: 3901-3907

Jeong, J. and Connolly, E.L. 2009. Iron uptake mechanisms in plants: Functions of the *FRO* family of ferric reductases. Plant Sci. 176:709-714

Juven-gershon, T. and Kadonaga, J.T. 2010. Regulation of gene expression via the core promoter and the basal transcriptional machinery. Dev. Biol. 339:225-229

Kirst, M., Johnson, A.F., Baucom, C., Ulrich, E., Hubbard, K., Staggs, R., Paule, C., Retzel, E., Whetten, R. and Sederoff, R. 2003. Apparent homology of expressed genes from wood-forming tissues of loblolly pine (*Pinus taeda* L.) with *Arabidopsis thaliana*. Proc. Natl. Acad. Sci. USA 100:7383-7388

Kobayashi, T. and Nishizawa, N.K. 2012. Iron uptake, translocation, and regulation in higher plants. Annu. Rev. Plant Biol. 63:131-152

Larionov, A., Krause, A. and Miller, W. 2005. A standard curve based method for relative real time PCR data processing. BMC Bioinformatics 6:62

Legay, S., Guignard, C., Ziebel, J. and Evers D. 2012. Iron uptake and homeostasis related genes in potato cultivated in vitro under iron deficiency and overload. Plant Physiol. Biochem. 60:180-189

Li, P., Qi, J.L., Wang, L., Huang, Q.N., Han, Z.H. and Yin, L.P. 2006. Functional expression of MxIRT1, from *Malus xiaojinensis*, complements an iron uptake deficient yeast mutant for plasma membrane targeting via membrane vesicles trafficking process. Plant Sci. 171:52-59

Lin, Y.F., Liang, H.M., Yang, S.Y., Boch, A., Clemens, S., Chen, C.C., Wu, J.F., Huang, J.L. and Yeh, K.C. 2009. *Arabidopsis IRT3* is a zinc-regulated and plasma membrane localized zinc/iron transporter. New Phytol. 2182:392-404

Lodhi, M.A., Ye, G.N., Weeden, N.F. and Reisch, B.I. 1994. A simple and efficient method for DNA extraction from grapevine cultivars and *Vitis* species. Plant Mol. Biol. Rep. 12:6-13

Marschner, H.1995. Mineral Nutrition of Higher Plants, 2nd ed., Academic Press, London, UK.

Maston, G.A., Evans, S.K. and Green, M.R. 2006. Transcriptional regulatory elements in the human genome. Anne. Rev. Genomics Hum. Genet. 7:29-59

Mori, S. 1999. Iron acquisition by plants. Curr. Opin. Plant Biol. 2:250-253

Morrissey, J. and Guerinot, M.L. 2009. Iron uptake and transport in plants: the good, the bad, and the ionome. Chem Rev. 109:4553-4567

Mukherjee, I., Campbell, N.H., Ash, J.S. and Connolly, E.L. 2006. Expression profiling of the *Arabidopsis* ferric chelate reductase (FRO) gene family reveals differential regulation by iron and copper. Planta 223:1178-1190

Murashige, T. and Skoog, F. 1962. A revised medium for rapid growth and bioassays with tobacco tissue culture. Physiol. Plant 15:473-497

Olsen, R.A., Clark, R.B. and Bennett, J.H. 1981. The enhancement of soil fertility by plant roots. Am. Scientist 69:378-384

Ong, C. and Corces, V.G. 2011. Enhancer function: new insights into the regulation of tissue-specific gene expression. Nat. Rev. Genet. 12:283-293

Peirson, S.N., Butler, J.N. and Foster, R.G. 2003. Experimental validation of novel and conventional approaches to quantitative real-time PCR data analysis. Nucleic Acids Res. 31:e73

Pennacchio, L.A., Bickmore, W., Dean, A., Nobrega, M.A. and Bejerano, G. 2013. Enhancers: Five essential questions. Nature Rev. Genet. 14:288-295

Qu. S.C., Huang, X.D., Zhang, Z., Yao, Q.H., Tao, J.M., Qiao, Y.S. and Zhang, J.Y. 2005. Agrobacterium-mediated transformation of *Malus robusta* with tomato iron transporter gene. J Plant Physiol Mol Biol 31:235-240

Quesada, T., Li, Z., Dervinis, C., Li, Y., Bocock, P.N., Tuskan, G.A., Casella, G., Davis, J.M. and Kirst, M. 2008. Comparative analysis of the transcriptomes of *Populus trichocarpa* and *Arabidopsis thaliana* suggests extensive evolution of gene expression regulation in angiosperms. New Phytol. 180:408-420

Ravet, K., Touraine, B., Boucherez, J., Briat, J.F. Gaymard, F. and Cellier, F. 2009. Ferritins control interaction between iron homeostasis and oxidative stress in *Arabidopsis*. Plant J. 57:400-412

Robinson, N.J., Procter, C.M., Connolly, E.L. and Guerinot, M.L. 1999. A ferric-chelate reductase for iron uptake from soils. Nature 397:694-697

Rogers, E.E., Eide, D.J. and Guerinot, M.L. 2000. Altered selectivity in an *Arabidopsis* metal transporter. Proc. Natl. Acad. Sci. USA 97:12356-12360

Römheld, V. 1987. Different strategies for iron acquisition in higher plants. Physiol. Plant 70:231-234

Römheld, V. and Marschner, H. 1986. Evidence for a specific uptake system for iron phytosiderophores in roots of grasses. Plant Physiol. 80:175-180

Santi, S. and Schmidt, W. 2009. Dissecting iron deficiency-induced proton extrusion in *Arabidopsis* roots. New Phytol. 183:1072-1084

Santi, S., Cesco, S., Varanini, Z. and Pinton, R. 2005. Two plasma membrane H+-ATPase genes are differentially expressed in iron-deficient cucumber plants. Plant Physiol. Biochem. 43:287-292

Shanmugam, V., Lo, J., Wu, C., Wang, S., Lai, C., Connolly, E.L., Huang, L. and Yeh, K. 2011. Differential expression and regulation of iron-regulated metal transporters in *Arabidopsis halleri* and *Arabidopsis thaliana* – the role in zinc tolerance. New Phytol. 190:125-137

Shin, L.J., Lo, J.C., Chen, G.H., Callis, J., Fu, H. and Yeh, K.C. 2013. IRT1 degradation factor1, a ring E3 ubiquitin ligase, regulates the degradation of iron-regulated transporter1 in *Arabidopsis*. Plant Cell 25:3039-3051

Spilianakis, C.G., Lalioti, M.D., Town, T., Lee, G.R. and Flavell, R.A. 2005. Interchromosomal associations between alternatively expressed loci. Nature 435:637-645

Takagi, S. 1976. Naturally occurring iron-chelating compounds in oat- and rice-root washing. I. Activity measurement and preliminary characterization. Soil Sci. Plant Nutri. 22:423-433

Talke, I.N., Hanikenne, M. and Kramer, U. 2006. Zinc-dependent global transcriptional control, transcriptional deregulation, and higher gene copy number for genes in metal homeostasis of the hyperaccumulator *Arabidopsis halleri*. Plant Physiol. 142:148-167

Thavarajah, D., Thavarajah, P., Sarker, A. and Vandenberg, A. 2009. Lentils (*Lens culinaris* Medikus Subspeices *culinaris*): A whole food for increased iron and zinc intake. J. Agri. Food Chem. 57:5413-5419

Thomas, M.C. and Chiang C.M. 2006. The general transcription machinery and general cofactors. Crit. Rev. Biochem. Mol. Biol. 41:105-178

Tuskan, G., Difazio, S., Jansson, S., et al. 2006. The genome of black cottonwood, *Populus trichocarpa* (Torr. & Gray). Science 313:1596-1604

Varotto, C., Maiwald, D., Pesares, P., Jahns, P., Salamini, F. and Leister, D. 2002. The metal ion transporter IRT1 is necessary for iron homeostasis and efficient photosynthesis in *Arabidopsis thaliana*. Plant J. 31:589-599

Vert, G., Barberon, M., Zelazny, E., Seguela, M., Briat, J.F. and Curie, C. 2009. *Arabidopsis* IRT2 cooperates with the high-affinity iron uptake system to maintain iron homeostasis in root epidermal calls. Planta 229:1171-1179

Vert, G., Briat, J.F. and Curie, C. 2001. *Arabidopsis* IRT2 gene encodes a root-periphery iron transporter. Plant J. 26:181-189

Vert, G., Grotz, N., Dedaladechamp, F., Gaymard, F., Guerinot, M.L., Briat, J.F. and Curie, C. 2002. *IRT1*, an *Arabidopsis* transporter essential for iron uptake from soil and for plant growth. Plant Cell 14:1223-1233

Waters, B.M. and Sankaran, R.P. 2011. Moving micronutrients from the soil to the seeds: Genes and physiological processes from a biofortification perspective. Plant Sci. 180:562-574

Waters, B.M., Lucena, C., Romera, F.J., Jester, G.G., Wynn, A.N., Rojas, C.L., Alcantara, E. and Perez-Vicente, R. 2007. Ethylene involvement in the regulation of the H(+)-ATPase *CsHA1* gene and of the new isolated ferric reductase *CsFRO1* and iron transporter *CsIRT1* genes in cucumber plants. Plant Physiol. Biochem. 45:293-301

Weigel, D and Glazebrook, J. 2006.Transformation of *Agrobacterium* using the freeze-thaw method. Cold Spring Harb. Protoc. doi:10.1101/pdb.prot4666

Winterbourn, C.C. 1995. Toxicity of iron and hydrogen peroxide: the Fenton reaction. Toxicol. lett. 82-83:969-974.

Wu, H., Li, L., Du, J., Yuan, Y., Cheng, X. and Ling, H.Q. 2005. Molecular and biochemical characterization of the Fe(III) chelate reductase gene family in *Arabidopsis thaliana*. Plant Cell Physiol. 46:1505-1514

Xiong, H., Guo, X., Kobayashi, T., Kakei, Y., Nakanishi, H., Nozoye, T., Zhang, L., Shen, H., Qiu, W., Nishizawa, N.K. and Zuo, Y. 2014. Expression of peanut iron regulated transporter 1 in tobacco and rice plants confers improved iron nutrition. Plant Physiol. Biochem. 80:83-89

Yang, X., Jawdy, S., Tschaplinski, T.J. and Tuskan, G.A. 2009. Genome-wide identification of lineage-specific genes in *Arabidopsis*, *Oryza* and *Populus*. Genomics 93:473-480

CHAPTER V. MOLECULAR CHARACTERIZATION OF THE BASIC HELIX-LOOP-HELIX (*BHLH*) GENES THAT ARE DIFFERENTIALLY EXPRESSED AND INDUCED BY IRON DEFICIENCY IN *POPULUS*

Abstract

The basic helix-loop-helix (*bHLH*) proteins play an important role in gene regulation by binding to specific DNA sequences affecting the rate of transcription. Five orthologs of eight *Arabidopsis bHLH* genes responding to iron deficiency in *Populus* were selected as candidate genes based on microarray analyses and previous studies. Open reading frame (ORF) regions of two *bHLH* genes (*PtFIT* and *PtIRO*) encoding a basic helix-loop helix protein were isolated from the iron deficiency susceptible (PtY) and tolerant (PtG) genotypes of *Populus tremula* L. 'Erecta'. The ORFs of *PtFIT* and *PtIRO* contain 939 and 795 bp nucleotides, respectively. Gene sequence analyses showed that each of the two genes was identical in PtG and PtY. Phylogenetic analysis revealed that *PtFIT* was clustered with the *bHLH* genes regulating iron deficiency responses in *Arabidopsis*, *Lycopersicon esculentum*, and *Malus xiaojinensis*, while *PtIRO* was clustered with another group of the *bHLH* genes that regulate iron deficiency responses in a *FIT* independent pathway. Tissue-specific expression analysis indicated that *PtFIT* was only expressed in the root, while *PtIRO* was rarely detected in all tested tissues. Real-time PCR showed that *PtFIT* was up-regulated in roots under the iron deficient condition. A higher level of *PtFIT* transcripts was detected in PtG than in PtY. Pearson Correlation Coefficient calculation suggested that there was a strong positive correlation (r=0.94) between *PtFIT* and *PtIRT1* in PtG, while a weak correlation (r=0.49) was observed in PtY. It suggests that the chlorosis tolerance of PtG may be regulated by the *PtFIT*-dependent iron deficiency response pathway. The *PtFIT*-transgenic poplar plants had an increased expression level of *PtFIT* and *PtIRT1* responding to

iron deficiency. One *PtFIT*-transgenic line (TL2) accumulated more Fe under the iron sufficient condition and had enhanced iron deficiency tolerance with higher chlorophyll content and Chl a/b ratio under the iron deficient condition than the control plants. Thus, our results indicated that *PtFIT* is involved in iron deficiency response and overexpression of *PtFIT* would enhance the tolerance to iron deficiency in *Populus*.

Introduction

Iron deficiency induced chlorosis causes yield loss and poor quality of crops, particularly in calcareous and high pH soils. Iron deficiency is not caused by the lack of iron in the soil, but rather the low availability for plants to absorb (Römheld and Marschner, 1986; Guerinot and Yi, 1994). Higher plants acquire iron from the soil through two strategies, reduction-based and chelation-based (Römheld and Marschner, 1986; Kobayashi and Nishizawa, 2012). Non-graminaceous plants (known as Strategy I species) acquire iron through the reduction-based strategy, which is accomplished by reducing Fe(III) to absorbable Fe(II) and then the absorbable Fe(II) is transported into the root by the *IRT1* transporter (Eide et al., 1996; Robinson, et al., 1999). Graminaceous plants (known as Strategy II species) produce Fe(III) chelators, mugineic acid family phytosiderophores (MAs), to form a complex of Fe(III)-MAs that is transported into the root by *YS1* (*Yellow stripe 1*) or YSL (*Yellow stripe 1-like)* transporter (Takagi, 1976; Curie et al., 2001; Murata et al., 2006; Inoue et al., 2009). Research has revealed that two groups of genes, *Ferric reductase oxidase* (*FRO*) and *Iron-regulated transporter* (*IRT*), are involved in iron reduction and transport in Strategy I species (Eide et al., 1996; Robinson, et al., 1999). When plants are exposed to the iron deficiency condition, the *FRO* and *IRT* genes are induced to reduce Fe(III) to Fe(II) and to regulate the transport of Fe(II) in plants (Eide et al., 1996; Vert et al., 2001; Jeong and Connolly, 2009).

Plants can survive under various stressful conditions by regulating the expression of genes that are involved in many biological changes. Gene regulation could be achieved by many ways, such as DNA methylation, transcriptional and post-transcriptional regulation, or regulation of translation (Latchman, 2007). Transcriptional regulation refers to the change at gene expression level via altering the transcription rate. Transcription factors are proteins that bind to a specific region of a promoter to control the transcription rate. As a large family of transcription factors, the *basic helix-loop-helix* (*bHLH*) proteins play an important role in regulating genes involved in iron deficiency responses in plants. A *bHLH* transcription factor (*LeFER*) isolated from tomato offered the first clue to know how iron deficiency responses are regulated by plants (Ling et al., 2002). The *fer* mutant in tomato failed to induce *LeIRT1* expression under the iron deficient condition, indicating the direct role of *LeFER* in regulating the *LeIRT1* gene. In addition, *LeFER* expression was suppressed by iron sufficiency at the post-transcriptional level (Brumbarova et al., 2005). An ortholog of *LeFER* named *AtFIT1* (*FER-like iron deficiency-induced transcription factor 1*, also known as *AtbHLH29* or *AtFRU*) is required for inducing the iron mobilization genes in *Arabidopsis* (Jakoby et al., 2004; Yuan et al., 2005). The *AtFIT1* gene regulates several iron deficiency inducible genes with known or putative functions in iron homeostasis, including *AtFRO2* and *AtIRT1* (Colangelo and Guerinot, 2004). Colangelo and Guerinot (2004) reported that *AtFIT1* regulated *AtFRO2* at the level of mRNA accumulation and *AtIRT1* at the level of protein accumulation. Further study demonstrated that with the co-expression of another two *AtbHLH* transcription factors, forming *AtFIT1*/*AtbHLH38* and *AtFIT1/AtbHLH39* complexes, *AtFRO2* and *AtIRT1* could be constitutively expressed even under the iron sufficient condition (Yuan et al., 2008). Additionally, another two *AtbHLH* transcription factors (*AtbHLH100* and *AtbHLH101*) within the same subgroup of *AtbHLH38* and *AtbHLH39*

were strongly induced by iron deficiency in the root and leaf of *Arabidopsis* (Wang et al., 2007). Sivitz et al. (2012) proposed that rather than the *AtFIT1* target genes, *AtbHLH100* and *AtbHLH101* likely regulate genes involved in the distribution of iron within the plant, suggesting that *AtbHLH100* and *AtbHLH101* play an *AtFIT1*-independent regulation role in iron deficiency responses. With a different opinion, Wang et al. (2013) proposed that both *AtbHLH100* and *AtbHLH101* could interact with *AtFIT1* according to the yeast two-hybrid analysis and bimolecular fluorescence complementation assay. Furthermore, Long et al. (2010) reported that in addition to *AtFIT1* acting as a master regulator in the iron deficiency response, *POPEYE* (*AtPYE,* also known as *AtbHLH047*) expressed specifically in the pericycle was also responding to iron deficiency. *AtPYE* helps maintain iron homeostasis by regulating the expression of known iron homeostasis genes and other genes involved in transcription, development, and stress response according to microarray data. Additionally, *AtPYE* interacts with *AtPYE* homologs, including *IAA–Leu Resistant3* (*AtILR3,* also named as *bHLH105*) or *AtbHLH115* that is involved in metal ion homeostasis to regulate the downstream target genes. In other species, Legay et al. (2012) proposed that in potato, the expression of the *FER*-like transcription factor that share 90% identities with the *LeFER* gene was also influenced by iron status and a strong positive correlation between the expressions of the *FER*-like transcription factor and *IRT1* was observed. In woody plants, three *bHLH* genes (*MxbHLH01*, *MxIRO2*, and *MxFIT*) were isolated and characterized in *Malus xiaojinesis*. The *MxbHLH01* expression was restricted to the root and up-regulated under the iron deficient condition and *MxbHLH01* might interact with other proteins to regulate genes in response to iron deficiency (Xu et al., 2011). The *MxIRO2* gene was induced in the root and leaf of *Malus xiaojinesis* under iron deficiency. It might form a heterodimer or multimer with other transcription factors to control the expression of genes related to iron

absorption (Yin et al., 2013). The *MxFIT* gene was up-regulated in roots under iron deficiency at both mRNA and protein levels, while almost no expression was detected in leaves irrespective of iron supply. The transgenic *Arabidopsis* plants with *MxFIT* had increased *AtIRT1* and *AtFRO2* transcripts in roots under the iron deficient condition, showing a stronger resistance to iron deficiency (Yin et al., 2014).

In a previous study described in Chapter IV, the *PtIRT1* gene from *Populus tremula* was cloned and its expression was strongly induced by iron deficiency; particularly, the increment of *PtIRT1* transcripts was much greater in the iron deficiency tolerant clone (PtG) than in the iron deficiency susceptible clone (PtY) of *Populus tremula*. However, overexpression of the *PtIRT1* gene in other transgenic poplar species did not enhance Fe accumulation compared to the wild type regardless of iron status. It indicated that some transcriptional control mechanisms might be involved in regulating *PtIRT1* in iron uptake and transport in poplar. Therefore, we cloned and characterized the *bHLH* genes from both iron deficiency tolerant and susceptible clones of *Populus tremula* and overexpressed them in other poplar species. The results would offer a view of how transcription factors regulate genes in response to iron deficiency and further strengthen the understanding of iron deficiency response mechanisms in woody species.

Materials and methods

Discovery of the *bHLH* candidate genes in response to iron deficiency in *Populus*

To identify *bHLH* proteins that may be in response to iron deficiency in *Populus*, the expression profile of the *Arabidopsis bHLH* genes in the root of *Arabidopsis* under iron deficiency at various time points was analyzed based on the published microarray data in NCBI. A total of 167 *bHLH* genes in *Arabidopsis* predicted by Carretero-Paulet et al. (2010) were used in this study. Microarray data were downloaded from the Gene Expression Omnibus under the

series entry GSE10502 (http://www.ncbi.nlm.nih.gov/geo/query/acc.cgi?acc=GSE10502). The expression data of the *AtbHLH* genes were extracted from GSE10502 using BRB-Array Tools software (Simon et al., 2007). All extracted data were normalized based on the mean expression value of each gene and analyzed and graphed using the mean of Multi Experiment Viewer software (Saeed et al., 2006). Genes were hierarchically clustered based on 'Pearson's correlation' distance matric and 'average linkage' method. Analysis of variance (ANOVA) was performed to identify the *AtbHLH* genes that expressed at a significantly different level in each treatment at the level of $P \leq 0.01$. The output genes were used as queries to BlastP their orthologs in *Populus trichocarpa* in NCBI. The putative orthologous genes showing high similarity to the *AtbHLH* genes in response to iron deficiency were considered as the candidates that may also respond to iron deficiency in *Populus.*

Plant materials and growth conditions

Iron deficiency tolerant (PtG) and susceptible (PtY) clones of *Populus tremula* L. 'Erecta' was used in this study. Plants were maintained and grown in a hydroponic system comprised of a 30-hole PVC plate, black plastic container (42 × 34 × 13 cm), Hoagland's solution, and an air pump. The PVC plate was floated on the solution that was prepared according to Hoagland and Arnon (1939). Each container contained seven liters of Hoagland's solution that was aerated with an air pump (TOPFIN Aquarium Air Pump, Model: AIR-8000) and refreshed every week. Each hole on the plate held one plant. The container was then covered by plastic film to maintain the moisture. To acclimate the plants, the film was gradually removed from the container after one week. For the iron sufficient treatment, plants were grown in full strength Hoagland's solution containing 30 μM Fe(II)-ethylenediaminetetraacetic acid (EDTA).

For the iron deficient treatment, Fe(II)-EDTA was removed from the Hoagland's solution and 200 μM ferrozine was added.

RNA extraction and cDNA preparation

Total RNA was isolated using the QIAGEN RNeasy Plant Mini Kit (QIAGEN Inc, Valencia, CA, USA) according to the manufacturer's instructions. RNA was isolated from three biological replicates of each treatment. Prior to cDNA synthesis, the RNA was quantified by a NanoDrop ND-1000 spectrophotometer (Thermo Fisher Scientific Inc., Waltham, MA, USA) and agarose gel electrophoresis. A total of 1 μg RNA was treated with gDNA wipeout buffer to eliminate possible contaminating genomic DNA and then subjected to reverse transcription with RT primer mix (oligo-dT and random primers) and unique QIAGEN Omniscript and Sensiscript reverse transcriptases according to the manufacturer's instructions of the QuantiTect Reverse Transcription Kit (QIAGEN Inc, Valencia, CA, USA).

Gene cloning and sequence analysis

The open reading frame (ORF) region of each candidate gene was cloned from *Populus tremula* using the homology cloning method. Primers were designed using the PrimerSelect module of the DNASTAR Lasergene® software package (DNASTAR, Inc., Madison, WI, USA). All primers used for gene cloning and RT-PCR were listed in Table 5.1. The PCR was performed according to the instructions of the Elongase® Enzyme Mix (Invitrogen™, Carlsbad, CA, USA). Target PCR products were purified using the QIAquick Gel Extraction Kit (QIAGEN Inc, Valencia, CA, USA) and then ligated into the pGEM-T easy vector (Promega, Madison, WI, USA). Plasmid DNA was extracted from the white colonies grown on indicator plates containing X-gal and IPTG, using a PerfectPrep™ Spin Mini Kit (5 PRIME Inc., Gaithersburg, MD, USA) and sent for sequencing at the Iowa State University DNA Facility (Ames, IA, USA). The

domains of putative proteins were analyzed using SMART (http://smart.embl-heidelberg.de/). A phylogenetic tree was constructed using the predicted amino acid sequences of the *bHLH* genes from *Populus* and other species by the MegAlign module of the DNASTAR Lasergene® software package.

Evaluation of the expression profile of the *bHLH* genes using semi-quantitative RT-PCR

The expression profile of the *bHLH* genes in various poplar tissues including the root tip, root, phloem, xylem, mature leaf, young leaf, and shoot tip was analyzed using semi-quantitative RT-PCR. Samples were collected from PtG and PtY grown under the iron sufficient condition. Primers corresponding to the *PtbHLH* genes and the *Populus* actin gene (NCBI accession no: XM_002298674.1) were designed using the PrimerSelect module of the DNASTAR Lasergene® software package and listed in Table 5.1. Prior to RT-PCR, the quality of cDNA was assessed by PCR using actin-specific primers designed to span introns to detect genomic DNA contamination. PCR amplification was carried out in a 16 µl reaction that consisted of 5 ng cDNA template, 0.375 µM of each primer, 0.2 mM dNTP, 1.5 mM $MgCl_2$, 1×Green GoTaq® Flexi buffer, and 5 U *Taq* DNA Polymerase. The amplification conditions were: denaturing for 30 s at 94 °C (3 min before the first cycle), annealing for 40 s at 56 °C, and extension for 50 s at 72 °C (5 min after the final cycle) for 30 cycles. PCR products were separated in a 2% agarose gel at 110 volts (V) for 30 min. The gel was visualized under UV light and images were captured using a AlphaImager® Gel Documentation System (Proteinsimple Inc., Santa Clara, California, USA).

Expression quantification of the *bHLH* genes responding to iron deficiency using real-time quantitative PCR

The expression of the *bHLH* genes in the root of the poplar plant responding to iron deficiency was evaluated by real-time quantitative PCR using an ABI 7900HT Fast Real-Time PCR System (Applied Biosystems, Foster City, CA, USA). Samples for RNA extraction were collected from PtG and PtY plants after they were transferred to the iron deficient solution for 0, 0.5, 1, 3, and 6 days. Each treatment had three biological replicates with 10 individual plants per replicate. Gene specific primers were designed based on the sequences of the *PtbHLH* genes and *PtTIF5α* (NCBI accession no: CV251327.1) was used as the internal control gene (Table 5.1). Amplification conditions were: (1) incubation at 95 °C for 5 min; (2) cDNA amplification for 35 cycles at 95 °C for 15 s, 56 °C for 20 s, and 72 °C for 30 s. To evaluate amplification specificity, melting curve analysis was performed at the end of each PCR run according to the manufacturer's recommendation. The melting curve temperature profile was generated through the cycle of 95 °C for 1 min, 60 °C for 1 min, and heating to 95 °C in 20 min. Each sample had two technical replicates. Real-time PCR data were exported from ABI 7900HT software version SDS v2.2.

The absolute quantity of the target gene was determined according to the methods of Peirson et al. (2003) and Larionov et al. (2005). In brief, the artificial plasmid DNA template containing the real-time PCR amplicons of the target gene was constructed using the pGEM-T easy vector system. The purified plasmid DNA was diluted at 1:10 ratio from 10^{-2} ng/µl to 10^{-6} ng/ µl. The standard curve was generated by the Absolute Quantification of ABI 7900HT Fast Real-Time PCR system according to the manufacturer's instructions. The copy number corresponding to each ng of plasmid DNA was calculated based on the method at

http://cels.uri.edu/gsc/cndna.html. The amplification efficiency was calculated based on the slope of the standard curve at http://www.thermoscientificbio.com/webtools/qpcrefficiency/. The final expression data was presented as a ratio of the copy number of *PtbHLHs* to that of *PtTIF5α.*

Expression vector construction and plant transformation

The *Suppro::PtbHLH* vector was constructed using the pCAMBIA S1300 expression vector system (Figure 4.2). Gene transformation was carried out using *Agrobacterium*-mediated method according to Dai et al. (2003) and Han et al. (2000). Briefly, leaves of *P. canescens* × *P. grandidentata* ('Cl6') were infected with *Agrobacterum tumefaciens* strain EHA 105 harboring the *Suppro::PtbHLH* vector for 30 min and then placed in woody plant medium WPM (Lloyd and McCown, 1980) containing 10 μM 6-benzylaminopurine (BA), 5 μM naphthaleneacetic acid (NAA) and 100 μM acetosyringone for 2-3 days in the dark. Co-cultivated leaves were rinsed with sterile water 3 times and placed in the selection medium (WPM with 10 μM BA and 5 μM NAA) supplemented with 5 μM hygromycin for callus induction under the dark condition. Four weeks later, induced calli were transferred to the shoot induction medium (WPM with 0.05 μM thidiazuron (TDZ) supplemented with 5 μM hygromycin) under a 16/8 h photoperiod condition. After another four weeks, the individual regenerated-shoots were rooted in ½ MS medium supplemented with 0.5 μM NAA and 5 μM hygromycin. Verified transgenic lines were proliferated and grown in the hydroponic culture system.

Molecular characterization of transgenic events

Transgenic lines were confirmed by PCR with the specific primers located in the flanking region of the insertions according to the method of Dai et al. (2003) (Table 5.1). The expression level of *PtFIT* and *PtIRT1* was determined in the root of transgenic plants grown under either iron sufficient or deficient conditions by real-time quantitative PCR as described above.

Table 5.1. Primers used in this study.

Primer	Sequence (5'-3')	Application
PtFIT-F3	GTATCTTCTAGAAAAGAATGGATAGGATGGATGA	*PtFIT* cloning
PtFIT-R3	CATAGAGAGCTCAGGGCTAAACAGATGGATT	
PtIRO-F2	TAATAACCCTCCAACTAATCCACA	*PtIRO* cloning
PtIRO-R2	GAAGGTTTTTGCGACAGTATCTAA	
PtFIT-F1	ACCGCCACAACGACTAAGAAGAC	Semi-quantitative/real-time quantitative RT-
PtFIT-R1	AACCAAGGACCGCAAAGCATA	PCR for *PtFIT*
PtIRO-F2	TAATAACCCTCCAACTAATCCACA	Semi-quantitative/real-time quantitative RT-
PtIRO-R6	CATCTCTAAAGCTGCACTGTTCAT	PCR for *PtIRO*
PtAct1-F7	ATGGTTGGAATGGGGCAGAAG	Semi-quantitative RT-PCR internal control
PtAct1-R7	CGAAGGATGGCGTGTGGA	*PtAct1*
PtTIF5α-F	GACGGTATTTTAGCTATGGAATTG	Real-time quantitative PCR for reference
PtTIF5α-R	CTGATAACACAAGTTCCCTGC	*PtTIF5α*
T-DNA-F	ACGTCGCATGCTCCCGG	Gene transfer confirmation
T-DNA-R	CATATGGTCGACCTGCAG	

Physiological analysis of transgenic plants grown under the iron deficient condition

The content of chlorophyll and carotenoids, Chl a/b ratio, and the content of Mn, Zn, Fe and Cu in the control and transgenic plants grown in either iron sufficient or iron deficient condition were determined. Leaves were collected at day 9 after the treatment. The content of chlorophyll a, chlorophyll b, and carotenoids was determined following the method of Lichtenthaler (1987). Briefly, chlorophyll was extracted from about 0.2 g ground leaves using 1.8 ml 80% acetone overnight at 4°C. After centrifugation at 10,000 rpm for 8 min, the absorbance of the combined 20 µl supernatant extractions with 980 µl 80% acetone was measured at 470 nm, 646.8 nm, and 663.2 nm using a BECKMAN DU-600 spectrophotometer (Beckman Coulter Inc. CA) with 80% acetone as the reference for the spectrophotometer. The concentration of chlorophyll in each cuvette (test conc.) was calculated as follows: Chl a = 12.25A663.2-2.79A646.8; Chl b = 21.50A646.8-5.10A663.2; Chl a+b=7.15A663.2+18.71A646.8; carotenoids (xanthophylls and β-carotene) = (1000A470-1.82Chla-85.02Chlb)/198. The final chlorophyll concentration (mg/kg FW) was calculated using the equation: Conc. = test conc.×1000×1.8/20/sample weight. For determining the content of mineral elements, leaf samples were oven-dried at 65°C for 2 days and subjected to leaf tests in the North Dakota State University Cereal Science lab according to the method of Thavarajah et al. (2009).

Statistical analysis

Data were expressed as mean±SE. An unpaired two-tailed t-test was used to analyze significant differences between the treatment and the control.

Results

Discovery of the *bHLH* candidate genes in response to iron deficiency in *Populus*

A total of 117 *AtbHLH* genes had the corresponding probes in the array of GSE10502 containing 22,810 genes based on the microarray gene annotation database. Figure 5.1a illustrates the expression pattern of individual *AtbHLH* genes. The seven time points of the iron deficiency treatment (0, 3, 6, 12, 24, 48, and 72 h) were clustered into three groups: Group 1 included 0 and 3 h treatment; group 2 included 6, 12, and 24 h treatment, and Group 3 contained 48 and 72 h treatment. A significant difference in gene expression was observed between group 1 and 3, indicating that the *bHLH* genes might respond to iron deficiency at 3 h after the treatment and such a response could be clearly observed at 48 h after the treatment. According to the ANOVA analysis, 25 *AtbHLH* genes showed significant differences in the level of expression at seven time points (Figure 5.1b). Of these genes, nine (*At007*, *At039ORG3*, *At047*, *At059UN12*, *At093*, *At101*, *At105ILR3*, *At115*, and *At143*) were up-regulated and the rest of genes were down-regulated by iron deficiency. Previous research confirmed that *At105ILR3*, *At101*, *At115*, *At039ORG3*, and *At047* were transcription factors that positively regulate iron deficiency responses in plants (Wang et al., 2007, 2013; Yuan et al., 2008; and Long et al., 2010). In other research, the *At093* gene was found to be involved in stomatal development (Ohashi-Ito and Bergmann, 2006) and *At059UN12* may be related to fertilization (Pagnussat et al., 2005). No research was reported regarding the function of *At007*and *At143.* Therefore, the orthologs of *At105ILR3*, *At101*, *At115*, *At039ORG3*, and *At047* in *Populus trichocarpa* were considered as the candidate genes that may regulate responses to iron deficiency in *Populus*. In addition, *At029 FRU*, *At038ORG2*, and *At100* likely play an important role in regulation of iron deficiency. No corresponding probes of *At038ORG2* and *At100* in the microarray were identified and the P

value of *At029 FRU* was 0.024 (> 0.01) according to the ANOVA analysis. All eight orthologs in *Populus* are listed in Table 5.2.

Table 5.2. The BlastP identified candidates of the *bHLH* genes related to iron deficiency response in *Populus.*

Arabidopsis accessions	*Populus* accessions	Query cover	E-value	Identity
At029FRU (At2G28160)	XP_002313541.2	95%	5.00E-86	50%
At038ORG2 (At3G56970)	XP_002307969.2	97%	7.00E-51	48%
	XP_002323250.2	97%	3.00E-49	47%
At039ORG3(At3G56980)	XP_002307969.2	93%	1.00E-45	47%
	XP_002323250.2	94%	3.00E-41	43%
At047(At3G47640)	XP_002303343.1	91%	1.00E-59	51%
At100(At2G41240)	XP_002307969.2	94%	2.00E-39	41%
	XP_002323250.2	94%	3.00E-36	42%
At101(At5G04150)	XP_002307969.2	93%	2.00E-39	44%
At105ILR3 (At5G54680)	XP_002316971.1	100%	1.00E-93	68%
At115(At1G51070)	XP_002316971.1	64%	1.00E-75	69%

Cloning and sequence analysis of *PtFIT* and *PtIRO*

The open reading frame (ORF) regions of two candidate genes were amplified from the cDNA of *Populus tremula* (PtG and PtY). The PCR primers were designed according to the corresponding nucleotide sequence information of XP_002313541.2 and XP_002323250.2. Nucleotide sequence alignment revealed that either of two genes was identical in both PtG and PtY. Based on their similarity to the *bHLH* genes, the two genes were named *PtFIT* and *PtIRO (iron-related transcription factor)*, respectively (Figure 5.2). The 939 bp ORF of *PtFIT* encoded a deduced protein of 313 amino acid residues with a molecular weight of 34.9 kDa and an

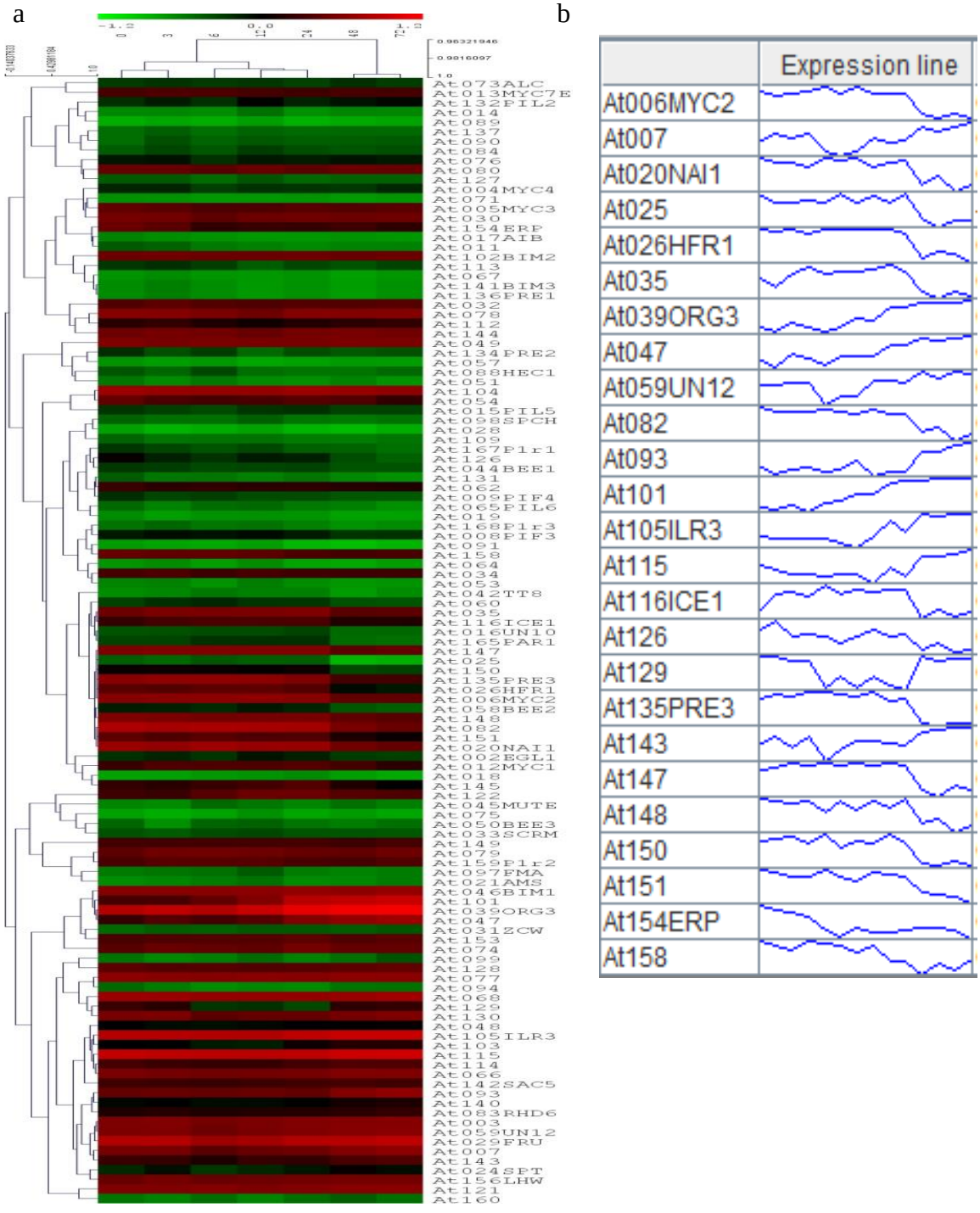

Figure 5.1. Expression profiles of the *AtbHLH* genes in response to iron deficiency at different time points after the iron deficient treatment. a: Microarray analysis of the 117 *AtbHLH* genes. Genes and samples are ordered based on a hierarchical clustering analysis; b: Expression patterns of 25 *AtbHLH* genes showing significant differences at different time points.

isoelectric point of 4.74. The 795 bp ORF of *PtIRO* encoded a deduced protein of 265 amino acid residues with a molecular weight of 30.0 kDa and an isoelectric point of 6.55. Deduced amino acid sequence analysis revealed that *PtFIT* showed 14.0% - 57.1% identity to other *bHLH* genes (57.15% to *AtbHLH29* and 55.7% to *MxFIT*). The *PtIRO* also showed 14.3% - 54.7% identity to other *bHLH* genes (54.7% to *MxIRO2*). Alignment analysis of amino acid sequences showed that *PtFIT* and *PtIRO* contained the conserved bHLH domain (Pfam accession: PF00010) (Figure 5.3). Phylogenetic analysis suggested that the bHLH proteins could be divided to two subgroups (Figure 5.4). *PtFIT* was clustered with *AtbHLH29*, *LeFER*, *MxbHLH01*, and *MxFIT*, while *PtIRO* was clustered with the rest of *bHLHs*. The distinct structures between these two subgroups might lead to the divergence in their functions. A similar result was reported by Carretero-Paulet et al. (2010) where *AtbHLH29* and *AtbHLH38/AtbHLH39* belong to two different subfamilies and play different roles.

Percent Identity

Divergence

	1	2	3	4	5	6	7	8	9	10	11	12	13	
1		34.1	16.0	60.3	63.3	30.4	14.7	15.5	16.9	39.7	30.5	15.0	42.4	1
2	137.1		14.4	39.7	39.3	32.1	13.6	13.9	15.4	37.4	31.7	14.5	38.3	2
3	309.0	342.0		14.5	17.5	15.4	48.3	47.6	52.1	14.6	14.2	57.1	14.9	3
4	56.1	112.5	339.0		80.7	32.6	13.6	15.2	16.6	44.0	31.5	14.0	45.9	4
5	50.0	114.2	282.0	22.4		31.9	15.0	17.1	19.4	44.9	30.3	16.9	43.5	5
6	157.7	147.3	319.0	144.7	148.5		13.7	14.1	16.7	36.0	69.7	15.9	35.5	6
7	335.0	365.0	84.5	362.0	328.0	362.0		50.0	46.9	15.4	12.3	49.3	14.3	7
8	317.0	354.0	86.5	325.0	287.0	352.0	79.9		70.1	15.5	11.7	51.3	15.5	8
9	291.0	321.0	74.4	298.0	253.0	296.0	88.5	38.1		14.3	16.0	55.7	16.1	9
10	112.4	121.9	337.0	97.4	94.6	128.1	319.0	319.0	344.0		34.0	14.8	54.7	10
11	156.6	149.6	347.0	150.8	158.1	38.8	403.0	430.0	309.0	137.3		14.3	35.3	11
12	330.0	342.0	62.7	354.0	291.0	309.0	81.8	76.4	65.7	332.0	344.0		14.7	12
13	102.9	118.3	332.0	91.4	99.0	130.1	344.0	317.0	307.0	68.1	131.3	337.0		13
	1	2	3	4	5	6	7	8	9	10	11	12	13	

AtbHLH100 NP_181657
AtbHLH101 ADY38577
AtbHLH29 NP_850114
AtbHLH38 NP_191256
AtbHLH39 NP_191257
HvIRO2 BAF30424
LeFER NP_001234654
MxbHLH01 ADY38577
MxFIT
MxIRO2
OsIRO2 FAA00382
PtFIT
PtIRO

Figure 5.2. Deduced amino acid sequence similarity of the *PtFIT* and *PtIRO2* genes with other *bHLH* proteins calculated by ClustalW. The accession numbers of studied proteins follow the gene names. The corresponding sources are: *Lycopersicon esculentum* (*Le*), *Malus xiaojinensis* (*Mx*), *Arabidopsis thaliana* (*At*), *Oryza sativa* (*Os*), and *Hordeum vulgare* (*Hv*).

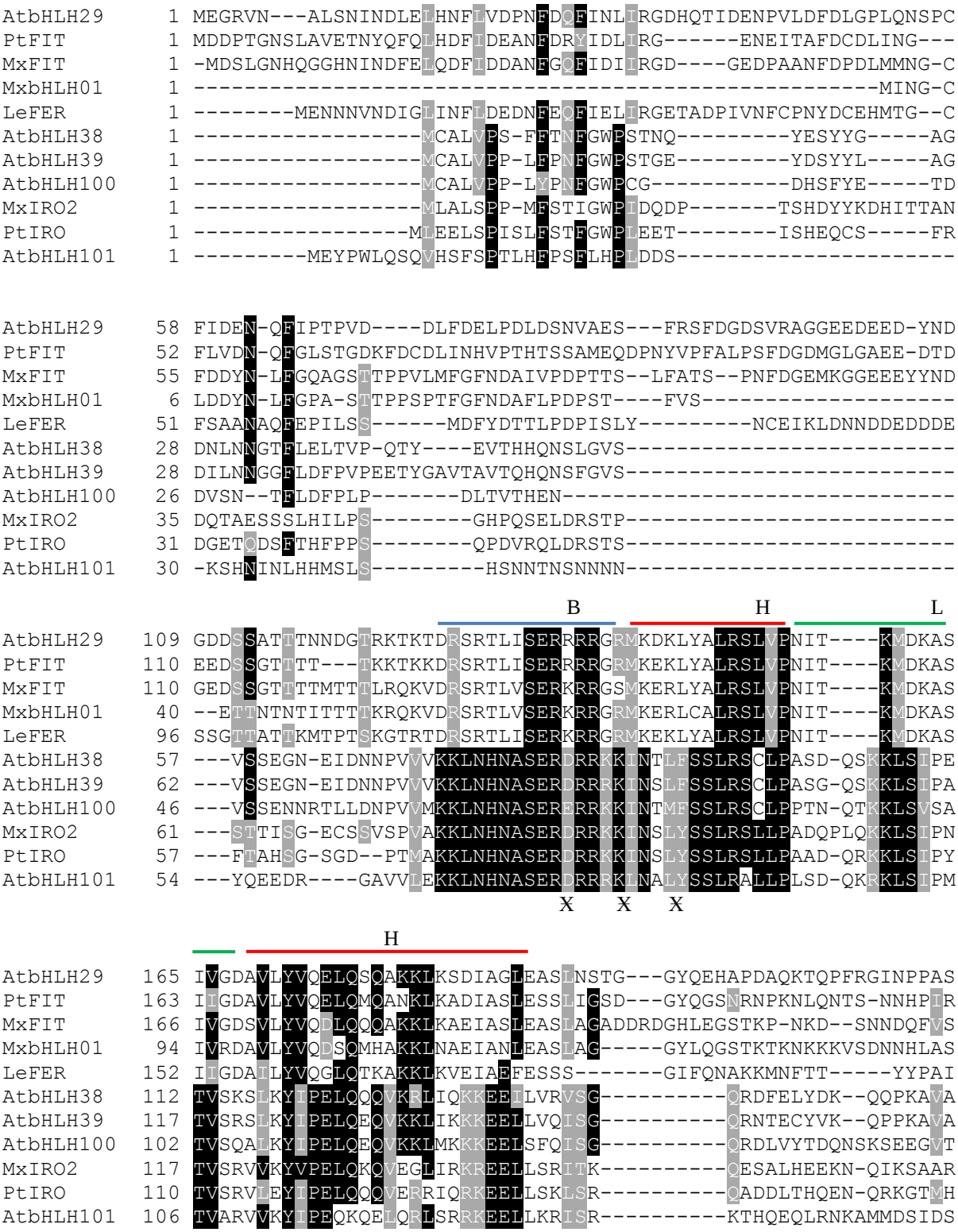

Figure 5.3. Amino acid alignment of the *bHLH* genes in this study. The *bHLH* conserved domain is indicated with lines. Shaded areas represent identical residues (black) or similar residues (gray) found in most of the proteins. 'X' indicates the motifs.

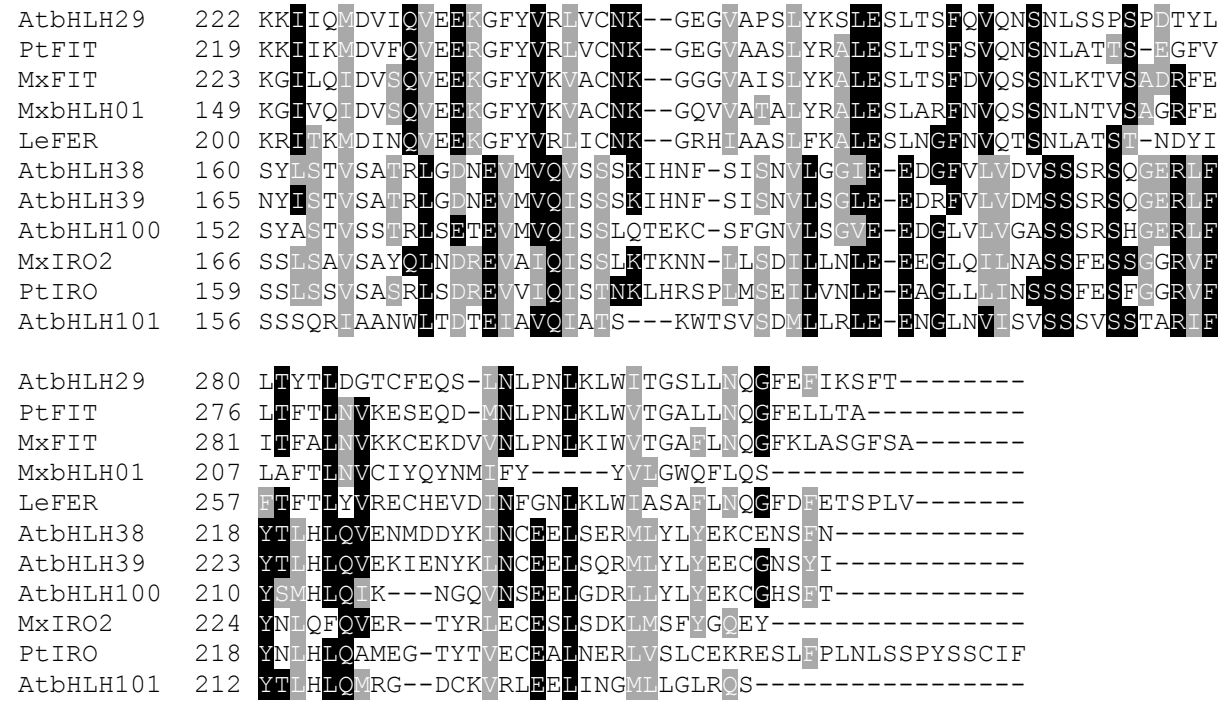

Figure 5.3. Amino acid alignment of the *bHLH* genes in this study (continued). The *bHLH* conserved domain is indicated with lines. Shaded areas represent identical residues (black) or similar residues (gray) found in most of the proteins. '**X**' indicates the motifs.

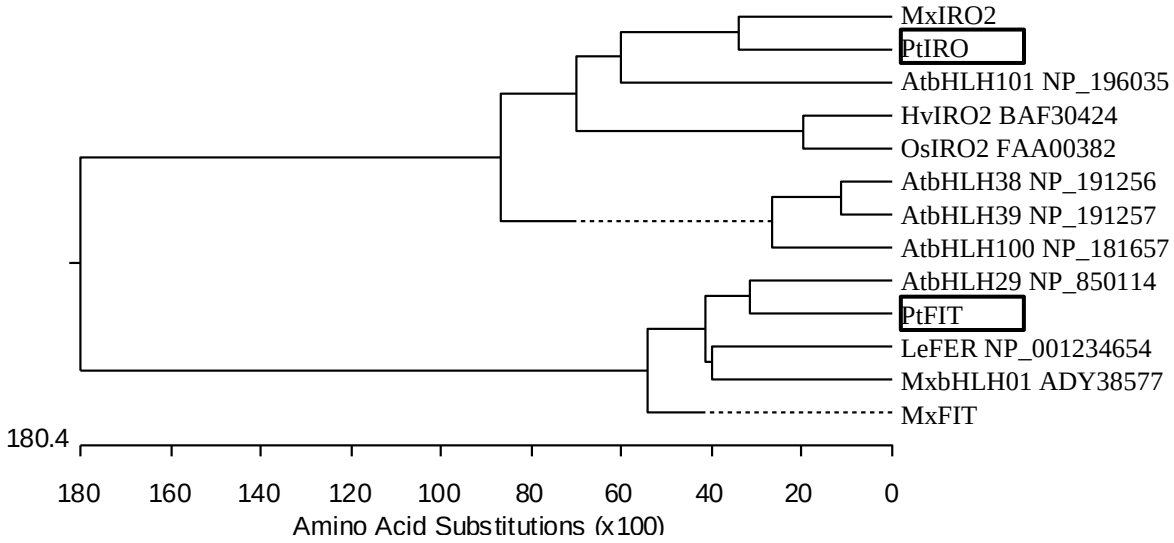

Figure 5.4. A phylogenetic tree of the *PtFIT*, *PtIRO2*, and other *bHLH* genes constructed by ClustalW. The accession numbers of studied proteins follow the gene names. *PtFIT* and *PtIRO* are framed. The corresponding sources are: *Lycopersicon esculentum* (*Le*), *Malus xiaojinensis* (*Mx*), *Arabidopsis thaliana* (*At*), *Oryza sativa* (*Os*), and *Hordeum vulgare* (*Hv*).

Expression analysis of *PtFIT* and *PtIRO*

The expression of *PtFIT* and *PtIRO* in the root tip, root, phloem, xylem, mature leaf, young leaf, and shoot tip of both PtG and PtY was determined using semi-quantitative PCR. As shown in Figure 5.5, *PtFIT* expressed only in the root tip and root, while a weak expression of *PtIRO* was detected in the young leaf and shoot tip. A real-time quantitative PCR was conducted to evaluate the expression profile of *PtFIT* in the root responding to iron deficiency at different times after the iron deficiency treatment (Figure 5.6). Results showed that a slight decrease of the *PtFIT* transcript was detected at day 0.5, then gradually increased and peaked at day 6 in PtG. In PtY, the expression of *PtFIT* showed the first peak at day 1, and then decreased until day 3. The second expression peak of *PtFIT* in PtY was detected at day 6. The expression level of *PtFIT* at day 6 was more than 2-fold higher in PtG than in PtY.

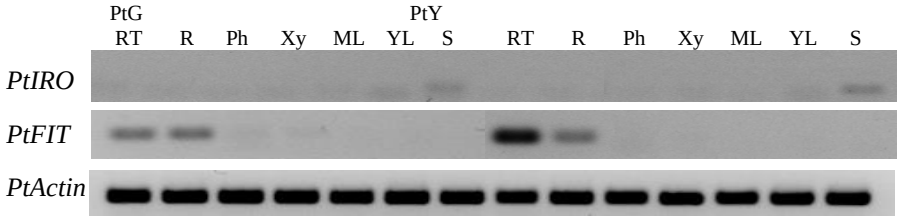

Figure 5.5. Tissue-specific expression of *PtFIT* and *PtIRO* in PtG and PtY determined by semi-quantitative PCR. PtG: iron chlorosis tolerant clone of *Populus tremula*; PtY: iron chlorosis susceptible clone of *Populus tremula*; RT: root tip; R: root; Ph: phloem; Xy: xylem; ML: mature leaf; YL: young leaf; ST: shoot tip.

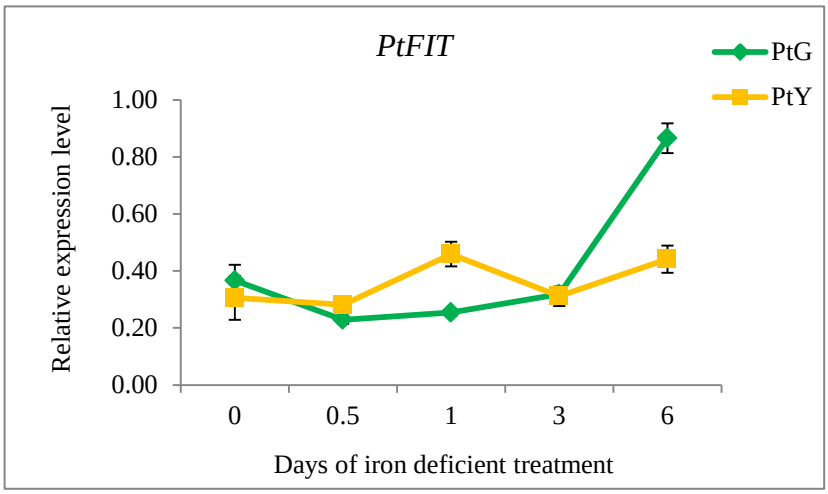

Figure 5.6. Relative expression level of *PtFIT* in the root of PtG and PtY responding to iron deficiency at 0, 0.5, 1, 3, and 6 days. The relative expression is quantified by real-time PCR and normalized to the *PtTIF5α* gene.

Overexpression of the *PtFIT* gene in *P. canescens* × *P. grandidentata* 'Cl6'

Overexpression of the *PtFIT* gene was confirmed in five independent transgenic lines of *P. canescens* × *P. grandidentata* 'Cl6'. One line with the empty vector (no *PtFIT*) was the control (NC). As shown in Figure 5.7, the expression level of *PtFIT* in transgenic lines decreased under the iron sufficient condition except TL5 that was similar to NC. Under the iron deficient condition, the expression of *PtFIT* significantly increased except in TL13. Two transgenic lines (TL12 and TL5) showed a significantly higher expression level of *PtFIT* than the control under iron deficiency. The expression pattern of *PtIRT1* in *PtFIT*-transgenic lines was also evaluated. Similar to that of *PtFIT*, the expression of *PtIRT1* was also inhibited under iron sufficiency and dramatically enhanced under iron deficiency (Figure 5.7). Compared to NC, *PtIRT1* transcripts in transgenic plants were reduced more than half under the iron sufficient condition, while *PtIRT1* transcripts were significantly increased in TL10 compared to NC under iron deficiency.

On the other hand, *PtIRT1* transcripts were increased 2.44 times in NC and 3.38-13.43 times in transgenic plants under the iron deficient condition.

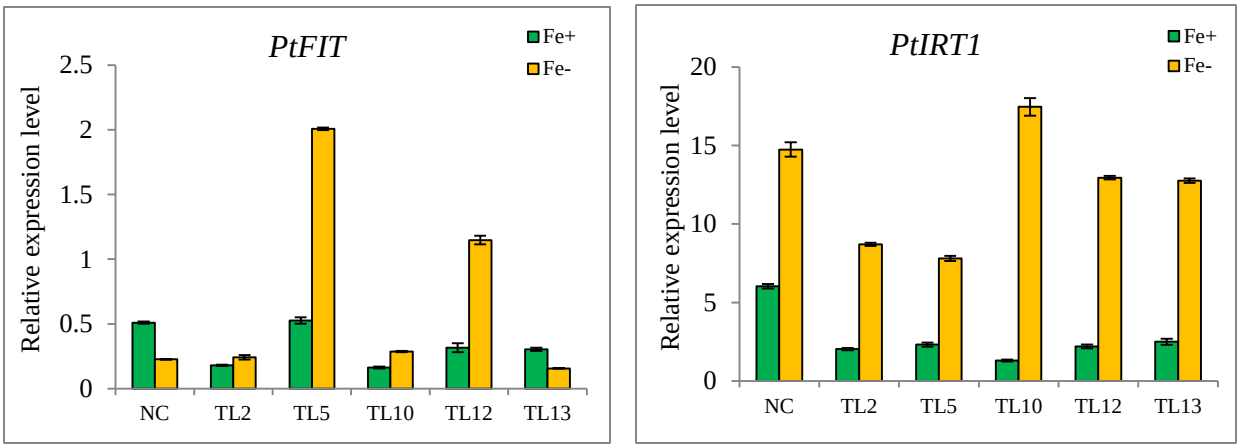

Figure 5.7. Quantitative assay of *PtFIT* and *PtIRT* expression in transgenic poplar plants. Plants were grown under iron sufficiency (Fe+) or deficiency (Fe-). NC: the transgenic line with the empty vector (no target gene). The relative expression is quantified by real-time PCR and normalized to the *PtTIF5α* gene.

Physiological analysis of the *PtFIT*-transgenic lines responding to iron deficiency

The contents of chlorophyll and mineral elements in the *PtFIT*-transgenic leaves were determined. As shown in Figure 5.8 and 5.9, no significant increase of chlorophyll (Chl a+b), Chl a/b ratio, or carotenoids was observed in transgenic lines under the iron sufficient condition. Under the iron deficient condition, the chlorophyll content decreased in TL10 and TL13 as well as in NC, but no significant changes in TL12, TL2, and TL5 were detected. The Chl a/b ratio also decreased under iron deficiency in all transgenic plants as well as in NC. TL2 had the highest Chl a/b ratio in all transgenic lines (Figure 5.8). Similarly, iron deficiency significantly decreased the content of carotenoids in NC, while no significant changes in transgenic plants except TL2 (Figure 5.9). The contents of Mn, Zn, Cu, and Fe in leaves of the transgenic plants under the iron deficient or sufficient condition were determined (Figure 5.10). In general, iron

deficiency showed no effect on Mn content, but slightly lowered the Zn content. Iron content was significantly decreased and Cu content was significantly increased under iron deficiency. Under the iron sufficient condition, transgenic lines accumulated more Zn and Fe with the exception that TL5 had a similar Fe content to NC. Under iron deficiency, TL2 and TL5 accumulated more Zn than other lines and NC; while no significant difference in Fe, Mn, or Cu content was found among all transgenic and NC lines.

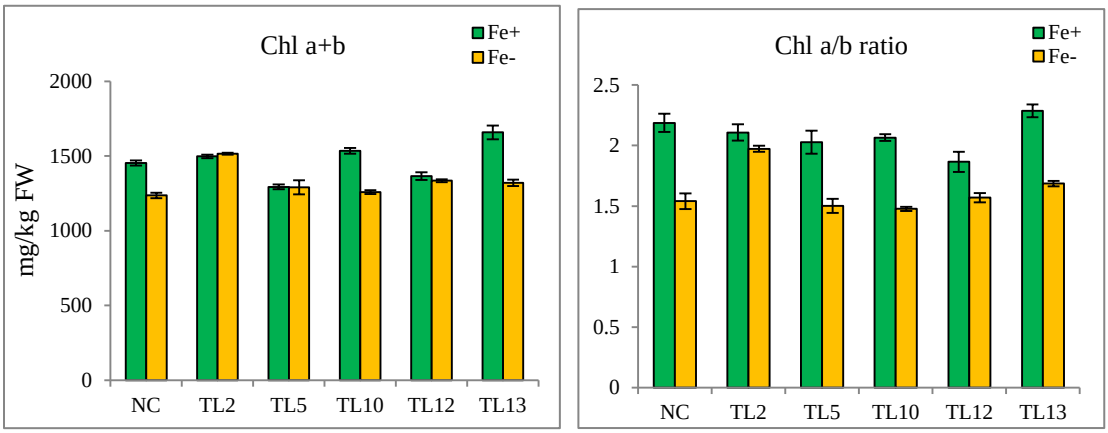

Figure 5.8. Chlorophyll content and Chl a/b ratio in the *PtFIT*-transgenic poplar lines under iron sufficient (Fe+) and deficient (Fe-) conditions. NC: the transgenic line with the empty vector (no target gene).

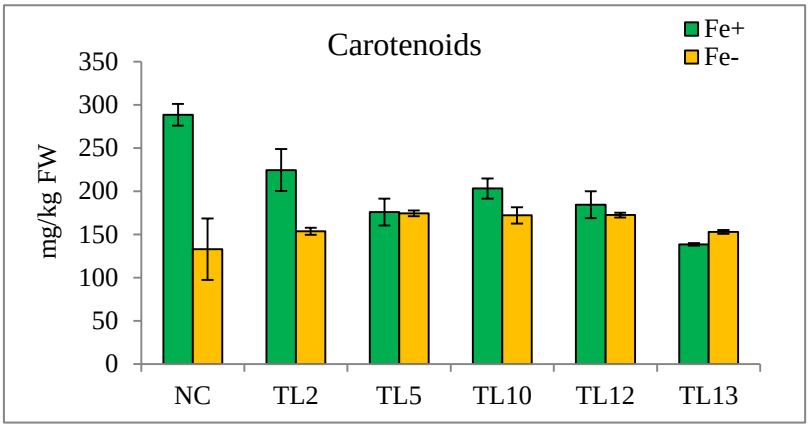

Figure 5.9. Carotenoid content in the *PtFIT*-transgenic poplar lines under iron sufficient (Fe+) and deficient (Fe-) conditions. NC: the transgenic line with the empty vector (no target gene).

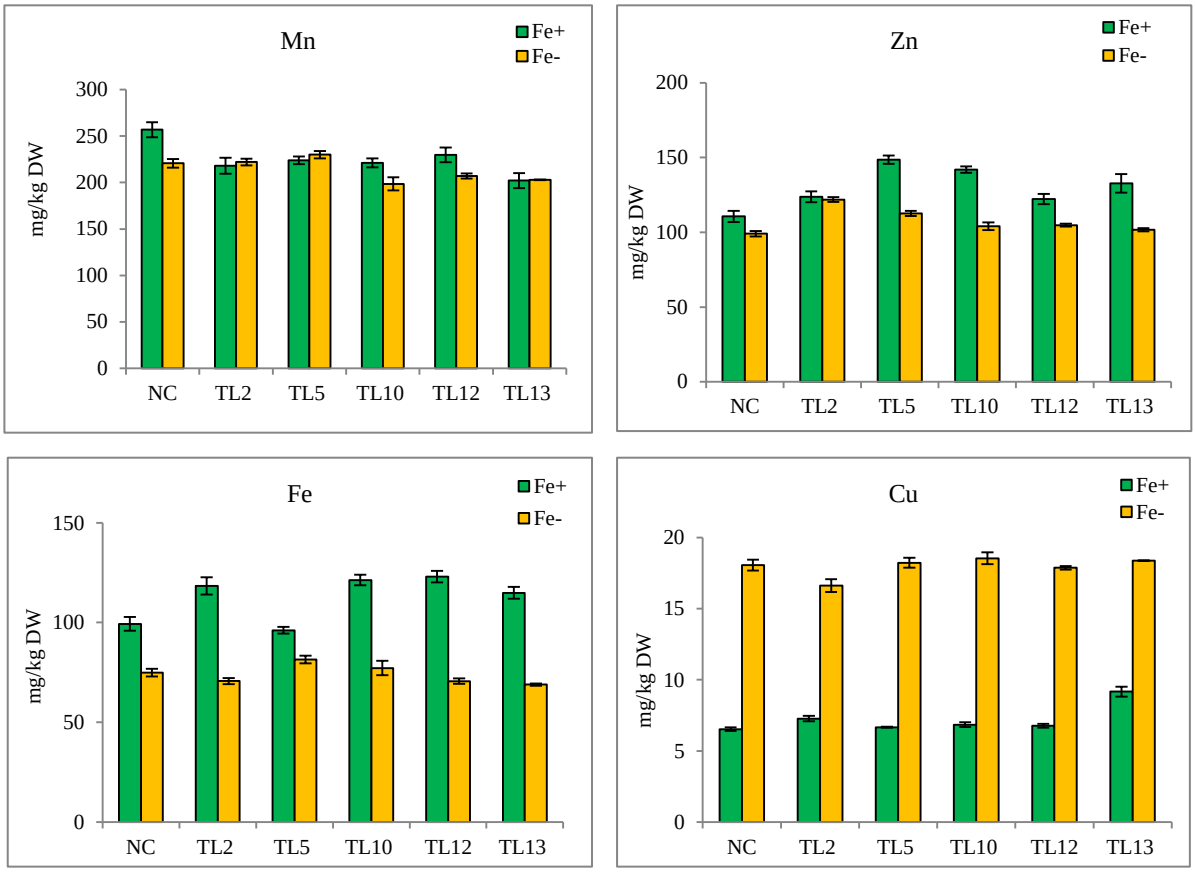

Figure 5.10. The content of Mn, Zn, Fe, and Cu in the leaf of the *PtFIT*-transgenic poplar lines under iron sufficient (Fe+) and deficient (Fe-) conditions. NC: the transgenic line with the empty vector (no target gene).

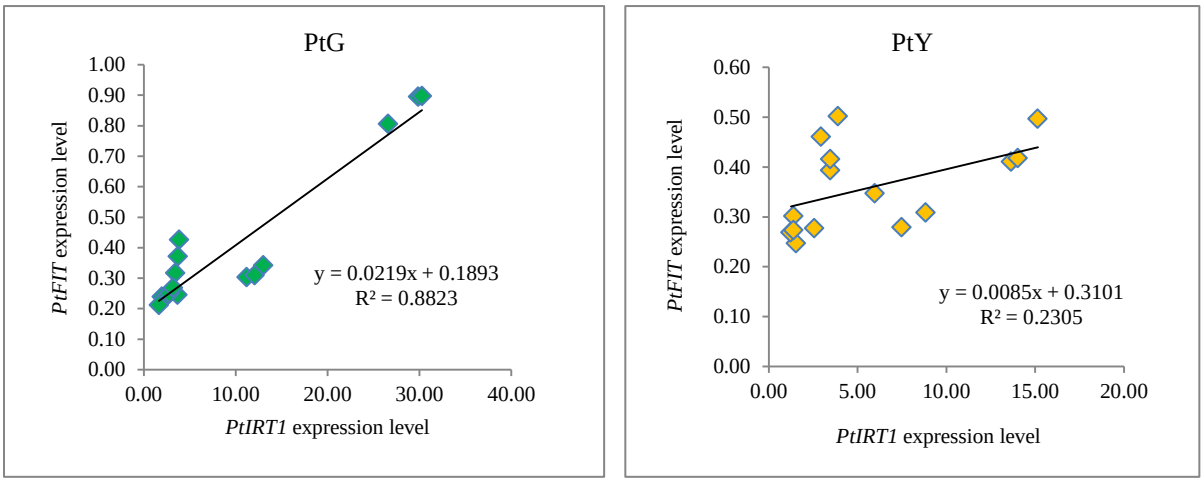

Figure 5.11. Correlation between the expression levels of *PtIRT1* and *PtFIT* responding to iron deficiency calculated by Pearson Correlation Coefficient Calculator. Expression levels are normalized as a ratio to the *PtTIF5α* gene.

Discussion

The basic helix-loop-helix (*bHLH*) is an important family of transcription factors (Massari and Murre, 2000). In this study, the orthologs of the *AtbHLH* genes responding to iron deficiency in *Populus* were discovered using microarray data. Microarray is a useful tool to explore the genes responding to changes of the environmental conditions. In *Arabidopsis*, the microarray method has been used to analyze the genome-wide responses of genes to iron deficiency, such as the differential expression in different tissues (shoots, roots, or leaves) or under different Fe supply conditions (Dinneny et al., 2008; Buckhout et al., 2009; Li and Schmidt, 2010; Long et al., 2010; Schuler et al., 2011; Ivanov et al., 2012; Sivitz et al., 2012; Waters et al., 2012).We analyzed the expression profile of the *AtbHLH* genes in response to iron deficiency in the root using the microarray data submitted by Dinneny et al.(2008). Twenty-five *AtbHLH* genes showed the responses to iron deficiency (Figure 5.1b). Among them, three up-regulated genes (*At039ORG3*, *At047*, and *At101)* were also confirmed by other microarray analyses that involved in iron deficiency responses (Sivitz et al., 2012; Waters et al., 2012). Five orthologs of *AtbHLH* were identified in *Populus trichocarpa* according to the BlastP result and two out of five (*PtFIT* and *PtIRO*) that are homologues of XP_002313541.2 and XP_002323250.2 were cloned from *Populus tremula*.

Amino acid sequence analyses revealed that the *bHLH* domain sequences of *PtFIT* and *PtIRO* had the highest similarity with *AtbHLH29* and *MxIRO2*, respectively (Figure 5.2). *AtbHLH29* and *MxIRO2* functioned as regulators of the genes responding to iron deficiency (Colangelo and Guerinot, 2004; Jakoby et al., 2004; Yuan et al., 2005; Yin et al., 2013). Phylogenetic analysis showed that the two iron deficiency regulators were clustered into two groups (Figure 5.4). The *PtFIT* protein contained the typical threonine-glutamate-arginine (T-E-

R) motif in the basic region of the *bHLH* domain at positions 5-9-13, as other members in the same subgroup. Differently, the feature showed in the *PtIRO* protein was histidine-glutamate-arginine (H-E-R) (Figure 5.3). Research showed that H-E-R could bind to the G-box (5'-CACGTG-3') of a promoter and T-E-R was bound to a variation of the E-box (5'-CANNTG-3') hexanucleotide sequence, revealing the different roles of the *FIT* and *IRO* genes in regulating iron deficiency response in plants(Heim et al., 2003; Li et al., 2006). Information in this study suggests that *PtFIT* and *PtIRO* cloned from *Populus tremula* belong to the *bHLH* family and may function differently in iron deficiency response in *Populus*.

The up-regulated expression of *PtFIT* was observed and more transcripts were detected in roots under iron deficiency (Figure 5.5 and 5.6). Similar responses of *AtbHLH29* and M*xFIT* were also reported (Jakoby et al., 2004; Yin et al., 2014). However, very weak expression of *PtIRO* was detected in the shoot tip of *Populus tremula* (Figure 5.5), which is different from the *MxIRO2* gene that expressed in the leaf and root of *Malus xiaojinensis* under iron sufficiency (Yin et al., 2013). It indicates that *PtIRO* may have a different function from *MxIRO2* and further research is needed to evaluate the possible function of *PtIRO* related to iron deficiency responses. This study also showed that the expression of *PtFIT* was higher in PtG than PtY at day 6 after the iron deficiency treatment. Research in *Arabidopsis* indicated that *AtIRT1* is a major downstream gene regulated by *AtFIT1* (Colangelo and Guerinot, 2004; Jakoby et al., 2004; and Yuan et al., 2005). In this study, the correlation between *PtIRT1* and *PtFIT* responding to iron deficiency was strongly positive (r=0.94) between *PtIRT1* and *PtFIT* in PtG (Figure 5.11), but the correlation in PtY was weak (r=0.49). This indicates that *FIT* in PtG functioned well in regulating *IRT1* to respond to iron deficiency as reported in *Arabidopsis* (Colangelo and Guerinot, 2004; Jakoby et al., 2004; and Yuan et al., 2005); however, in PtY, the regulation

function of *FIT* might be inhibited or needs to be induced by other factors (Yuan et al., 2008) and lack of those factors or lack of connections between those factors may explain such a weak correlation between *PtFIT* and *PtIRT*.

To further characterize the gene function, *PtFIT* driven by a constitutive super promoter (a trimer of the octopine synthase transcriptional activating element affixed to the mannopine synthase 2' transcriptional activating element plus minimal promoter) was transferred into another poplar species (*P. canescens* × *P. grandidentata* 'Cl6'). No enhanced constitutive expression of the *PtFIT* gene in transgenic lines was detected in this study. The transgenic plants had a relatively lower expression level of *PtFIT* under the iron sufficient condition compared to the control, while the expression of *PtFIT* was induced by iron deficiency in most transgenic plants (Figure 5.7). This indicates that there might be other factors regulating the expression of *PtFIT* and these factors can be activated by iron deficiency. As expected, the expression of *PtIRT1* in *PtFIT*-transgenic plants was also inhibited by iron sufficiency and induced by iron deficiency (Figure 5.7). Additionally, the fold change of the *PtIRT1* transcript was much greater in transgenic lines than in the control (Table 5.3). Previous research showed a similar result to which *AtIRT1* transcripts were not accumulated under the iron sufficient condition, but increased under the iron deficient condition in transgenic *Arabidopsis* plants overexpressing *AtFIT1* or *MxFIT*. This suggests that *PtFIT* might have the same function of inducing the expression of *PtIRT1* as *AtFIT1* and *MxFIT* have (Jakoby et al., 2004; Yuan et al., 2008; Yin et al., 2014). We predict that *PtFIT* could induce the expression of *PtIRT1* and might play an important role in regulation of iron transport under iron deficiency. Under iron sufficiency, the *PtFIT*-transgenic poplar lines accumulated more Fe than the control plant. Notably, one line (TL2) showed an increased chlorophyll (Chl a+b) content and Chl a/b ratio compared to the control even under

iron deficiency. This result is consistent with the findings in transgenic *Arabidopsis* in which overexpression of *MxFIT* increased chlorophyll content (Yuan et al., 2014). Interestingly, the TL2 line showed no enhanced Fe accumulation under iron deficiency, suggesting that TL2 might use iron more efficiently; therefore, overexpression of *PtFIT* could help increase the tolerance to iron deficiency in poplar trees.

In conclusion, two *bHLH* transcription factors (*PtFIT* and *PtIRO*) were cloned from *Populus tremula*. Functions of *PtFIT* in regulating iron deficiency were characterized. Results indicated that *PtFIT* might regulate *PtIRT1* to involve in regulation of iron deficiency response in *Populus*, which provides useful information for further understanding the mechanisms of iron deficiency response in poplar trees and other woody species.

References

Brumbarova, T. and Bauer, P. 2005. Iron-mediated control of the basic helix-loop-helix protein FER, a regulator of iron uptake in tomato. Plant Physiol. 137:1018-1026

Buckhout, T.J., Yang, T.J. and Schmidt, W. 2009. Early iron-deficiency-induced transcriptional changes in *Arabidopsis* roots as revealed by microarray analyses. BMC Genomics 10:147

Carretero-Paulet, L., Galstyan. A., Roig-Villanova, I., Martinez-Garcia, J.F., Bilbao-Castro, J.R. and Robertson, D.L. 2010. Genome-wide classification and evolutionary analysis of the bHLH family of transcription factors in *Arabidopsis*, poplar, rice, moss, and algae. Plant Physiol 153:1398-1412

Colangelo, E.P. and Guerinot, M.L. 2004. The essential basic helix-loop-helix protein FIT1 is required for the iron deficiency response. Plant Cell 16:3400-3412

Curie, C., Panaviene, Z., Loulergue, C., Dellaporta, S.L., Briat, J.F. and Walker, E.L. 2001. Maize *yellow stripe 1* encodes a membrane protein directly involved in Fe(III) uptake. Nature 409:346-49

Dai, W., Cheng, Z.M. and Sargent, W. 2003. Plant regeneration and *Agrobacterium*-mediated transformation of two elite aspen hybrid clones from in vitro leaf tissues. In Vitro Cell Dev. Biol. Plant 39:6-11

Dinneny, J.R., Long, T.A., Wang, J.Y., Jung, J.W., Mace, D., Pointer, S., Barron, C., Brady, S.M., Schiefelbein, J. and Benfey, P.N. 2008. Cell identity mediates the response of *Arabidopsis* roots to abiotic stress. Science 320:942-945

Eide, D., Broderius, M., Fett, J., and Guerinot, M.L. 1996. A novel iron-regulated metal transporter from plants identified by functional expression in yeast. Proc. Natl. Acad. Sci. USA 93:5624-28

Guerinot, M.L. and Yi, Y. 1994. Iron: Nutritious, noxious, and not readily available. Plant Physiol. 104:815-820

Heim, M.A., Jakoby, M., Werber, M., Martin, C., Weisshaar, B. and Bailey, P.C. 2003. The basic helix-loop-helix transcription factor family in plants: a genome-wide study of protein structure and functional diversity. Mol. Biol. Evol. 20:735-747

Hoagland, D.R. and Arnon, D.I. 1939. The water culture method for growing plants without soil. Calif. Agr. Expt. Sta. Circ. 347

Inoue, H., Kobayashi, T., Nozoye, T., Takahashi, M., Kakei, Y., Suzuki, K., Nakazono, M., Nakanishi, H., Mori, S. and Nishizawa, N.K. 2009. Rice *OsYSL15* is an iron-regulated iron(III)-deoxymugineic acid transporter expressed in the roots and is essential for iron uptake in earlygrowth of the seedlings. J. Biol. Chem. 284:3470-79

Ivanov, R., Brumbarova, T. and Bauer, P. 2012. Fitting into the harsh reality: regulation of iron-deficiency responses in dicotyledonous plants. Mol. Plant 5:27-42

Jakoby, M., Wang, H.Y., Reidt, W., Weisshaar, B. and Bauer, P. 2004. FRU(BHLH029) is required for induction of iron mobilization genes in *Arabidopsis thaliana*. FEBS Lett. 577:528-34

Jeong, J. and Connolly, E.L. 2009. Iron uptake mechanisms in plants: Functions of the *FRO* family of ferric reductases. Plant Sci. 176:709-714

Kobayashi, T. and Nishizawa, N.K. 2012. Iron uptake, translocation and regulation in higher plants. Annu. Rev. Plant Biol. 63:131-152

Larionov, A., Krause, A. and Miller, W. 2005. A standard curve based method for relative real time PCR data processing. BMC Bioinformatics 6:62.

Latchman, D.S. 2007. Gene regulation: a eukaryotic perspective. 5th edition. Taylor&Franics Group e-Library, New York, NY

Legay, S., Guignard, C., Ziebel, J. and Evers, D. 2012. Iron uptake and homeostasis related genes in potato cultivated in vitro under iron deficiency and overload. Plant Physiol. Biochem. 60:180-189

Li, X.X., Duan, X.P., Jiang, H.X., Sun, Y.J., Tang, Y.P., Yuan, Z., Guo, J.K., Liang, W.Q., Chen, L., Yin, J.Y., Ma, H., Wang, J. and Zhang, D.B. 2006. Genome-wide analysis of basic/helix-loop-helix transcription factor family in rice and *Arabidopsis*. Plant Physiol. 141:1167-1184

Lichtenthaler, H.K. 1987. Chlorophylls and carotenoids: pigments of photosynthetic membranes. Methods Enzymol. 148:350-382

Ling, H.Q., Bauer, P., Bereczky, Z., Keller, B. and Ganal, M. 2002. The tomato *fer* gene encoding a bHLH protein controls iron-uptake responses in roots. Proc. Natl. Acad. Sci. USA 99: 13938-13943

Long, T.A., Tsukagoshi, H., Busch, W., Lahner, B., Salt, D.E. and Benfey, P.N. 2010. The bHLH transcription factor POPEYE regulates response to iron deficiency in *Arabidopsis* roots Plant Cell 22:2219-2236

Massari, M.E. and Murre, C. 2000. Helix-loop-helix proteins: regulators of transcription in eukaryotic organisms. Mol Cell Biol 20:429-440

Murata, Y., Ma, J.F., Yamaji, N., Ueno, D., Nomoto, K. and Iwashita, T. 2006. A specific transporter for iron(III)-phytosiderophore in barley roots. Plant J. 46:563-572

Ohashi-Ito, K. and Bergmann, D.C. 2006. *Arabidopsis* FAMA controls the final proliferation/differentiation switch during stomatal development. Plant Cell 18:2493-2505

Pagnussat, G.C., Yu, H.J., Ngo, Q.A., Rajani, S., Mayalagu, S., Johnson, C.S., Capron, A., Xie, L.F., Ye, D. and Sundaresan, V. 2005. Genetic and molecular identification of genes required for female gametophyte development and function in *Arabidopsis*. Development 132:603 -614

Robinson, N.J., Procter, C.M., Connolly, E.L. and Guerinot, M.L. 1999. A ferric-chelate reductase for iron uptake from soils. Nature 397:694-697

Römheld, V. and Marschner, H. 1986. Evidence for a specific uptake system for iron phytosiderophores in roots of grasses. Plant Physiol. 80:175-180

Saeed, A.I., Bhagabati, N.K., Braisted, J.C. Liang, W., Sharov, V. Howe E.A., Li, j., Thiagarajan, M., White, J.A. and Quackenbush, J. 2006. TM4 microarray software suite. Methods Enzymol. 411: 134-193

Schuler, M., Keller, A., Backes, C., Philippar, K. Lenhof, H., and Bauer, P. 2011. Transcriptome analysis by GeneTrail revealed regulation of functional categories in response to alterations of iron homeostasis in *Arabidopsis thaliana*. BMC Plant Biol. 11:87

Simon, R., Lam, A., Li, M. Ngan, M., Menenzes, S. and Zhao, Y. 2007. Analysis of gene expression data using BRB-array tools. Cancer Inform. 3:11-17

Sivitz, A.B., Hermand, V., Curie, C. and Vert, G. 2012. *Arabidopsis bHLH100* and *bHLH101* control iron homeostasis via a FIT-independent pathway. PLoS ONE 7: e44843

Takagi, S. 1976. Naturally occurring iron-chelating compounds in oat- and rice-root washing. I. Activity measurement and preliminary characterization. Soil Sci. Plant Nutr. 22:423–33

Vert, G., Briat, J.F. and Curie, C. 2001. *Arabidopsis IRT2* gene encodes a root-periphery iron transporter. Plant J. 26:181-189

Wang, H.Y., Klatte, M., Jakoby, M., Baumlein, H., Weisshaar, B. and Bauer, P. 2007. Iron deficiency-mediated stress regulation of four subgroup Ib BHLH genes in *Arabidopsis thaliana*. Planta 226:897-908

Wang, L., Cui, Y., Liu, Y., Fan, H., Du, J., Huang, Z., Yuan, Y. Wu, H. and Ling, H.Q. 2013. Requirement and Functional Redundancy of Ib subgroup bHLH proteins for iron deficiency responses and uptake in *Arabidopsis thaliana*. Mol. Plant 6:503-513

Waters, B.M., McInturf, S.A. and Stein, R.J. 2012. Rosette iron deficiency transcript and microRNA profiling reveals links between copper and iron homeostasis in *Arabidopsis thaliana*. J. Exp. Bot. 63:5903-5918

Xu, H.M., Wang, Y., Chen, F., Zhang, X.Z. and Han, Z.H. 2011. Isolation and characterization of the iron-regulated MxbHLH01 gene in *Malus xiaojinensis*. Plant Mol. Biol. Report 29:936-942

Yin, L., Wang, Y., Yuan, M., Zhang, X., Pan, H., Xu, X. and Han, Z. 2013. Molecular cloning, polyclonal antibody preparation, and characterization of a functional iron-related transcription factor IRO2 from Malus xiaojinensis. Plant Physiol. Biochem. 67:63-70

Yin, L., Wang, Y., Yuan, M., Zhang, X., Xu, X. and Han, Z. 2014. Characterization of MxFIT, an iron deficiency induced transcriptional factor in *Malus xiaojinensis*. Plant Physiol. Biochem. 75:89-95

Yuan, Y, Wu, H., Wang, N., Li, J., Zhao, W., Du, J., Wang, D. and Ling, H.Q. 2008. FIT interacts with AtbHLH38 and AtbHLH39 in regulating iron uptake gene expression for iron homeostasis in *Arabidopsis*. Cell Res. 18:385-397

Yuan, Y., Zhang, J., Wang, D.W. and Ling, H.Q. 2005. AtbHLH29 of *Arabidopsis thaliana* is a functional ortholog of tomato FER involved in controlling iron acquisition in strategy I plants. Cell Res. 15:613-621

CHAPTER VI. GENERAL CONCLUSION

Iron deficiency causes a decrease of chlorophyll content and alteration of chlorophyll structure, resulting in plant chlorosis. Iron chlorosis can be seen in many plant species, particularly in plants grown in alkaline and calcareous soils, causing yield loss and poor quality. Molecular mechanisms of iron metabolism including uptake, transport, and utilization in many annual and herbaceous species, such as *Arabidopsis*, rice, and tomato have been well documented; however, very limited research has been done for woody plants.

Populus is a model woody species for both basic and applied research. The completion of the whole genome sequence of *Populus trichocarpa* largely facilitates research in molecular biology, genetics, and genomics for tree species. A few poplar species are also susceptible to iron chlorosis. Therefore, poplar is an ideal species to study iron uptake, transport, utilization, and metabolism for woody species.

The dissertation included two main parts: literature review and manuscripts. The literature review provided the general background of the importance of iron in plants, iron availability in the soil, plant responses to iron deficiency and its management, regulation of iron uptake, transport, and metabolism in plants as well as the general information about *Populus*. The second part contained three papers that were written in a refereed journal format. Paper 1 analyzed the physiological responses of *Populus tremula* to iron deficiency. Paper 2 reported the cloning and functional characterization of two iron-regulated transporter (*IRT*) genes in *Populus tremula*. Paper 3 discussed molecular cloning and characterization of the basic helix-loop-helix (*bHLH*) genes that may be involved in the regulation of iron deficiency responses in poplar trees.

Plant materials used in this study were two clonal trees of *Populus tremula* L.'Erecta' grown near each other with contrasting phenotypes (PtG: green leaves and PtY: yellow leaves).

Soil analysis showed that the soil where two trees were grown was slightly alkaline (pH 7.42-7.88). The quantity of major mineral elements (Fe, Zn, and Cu) in the soil was less than recommended. Leaf tests for the field-grown trees confirmed the differences in the content of dry matter, chlorophyll and carotenoids, Chl a/b ratio, and the content of Zn and Fe between the two trees. The hydroponic culture successfully induced the iron chlorosis and confirmed that the aforementioned differences were also significant between the two trees. Thus, the two trees showed the different tolerance to iron deficiency, which appeared to be the cause of contrasting phenotypes.

The iron-regulated transporter (*IRT)* genes play an important role in iron uptake and transport in plants. In this study, two *IRT* genes (*PtIRT1* and *PtIRT3*) were cloned from PtG and PtY to investigate their functions on iron uptake and transport and their responses to iron/zinc deficiency. Analysis of the deduced amino acids showed that both *PtIRT1* and *PtIRT3* were identical in PtG and PtY. They all contained the conserved ZIP domain with eight transmembrane regions (TM) and a ZIP signature sequence. Phylogenetic analysis suggested that *PtIRT1* may function as an iron transporter, while *PtIRT3* is more likely to be a zinc transporter. Analyses of gene expression indicated that *PtIRT1* only expressed in root tissues, while *PtIRT3* constitutively expressed in all tested tissues. However, the activity of the *GUS* gene derived by the promoter of *PtIRT1* was found both in the leaf and root of the transgenic tobacco lines. Expression analysis also showed that *PtIRT1* and *PtIRT3* were up-regulated by iron deficiency, while down-regulated by zinc deficiency. In addition, *PtIRT1* showed a higher expression level in PtG than in PtY under iron deficiency. Interestingly, *PtIRT1*-transgenic poplar plants showed an enhanced expression of *PtIRT1*, but no increased Fe accumulation. Transgenic tobacco lines with *PtIRT1*-pro::*GUS* showed an enhanced GUS activity in the root under iron deficiency,

indicating *PtIRT1*-pro was responding to iron deficiency and the promoter of *PtIRT1* might be regulated by the transcriptional factors.

Two basic helix-loop-helix (*bHLH*) transcription factors (*PtFIT* and *PtIRO*) were isolated from PtG and PtY and their responses to iron deficiency were analyzed. Gene sequence analyses showed that each of the two genes was identical in PtG and PtY. The expression of *PtFIT* was detected only in root tissues and up-regulated by iron deficiency; however, the expression of *PtIRO* was rarely detected in all tested tissues. A higher level of *PtFIRT* transcripts was detected in PtG than in PtY. A strong positive correlation (r=0.94) between *PtFIT* and *PtIRT1* in PtG was determined and such a correlation was very weak in PtY (r=0.49), indicating that PtG and PtY may have different mechanisms of regulating iron deficiency. The *PtFIT*-transgenic poplar plants had an enhanced Fe content under iron sufficiency. The expression of *PtFIT* and *PtIRT1* was significantly enhanced by iron deficiency compared to the control plant. One of the transgenic poplar lines (TL2) had a higher chlorophyll content and Chl a/b ratio than the control, revealing its enhanced tolerance to iron deficiency.

In conclusion, the iron chlorosis tolerant tree (PtG) could accumulate more Fe than the susceptible one (PtY) under iron deficiency, which might attribute to a higher expression level of *PtFIT* and *PtIRT1* responding to iron deficiency. Transgenic plants with *PtFIT* showed an increased tolerance to iron deficiency. This research facilitates the understanding of iron uptake, transport, and regulation in poplar trees. It would be valuable for further elucidation of the mechanisms of iron deficiency response in poplar and other tree species.